
Aus dem Fachbereich Pharmazie
der Johann Wolfgang Goethe-Universität
Frankfurt am Main

Institut für Biochemie I – Pathobiochemie

Impact of tumour microenvironmental factors on dendritic cell
differentiation and function

Dissertation for attaining the PhD degree of Natural Sciences

Submitted to the Faculty
of the Johann Wolfgang Goethe University
in Frankfurt am Main

by

Divya Sekar
Shimoga, India
Frankfurt 2012

Accepted by the Faculty of Pharmacy of the
Johann Wolfgang Goethe University as a dissertation.

Dean: Prof. Dr. rer. nat. Thomas Prisner
Expert assessor : Prof. Dr. rer. nat. Manfred Schubert-Zsilavecz
Expert co-assessor : Prof. Dr. rer. nat. B. Brüne

Date of the disputation:

विचारः परमं ज्ञानं

Inquiry is the highest wisdom

(Translated from Sanskrit)

INDEX

1	<i>Summary</i>	1
2	<i>Zusammenfassung</i>	4
3	<i>Introduction</i>	10
3.1	The inflammatory tumor microenvironment	10
3.2	Dendritic cells	13
3.3	DC subtypes and their role in immunity	13
3.4	Role of mDC in effector immunity	15
3.4.1	mDC in tumour tolerance induction	16
3.4.2	mDC and T cell interaction	16
3.4.3	DC-Treg interaction in tumour-bearers	18
3.4.4	Different states of immunosuppressive DC in tumour-bearing animals	18
3.4.5	Uptake of dying tumour cell-derived factors by DC	19
3.4.6	Types of cell death	19
3.4.7	Cell death-induced immune responses	21
3.5	pDC roles in immunotherapy	22
3.6	DC development	24
3.6.1	Precursors involved in DC subset development	24
3.6.2	Cytokines that shape pDC development and the myeloid progenitor hypothesis	26
3.6.3	Transcriptional machinery involved in pDC development	26
3.6.4	Hypoxia as a microenvironmental factor in hematopoiesis	28
3.7	Aims of this study	29
4	<i>Materials</i>	31
4.1	Chemicals and Reagents	31
4.2	Buffers and Solutions	33
4.3	Pre-made Buffers	36
4.4	Dye and beads	36
4.5	Kits	37
4.6	Antibodies	37
4.6.1	Human FACS antibodies:	37
4.6.2	Human Neutralizing antibodies	38

4.6.3	Murine FACS antibodies	39
4.6.4	Primary human antibodies:	40
4.6.5	Secondary human antibodies:	40
4.7	Microbeads:	40
4.8	Media and reagents for cell culture	40
4.9	Cytokines	41
4.10	ELISA	41
4.11	Stimulators and Inhibitors	41
4.12	Oligonucleotides	42
4.13	Cells and cell lines	43
4.14	Instruments	43
4.15	Plastic material	45
4.16	Software	45
5	<i>Methods</i>	46
5.1	Cell culture	46
5.2	Primary human immune cell isolation and expansion	46
5.3	Animals	46
5.4	Generation and maturation of plasmacytoid and myeloid DC	47
5.5	Isolation of primary pDC	47
5.6	Murine pDC generation from bone marrow and hypoxic culture	47
5.7	Preparation of tumour cell supernatants	48
5.8	DC-T cell co-culture	49
5.9	Treg isolation and CD39⁺ cell isolation	49
5.10	Stimulation of human monocyte-derived DC	49
5.11	Cytotoxicity assay	50
5.12	Flow cytometry of human DC	51
5.13	Murine Polychromatic flow cytometry	52
5.14	RNA isolation, cDNA synthesis and qPCR	53
5.15	Cytokine quantitation	53

5.16	T lymphocyte proliferation assay	54
5.17	Apoptotic cell phagocytosis assay	54
5.18	Western blot analysis	55
5.19	IFN-α intracellular staining (ICS)	55
5.20	IFN-α bioassay	55
5.21	Statistical analysis	55
6	<i>Results</i>	56
6.1	Ex-vivo mo-pDC generation and study under hypoxia	56
6.1.1	Generation and characterization of mo-pDC from human monocytes using Flt3-L	56
6.1.2	Expression of pDC developmental transcription factors by mo-pDC	60
6.1.3	Functional validation of mo-pDC	61
6.1.4	IFN- α production by mo-pDC	62
6.1.5	Augmenting IFN- α production by mo-pDC	64
6.1.6	Phenotypical differences between normoxia and hypoxia differentiated mo-pDC	66
6.2	Study of mice pDC development under the influence of HIF-1α and hypoxia	69
6.2.1	Increased pDC frequency in HIF-1 α ^{fl/fl} LysM-Cre mice	69
6.2.2	Hypoxia/HIF-1 represses pDC differentiation from whole bone marrow in vitro	70
6.2.3	Altered immune cell populations in Flt3L-expanded bone marrow cultures dependent on O ₂ supply	72
6.3	Generation of regulatory T cells by IL-27 secreting DC under the impact of apoptotic cell-derived factors	74
6.3.1	Priming with apoptotic tumour cell supernatants suppresses DC-dependent tumour cell killing	75
6.3.2	Accumulation of CD39/CD69-expressing FoxP3 ⁺ Treg in ACM-primed co-cultures	77
6.3.3	S1P in ACM confers suppression of cytotoxicity by activating S1PR4 on DC	82
6.3.4	ACM-primed DC secrete IL-27 to activate suppressive Treg	84
6.3.5	Suppression of cytotoxicity is reduced by interference with adenosine generation	89
7	<i>Discussion</i>	96
7.1	mo-pDC generation ex-vivo brought about by evoking pDC developmental genes	96
7.2	Under hypoxia mo-pDC development is halted to produce non-functional cells	99
7.3	Mouse pDC differentiation <i>in vitro</i> is inhibited by hypoxia-induced HIF-1	100
7.4	Apoptotic cell priming in reducing cytotoxicity and inducing Tregs in DC dependent priming	103

7.5	The Adenosine pathway is utilized by Treg to cause immunosuppression	105
8	<i>Concluding remarks</i>	<i>108</i>
9	<i>References</i>	<i>111</i>
10	<i>Publications</i>	<i>119</i>
11	<i>Acknowledgements</i>	<i>120</i>
12	<i>Curriculum Vitae</i>	<i>121</i>
13	<i>Ehrenwörtliche Erklärung</i>	<i>122</i>

LIST OF FIGURES

<i>Figure 1: Tumour microenvironmental stress factors.</i>	10
<i>Figure 2: Immune cells infiltrating the tumour microenvironment</i>	12
<i>Figure 3: DC play multiple roles in immunity.</i>	14
<i>Figure 4: Role of mDC in effector Th immunity</i>	15
<i>Figure 5: Modes of cell death and the factors released</i>	20
<i>Figure 6: Exposure of phagocytes to NC or AC-derived signals</i>	22
<i>Figure 7: pDC roles in immunity</i>	23
<i>Figure 8: DC subset development theories</i>	25
<i>Figure 9: Transcription factors (TF) involved in pDC development</i>	27
<i>Figure 10: Cytotoxicity assay was performed as depicted</i>	50
<i>Figure 11. Morphology of mo-pDC compared to mDC and macrophages</i>	57
<i>Figure 12. Mo-pDC differ in surface marker expression compared to mDC</i>	58
<i>Figure 13. Expression of pDC lineage determining transcription factor E2-2 and E2-2-controlled BDCA2.</i>	60
<i>Figure 14. Functional validation of mo-pDC versus mDC</i>	61
<i>Figure 15. IFN-α production by mo-pDC</i>	63
<i>Figure 16. Expression of E2-2, ID2 and E2-2-controlled BDCA2 in normoxia and hypoxia differentiated mo-pDC.</i>	66
<i>Figure 17. Mo-pDC generated under normoxia vs. hypoxia express different surface and functional markers</i>	68
<i>Figure 18: Generation of HIF-1αfl/fl LysM-Cre mice</i>	70
<i>Figure 19. Hypoxia-induced HIF-1 suppresses pDC differentiation in vitro</i>	71
<i>Figure 20. Differentiation of bone marrow under 5% O₂ blocks pDC differentiation and expands cDC.</i>	73
<i>Figure 21. Basal DC phenotype upon activation with tumour cell supernatants</i>	74
<i>Figure 22. Experimental outline</i>	75
<i>Figure 23. Viable cancer cell supernatants prime whereas supernatants of apoptotic cells suppress specific cytotoxicity.</i>	76
<i>Figure 24. Relative amounts of T cell subsets and FoxP3-expressing Tregs</i>	77
<i>Figure 25. Apoptotic cell supernatants induce CD39 and CD69-expressing Treg</i>	78
<i>Figure 26. Purity of isolated CD4⁺CD25⁺ Treg</i>	79
<i>Figure 27. Treg confer ACM-induced suppression of cytotoxicity</i>	80
<i>Figure 28. CD39 depletion restores ACM-induced suppression of cytotoxicity</i>	81
<i>Figure 29. ACM-dependent suppression of cytotoxicity functions through S1P receptors</i>	82
<i>Figure 30. S1PR4 on DC conveys ACM-dependent suppression of cytotoxicity</i>	83
<i>Figure 31. Addition of S1P to VCM mimics ACM</i>	84
<i>Figure 32. ACM-induced IDO expression and the effect of IDO inhibition on ACM-induced suppression of cytotoxicity.</i>	85

<i>Figure 33. Influence of ACM on cytokine induction</i>	86
<i>Figure 34. ACM induces IL-27 in DC in a S1PR4-dependent manner to generate Treg</i>	88
<i>Figure 35. OXA-ACM exhibits higher cytotoxicity compared to STS-ACM</i>	89
<i>Figure 36. IL-10 and TGF-β are not involved in suppressing cytotoxicity</i>	90
<i>Figure 37. Relative expression of ectonucleotidases CD39 or CD73 by T cells</i>	91
<i>Figure 38. Inhibition of ectonucleotidases and adenosine receptor A2a restores cytotoxicity</i>	92
<i>Figure 39. Surface profiling of doublet T cell populations.</i>	93
<i>Figure 40. CD39/CD69-expressing Treg are enriched in CD4+CD8+ doublet events.</i>	94
<i>Figure 41. CD69 neutralization reduces the doublet T cell population</i>	95
<i>Figure 42: Transcription factors (TF) profile during pDC development under normoxia and hypoxia</i>	97
<i>Figure 43: pDC development under normoxia and hypoxia</i>	101
<i>Figure 44: Pathway leading to suppression of anti-tumour immunity by apoptotic tumour cell priming of DC:</i>	106

LIST OF TABLES

<i>Table 1: Quantification of surface marker expression</i>	59
<i>Table 2: Surface marker expression at normoxia versus hypoxia'</i>	67

Abbreviations

A2a	adenosine receptor
AC	Apoptotic cells
ACM	Apoptotic cell conditioned medium
ANOVA	Analysis of variance
APS	Ammonium persulfate
ARNT	Aryl hydrocarbon receptor nuclear translocator
ATP	Adenosine triphosphate
ATRA	All-trans retinoic acid
BDCA	Blood dendritic cell antigen
BFA	Brefeldin A
BSA	Bovine serum albumin
CCR	C-C chemokine receptor
CD	Cluster of differentiation
CFSE	Carboxyfluorescein succinimidyl ester
CMAC	7-amino-4-chloromethylcoumarin
CpG	—C—phosphate—G—
CSF	Colony stimulating factor
CXCL	Chemokine (C-X-C motif) ligand
DMEM	Dulbecco's modified eagle medium
DMSO	Dimethylsulfoxide
DNA	Deoxyribonucleic acid
DTT	Dithiothreitol
EDTA	Ethylene diamine tetra acetate
FCS	Fetal calf serum
Flt3-L	Fms-related tyrosine kinase 3 ligand
FITC	Fluoresceinisothiocyanat
FMO	fluorescence minus one
GM-CSF	Granulocyte macrophage-colony stimulating factor
HIF	Hypoxia-inducible factor
HMGB	High-mobility group box
ICAM	Intercellular adhesion molecule
ID	Inhibitor of DNA-binding/differentiation proteins
IDO	indolamine-2,3-dioxygenase
IFN	Interferon
Ig	Immunoglobulin
IL	Interleukin
KCl	Potassium chloride
KH ₂ PO ₄	Potassium hydrogen phosphate

KHCO ₃	Potassium hydrogen carbonate
LPC	Lysophosphatidylcholine
LPS	Lipopolysaccharide
MCP	Monocyte chemotactic protein-1
MFG-EF	Milk fat globule-EGF factor
MgCl ₂	Magnesium chloride
MgSO ₄	Magnesium sulfate
MHC	Major histocompatibility complex
Na ₂ HPO ₄	Sodium hydrogen phosphate
NaCl	Sodium chloride
NC	Necrotic cells
NCM	Necrotic condition medium
NH ₄ Cl	Ammonium chloride
ODN	Oligonucleotides
OXA	Oxaliplatin
PBMCs	Peripheral blood mononuclear cells
PBS	Phosphate buffered saline
PI	Propidium iodide
PtdSer	Phosphatidylserine
RAGE	Receptor for Advanced Glycation Endproducts
RANTES	Regulated upon Activation, Normal T-cell Expressed, and Secreted
RPMI	Roswell park memorial institute
S1P	Sphingosine-1-phosphate
S1PR	S1P receptor
SD	Standard deviation
SDF	Stromal cell derived factor
SDS	Sodium dodecyl sulfate
STAT	Signal Transducers and Activators of Transcription
Sts	Staurosporine
Tc	cytotoxic T cells
TCR	T-cell receptor (TCR)
TEMED	Tetraethylendiamine
TGF	Transforming growth factor
Th	Helper T cells
TIM	T-cell immunoglobulin- and mucin-domain-containing molecule
TLR	Toll-like receptor
TNF	Tumor necrosis factor
UTP	Uridine triphosphate

VCM

Viable condition medium

VEGF

Vascular endothelial growth factor

1 Summary

Tumour cells that exhibit aberrant outgrowth have evolved various ways to escape detection by the immune system. In addition to modifications in the surface repertoire of its individual cells to avoid immune surveillance, the tumour exhibits alterations in its microenvironment. These are among others altered oxygen levels in the tumour core or shedding of biochemical factors by tumour cells that in turn modify the functions of phagocytes such as Dendritic cells (DC). DC are professional antigen-presenting cells, which play multiple roles in immunity, achieved by specialization into different functional subsets. Myeloid DC (mDC) are efficient in antigen presentation, thereby activating immunity, whereas plasmacytoid DC (pDC) act as rheostats of the immune system. pDC activate natural killer cells and cause activation of bystander mDC, but also interact with T cells to induce tolerance. This ambiguity positions pDC at the centre of inflammatory diseases such as cancer, arthritis and autoimmune diseases.

Protocols to generate human mDC *ex vivo* made it possible to engineer these cells to suit therapeutic needs. Unfortunately, a similar easily accessible system to generate human pDC was not available. A first goal of this study was therefore to develop a method to generate human pDC equivalents *ex vivo* from peripheral blood monocytes, termed mo-pDC (monocyte-derived pDC), using Fms-related tyrosine kinase 3 ligand (Flt3-L). Mo-pDC showed a characteristic pDC surface protein marker profile, as well as a low capacity to induce autologous lymphocyte proliferation and to phagocytose apoptotic debris in comparison to mDC. Furthermore, mo-pDC upregulated the pDC lineage-determining transcription factor E2-2 during differentiation and expressed the E2-2 target gene BDCA2. Importantly, mo-pDC produced high levels of interferon- α (IFN- α), the main functional parameter of pDC, when pre-treated with tumour necrosis factor- α (TNF- α) and/or when differentiated additionally with vitamin D3 or all-trans retinoic acid. When differentiated under hypoxia, E2-2 and its target gene BDCA2 were downregulated in mo-pDC. Furthermore, mo-pDC differentiated under hypoxia did not secrete

IFN- α , but produced high levels of other inflammatory cytokines. Hence, mo-pDC can be used to study differentiation and function of human pDC.

Strikingly, hypoxia also blocked differentiation of mouse pDC from bone marrow precursors. Hypoxia-inducible factor 1 α (HIF-1 α)-dependent repression of E2-2 via its transcriptional counterpart ID2 seemed to be a crucial factor in disturbing the differentiation of precursors into pDC, since pDC differentiation was normal when culturing HIF-1 α ^{fl/fl} LysM-Cre bone marrow under hypoxia. In addition, the differentiation of mouse pDC under hypoxia followed a similar transcription factor regulation pattern compared with human mo-pDC.

Hypoxia plays an important role in the pathogenesis of pulmonary disease, stroke, heart disease and cancer. In cancer, hypoxia is one of the tumour stress factors that topple anti-tumour immunity. Intrinsic immunosuppression is a major obstacle for successful therapy of tumours. Despite some progress, mechanisms how immunosuppression is induced and regulated in cancer patients are ill-defined. Besides hypoxia, a microenvironmental component that might prevent anti-tumour immunity is the presence of dying tumour cells. Apoptosis of tumour cells is abundant in tumour under steady-state conditions and is largely increased following conventional cancer ablation methods such as chemo- or radiotherapy. Shedding of apoptotic debris and/or secretion of factors to the tumour bed or draining lymph nodes might have a profound impact on professional phagocytes such as dendritic cells (DC) and the subsequent priming of lymphocyte responses. To clarify this, we exposed human myeloid DC to supernatants of living, apoptotic or necrotic human breast cancer cell supernatants, followed by their co-culture with autologous T cells. Priming with apoptotic debris prevented DC from establishing cytotoxicity towards living human tumour cells by inducing a regulatory T cell (Treg) population, defined by co-expression of CD39 and CD69. Immunosuppression via Treg was transferable to viable tumour cell-primed co-cultures and required the bioactive lipid sphingosine-1-phosphate (S1P), present in apoptotic cell supernatants and acting via S1P receptor 4 on DC to

induce IL-27 secretion. We propose that CD69-expression on CD39⁺ Treg enables them to interact with CD73-expressing CD8⁺ T cells to generate adenosine, which acts via adenosine receptor A2a on cytotoxic T cells to suppress their function. These findings might aid the understanding how dying tumour cells limit anti-tumour immunity and might provide cues to improve anti-tumour immunotherapy. In conclusion, the findings described here identify mechanisms how tumour microenvironmental factors influence human DC subtype function. Understanding these mechanisms can give valuable hints for choosing functional immunotherapy targets or chemotherapy regimens for the treatment of cancer.

2 Zusammenfassung

Um aberrant auszuwachsen zu können müssen Tumorzellen in vielfältiger Weise evolutive Prozesse durchlaufen, die es ihnen ermöglichen der Erkennung durch das körpereigene Immunsystem zu entkommen. Zusätzlich zur Modifikation der Oberflächensignatur einzelner Tumorzellen, zur Vermeidung einer effizienten Immun-Überwachung, weisen Tumore eine Modifikation ihrer Mikroumgebung auf. Diese Veränderungen entstehen einerseits passiv, z.B. durch veränderte Sauerstoffkonzentrationen überwiegend im Tumorkern, aber andererseits auch aktiv, durch die Freisetzung biochemischer Faktoren aus Tumorzellen. Diese Faktoren sind in der Lage die Funktion von Tumor-assoziierten Phagozyten, wie z.B. Dendritischen Zellen (DC) zu modifizieren. Solcherart durch die Tumormikroumgebung polarisierte Immunzellen fördern das Tumorstadium in vielfältiger Weise.

Bei DC handelt es sich um professionelle Antigen-präsentierende Zellen, die ihre vielfältigen Rollen im Immunsystem durch Spezialisierung in verschiedene funktionale Subtypen sicherstellen. Beispielsweise sind myeloische DC (mDC) besonders effizient in Hinsicht auf die Präsentation von Antigenen, wohingegen plasmazytoide DC (pDC) eher regulatorisch auf das Immunsystem einwirken. Sie sind in der Lage natürliche Killerzellen oder benachbarte mDC zu aktivieren, interagieren aber auch mit T Zellen um Immuntoleranz zu erzeugen. Diese doppelsinnige Funktionsweise positioniert pDC im Zentrum der Regulation inflammatorischer Erkrankungen zu denen u.a. die Karzinogenese, aber auch Arthritis und Autoimmunerkrankungen gehören.

Auch mDC spielen eine wichtige Rolle bei der Karzinogenese. Weiterhin wird ihnen ein großes Potential zur Initiation einer Anti-Tumor-Immunreaktion zugeschrieben. Humane mDC können *ex vivo* aus Monozyten hergestellt werden. Folgerichtig werden aus Monozyten hergestellte, funktionell maßgeschneiderte humane mDC schon heute zur Therapie von Tumoren

klinisch erprobt. In Mausmodellen wird das Anti-Tumor-Potential von *ex vivo* generierten mDC durch pDC extrem verstärkt. Leider war es bisher nicht möglich humane pDC in ausreichender Menge für therapeutische Applikationen, in Analogie zur Generierung von mDC, herzustellen.

Aus diesem Grund war ein erstes Ziel dieser Arbeit eine Methode zur Generierung von humanen pDC, oder zumindest Zellen mit äquivalenter Funktion, aus Vorläuferzellen zu entwickeln. In Analogie zur Herstellung von mDC wurden Monozyten peripherem Humanblut als Vorläuferzellen eingesetzt. Diese wurden mittels des Wachstumsfaktors *Fms-related tyrosine kinase 3 ligand* (Flt3-L) zu pDC-Äquivalenten differenziert, welche als *monocyte-derived pDC* (mo-pDC) bezeichnet wurden. In der Tat zeigten mo-pDC ein für humane pDC charakteristisches Oberflächenmarkerprofil, u.a. eine hohe Expression des Interleukin 3 (IL-3) Rezeptors CD123 und des *blood dendritic cell antigen 4* (BDCA4). Weiterhin zeigten mo-pDC eine geringe Expression des kostimulatorischen Moleküls CD86 und des toll-like receptor 4 (TLR4) welche für mDC charakteristisch sind. Auch funktional waren mo-pDC klar von mDC zu unterscheiden. Sie wiesen, im Vergleich zu mDC, eine geringe Kapazität zur Induktion der Proliferation autologer T Zellen auf. Auch die Phagozytose apoptotischer Zellen war in mo-pDC in Vergleich zu mDC verringert. Die Flt3-L-vermittelte Differenzierung von Monozyten zu pDC-Äquivalenten war auch auf der Ebene der Expression populationsspezifischer Transkriptionsfaktoren ersichtlich. Mo-pDC erwarben im Verlauf ihrer Differenzierung aus Monozyten eine kontinuierlich erhöhte Expression des pDC-spezifischen Transkriptionsfaktors E2-2 und exprimierten erhöhte Mengen des pDC-spezifischen Oberflächenmarkers BDCA2, welcher unter der transkriptionellen Kontrolle von E2-2 steht. Die wichtigste Funktion von pDC ist die Produktion großer Mengen von Interferon- α (IFN- α) in Antwort auf eine Virusinfektion oder Agonisten der Rezeptoren TLR7 und TLR9. Mo-pDC waren ebenfalls in der Lage große Mengen an IFN- α zu sekretieren, allerdings nur nach vorheriger Aktivierung mit Tumornekrosefaktor- α (TNF- α) und/oder wenn zu ihrer Differenzierung neben Flt3-L auch Vitamin D3 oder all-trans-Retinolsäure verwendet wurde. Nach der erfolgreichen Etablierung eines Protokolls zur Generierung von funktionalen pDC-Äquivalenten aus

humanen Monozyten war es das Ziel den Phänotyp dieser Zellen unter dem Einfluss eines Faktors der Tumormikroumgebung, in diesem Fall geringe Sauerkonzentrationen (Hypoxie), zu untersuchen. Die Differenzierung von Monozyten mittels Flt3-L unter Hypoxie veränderte die Differenzierung zu pDC in drastisch. Die Expression des spezifischen Transkriptionsfaktors E2-2 war stark vermindert, wie auch die Expression von BDCA2, CD86 und des Haupthistokompatibilitätskomplexes I (MHC I). Mo-pDC welche unter Hypoxie generiert wurden waren weiterhin nicht in der Lage IFN- α zu produzieren, sekretierten jedoch als Antwort auf eine Stimulation des TLR9 hohe Mengen anderer inflammatorischer Zytokine. Diese Daten zeigten zunächst, dass mo-pDC für das Studium von Differenzierung und Funktion humaner pDC eingesetzt werden können. Weiterhin lieferten sie Hinweise auf eine veränderte Differenzierung humaner pDC unter Hypoxie.

In einem nächsten Schritt wurde folglich untersucht, ob Hypoxie die Differenzierung von pDC auch aus deren physiologischen Vorläufern aus dem Knochenmark beeinflusst. Für diese Studien wurde ein gut etabliertes System unter Verwendung von Knochenmarkszellen der Maus eingesetzt. Diese wurden mit Flt3-L unter Normoxie oder Hypoxie zu pDC differenziert. In der Tat war die Differenzierung von Knochenmarkstammzellen zu pDC unter Hypoxie unterdrückt, was sich auch in der Expression von E2-2 widerspiegelte. Hypoxie aktiviert u.a. spezifische Transkriptionsfaktoren, die sogenannten Hypoxie-induzierten Faktoren (HIF). HIF-1 kann die Expression des funktionell antagonistischen Transkriptionsfaktors zu E2-2, *inhibitor of DNA binding 2* (ID2), induzieren. Interessanterweise war die Expression von ID2 in Knochenmarkskulturen unter Hypoxie induziert. Wurden jedoch Knochenmarkstammzellen von HIF-1 $\alpha^{fl/fl}$ LysM-Cre Mäusen, bei denen die Expression von HIF-1 in pDC-Vorläuferzellen ausgeschaltet ist, mit Flt3-L unter Hypoxie generiert, so war die Differenzierung zu pDC wiederhergestellt, die Expression von E2-2 normalisiert und die Induktion von ID2 unterdrückt. Zusammenfassend kann also gesagt werden, dass die Hypoxie-induzierte Aktivierung von HIF-1 die Differenzierung von pDC unterdrückt, wahrscheinlich in Abhängigkeit von ID2, was die Expression des pDC-

spezifischen Transkriptionsfaktors E2-2 verhindert. Hypoxie ist ein wichtiger Faktor der Mikroumgebung vieler pathologischer Zustände/Erkrankungen wie z.B. Schlaganfall, Herzinfarkt und Krebs. In Tumoren ist Hypoxie einer der Tumor-induzierten Stressfaktoren, die die Anti-Tumor-Immunantwort negativ beeinflussen. Da pDC eine potente Anti-Tumor-Immunantwort bewirken können, diese jedoch *in vivo* oft unterbleibt, könnte der hier aufgezeigte Mechanismus für das Verständnis der Hypoxie-induzierten Immunsuppression hilfreich sein und zur Entwicklung neuer innovativer Immuntherapien gegen Tumore beitragen.

Neben Hypoxie tragen viele andere Faktoren zur Immunsuppression in Tumoren bei. Diese intrinsische Immunsuppression ist eines der größten Hindernisse für die erfolgreiche Therapie von Tumoren, vor allem von soliden Tumoren. So wird z.B. der Erfolg einer Immuntherapie mit *ex vivo*-aktivierten DC oder T Zellen durch immunsuppressive Faktoren der Tumormikroumgebung gemindert. Obwohl es in den letzten 10 Jahren einige Fortschritte gegeben hat, sind die Mechanismen wie die Immunsuppression in Krebspatienten induziert und reguliert wird weiterhin weitestgehend unklar. Eine Komponente der Mikroumgebung in Tumoren ist das Vorhandensein sterbender Tumorzellen. Besonders physiologischer Zelltod, Apoptose, von Tumorzellen findet, im Kontrast zur generellen Sicht von Tumoren als Apoptose-resistente Entitäten, im Überfluss statt. Die Präsenz von sterbenden Tumorzellen kann dann durch konventionelle TumortheraPIen wie Chemo- oder Radiotherapie noch stark erhöht werden. Apoptotische körpereigene Zellen unterdrücken unter physiologischen Bedingungen das Immunsystem. Deshalb könnte das Freisetzen von apoptotischem Material oder die Sekretion von Faktoren aus sterbenden Tumorzellen in den Tumor selbst oder in assoziierte Lymphknoten einen starken Einfluss auf die Funktion von professionellen Phagozyten wie z.B. DC und die damit verbundene Aktivierung von tumoriziden Lymphozyten haben.

Zweites Ziel der vorliegenden Arbeit war es, den möglichen immunsuppressiven Einfluss von apoptotischen Tumorzellen auf die Funktion humaner mDC zu untersuchen. Humane, aus Monozyten hergestellte mDC

wurden zu diesem Zweck mit Überständen lebender, apoptotischer oder nekrotischer humaner Brustkrebszellen inkubiert, welche sowohl Fragmente apoptotischer Zellen (AC) als auch von AC freigesetzte Mediatoren enthalten. Solcherart aktivierte mDC wurden im Anschluß mit autologen T Zellen ko-kultiviert. Danach wurde das Potential der ko-kultivierten T Zellen zum Abtöten lebender Tumorzellen analysiert. Interessanterweise stattete die Aktivierung mit Überständen lebender Tumorzellen humane mDC mit der Fähigkeit aus tumorizide T Zellen zu induzieren, wohingegen die Aktivierung mit Überständen apoptotischer Tumorzellen diese Fähigkeit stark unterdrückte. Ko-Kultur von AC-aktivierten mDC mit autologen T Zellen resultierte in der Ausbildung einer Population von regulatorischen T Zellen (Treg), die durch die gleichzeitige Expression der Oberflächenmoleküle CD39 und CD69 charakterisiert war. Diese Treg Zellen waren kritisch für die Unterdrückung der Aktivierung von zytotoxischen T Zellen. Dies wurde durch Depletions- und Transferexperimente belegt. Depletion der CD39- und CD69-exprimierenden Treg Zellen aus AC-aktivierten Ko-Kulturen resultierte in der Aktivierung von T Zellen, welche effizient lebende Tumorzellen lysierten, und Zugabe der Treg Zellen zu Ko-Kulturen von mit lebenden Tumorzellen aktivierten mDC und autologen T Zellen unterdrückte die sonst ausgeprägte Generierung zytotoxischer T Zellen.

Die Ausprägung der CD39- und CD69-exprimierenden Treg Zell-Population war abhängig von der Freisetzung des bioaktiven Lipids Sphingosin-1-Phosphat (S1P), welches den S1P-Rezeptor 4 auf mDC aktivierte. Nach S1PR4 Aktivierung setzten mDC das immunregulatorische Zytokin IL-27 frei. Neutralisierung von IL-27 in AC-aktivierten Ko-Kulturen von mDC und T Zellen blockierte die Generierung von CD39- und CD69-exprimierenden Treg Zellen und resultierte deshalb in der Aktivierung zytotoxischer T Zellen. In einem nächsten Schritt wurde der Mechanismus der Treg Zell-induzierten Hemmung zytotoxischer T Zellen untersucht. Die Bildung von Adenosin in den Ko-Kulturen und die Aktivierung des Adenosin-Rezeptors A2a, potentiell auf zytotoxischen T Zellen, waren hierfür vonnöten. Erste Experimente lieferten Hinweise auf eine direkte Interaktion von CD69- und CD39-exprimierenden Treg Zellen mit CD73-exprimierenden zytotoxischen T Zellen. Da CD39 und

CD73 für die Bildung von Adenosin aus ATP benötigt werden, könnte die Interaktion von Treg Zellen und zytotoxischen T Zellen diese erst ermöglichen, was in der Folge in der Hemmung zytotoxischer T Zellen resultiert. Diese Beobachtungen können dem Verständnis von Mechanismen der Immunsuppression dienlich sein und könnten Hinweise zur Unterstützung einer effektiven Tumor-Immuntherapie liefern.

Zusammenfassend zeigen die hier präsentierten Ergebnisse wie Faktoren der Tumormikroumgebung die Funktion von humanen DC Subtypen beeinflussen können. Ein Verständnis der zugrundeliegenden Mechanismen kann wertvolle Informationen für die Wahl effektiver Immuntherapien oder Chemotherapien liefern und so die Therapie humaner Tumore unterstützen.

3 Introduction

3.1 The inflammatory tumor microenvironment

A growing tumour is constantly challenged by the immune system. Tumour cells exhibit certain unique alterations in surface antigens, metabolic output and release of peptide or lipid factors. Such factors released by tumour cells are shed into the tumour microenvironment or dumped into the draining lymph nodes. Ideally, these biochemical messages are used by immune cells to start and synchronise a tumour elimination network that include antigen-presenting and effector cells.

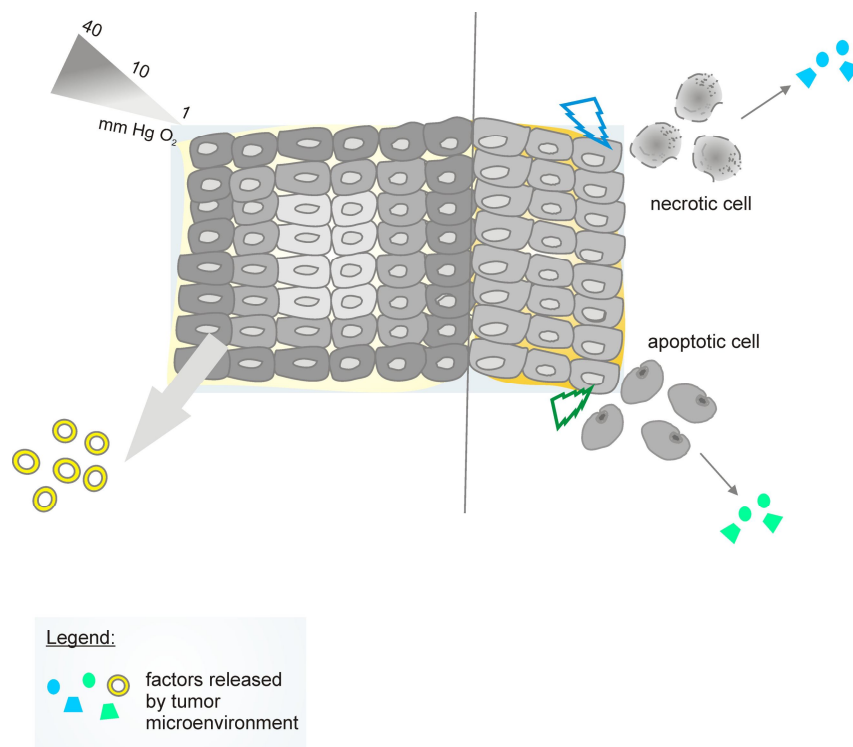


Figure 1: Tumour microenvironmental stress factors. A growing tumour exhibits stress factors such as: *left* an area with oxygen content as low as 1 mmHg at its core. Hypoxic tumour cells thus formed secrete various chemokines and cytokines that influence immunity; *right* Dying tumour cells are generated due to the tumour growth process or due to cancer-eradication treatments such as chemo- or radiotherapy. These tumour cells may undergo necrotic or apoptotic cell death thereby releasing respective immunomodulatory factors into the tumour microenvironment and the circulation.

However, in order to avoid their eradication, tumour cells have evolved strategies, which are largely dictated by their microenvironmental status. In this regard, stress factors that are most abundant in the tumour bed are the presence of 1) hypoxia and 2) dying tumour cells. Under these specialized conditions, the tumour sheds many factors that recruit immune cells from the bone marrow or from the circulation (**Figure 1**).

A growing tumour may secrete soluble interleukins, cytokines and chemokines (**Figure 2**). Factors such as monocyte chemoattractant protein-1 (MCP-1), colony stimulating factor-1 (CSF-1), vascular endothelial growth factor-A (VEGF-A), TNF α , and stromal cell derived factor-1 alpha (SDF-1 α) are secreted by hypoxic tumour cells to attract myeloid cells in general. Specifically, regulated upon activation, normal T-cell expressed and secreted (RANTES) and MCP-1 attract macrophages, β -defensin attracts mDC, IL-8 attracts mainly monocytes, chemokine (C-X-C motif) ligand 5 (CXCL5) recruits granulocytes [1] and CXCL12 attracts pDC [2]. Lymphocytes (NK cells, T cells, B cells) are also recruited by the tumour. For instance, tumour-secreted ligands binding to C-C chemokine receptor type 5 (CCR5) (chemoattractants MCP-2, MIP-1 α/β , RANTES) or CXCR3 (chemoattractants CCL9/10) on T cells recruits them to the tumour microenvironment [3]. In addition, a tumour under hypoxic stress releases VEGF, which promotes neo-angiogenesis during which, recruitment and proliferation of endothelial cells secures blood supply to the growing tumour.

Of all the immune cells that infiltrate tumour tissues or lymph nodes of tumour-bearing animals/patients, antigen presenting cells (APC) such as DC are crucial in modulating immunity. DC are phagocytes that fulfil various tasks in immunity. They shape the tumour immunity towards anti-tumour inflammation or tolerance, depending on the microenvironmental factors that they are exposed to.

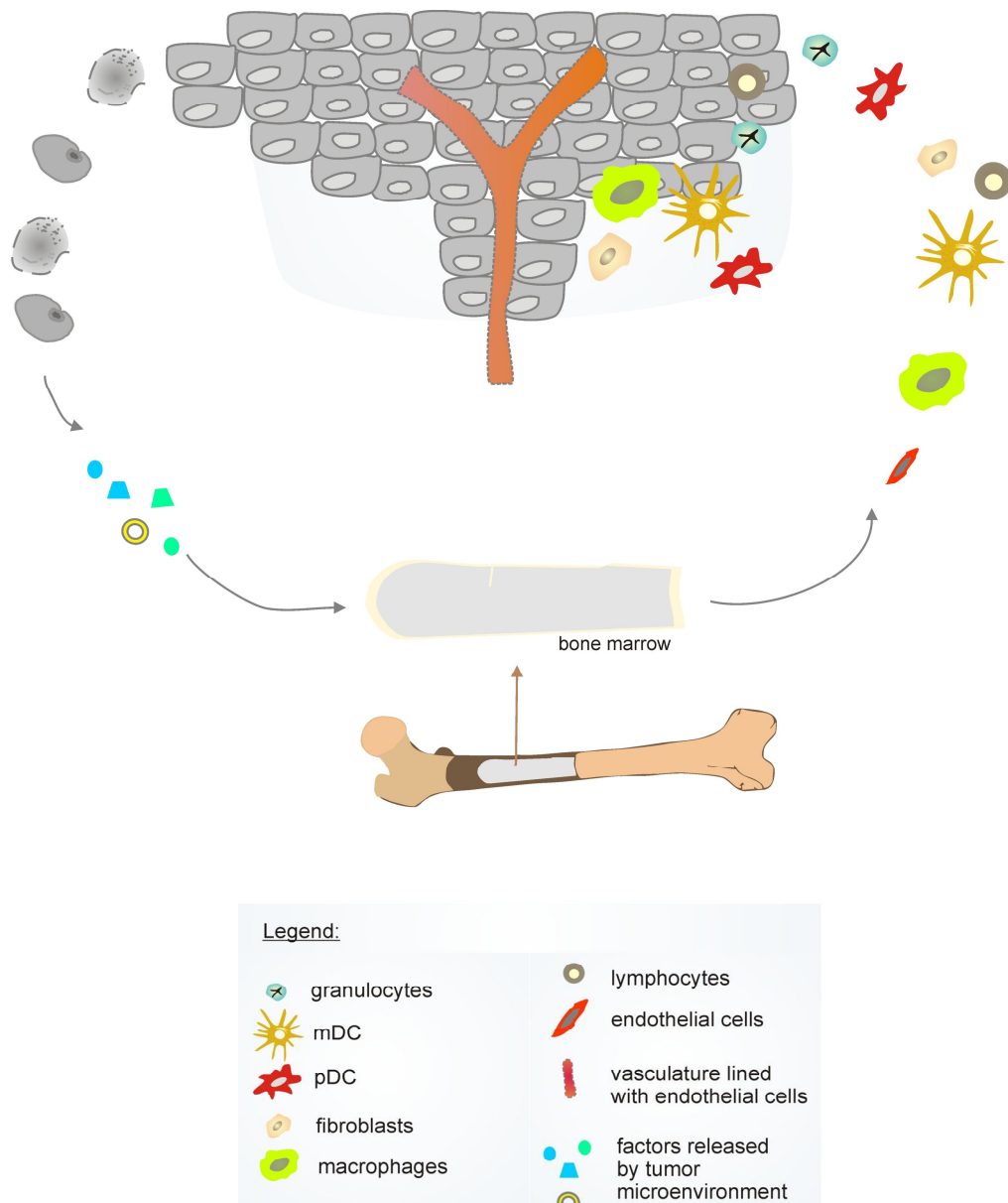


Figure 2: Immune cells infiltrating the tumour microenvironment. *From top left:* Tumour shed cytokines and chemokines which attract various immune cell populations from the bone marrow or bloodstream. These immune cells include lymphocytes such as NK, T and B cells and myeloid cells such as granulocytes, monocytes, macrophages or mDC. In addition, pDC and fibroblasts are also recruited to the tumour bed. The tumour needs to develop vasculature to support the newly proliferating tissue. For this purpose, the tumour sheds factors that attract endothelial cells.

3.2 Dendritic cells

The interaction pattern of living organisms amongst each other extends beyond a predator-prey relationship to include an internal 'sensing-reacting' relationship. This interaction is brought about by a highly evolved network of immune cells. Higher organisms are constantly confronted with externally-derived antigens that can be microbial or viral, or self-antigens that are e.g. tumoural in nature. For eradication of the invaders, the cells of the immune system have evolved a repertoire of receptors to 'sense' the antigens and engulf them through sophisticated antigen uptake machinery. After which, these cells aptly termed APC, train the effector immune cells to 'react' and mount an immune response against the antigen-bearing invaders. This ultimately leads to the eradication of the latter. Antigen sensing and presentation are the two key functions of these specialized cells that include macrophages and DC. DC are the professional APC of the immune system that link the innate and adaptive immunity. DC display a wide array of antigen-capturing molecules on their surface and in intracellular compartments. For instance, molecules such as TLR4 on the surface of DC serve to capture microbial antigens such as lipopolysaccharide (LPS) or intracellular molecules like TLR7/9 recognize CpG sequences in bacterial genomes or viral DNA/RNA. In addition to capturing antigens and presenting them to effector T cells of the adaptive immunity, DC are also important for B cell activation, proliferation and antibody production [4].

3.3 DC subtypes and their role in immunity

DC are highly plastic cells that appear in the 'twilight zone' of the immune system, under more than one classification of immunity. 1) DC bridge the interface between peripheral tissues and lymphoid tissues, 2) depending on the environment that foster them, they can be immunostimulatory or tolerogenic in nature. DC exert multiple roles in immunity (**Figure 3**) that include activation of innate immune cells, antigen-presentation to T cells, mounting immunological tolerance and anti-viral responses.

The varied functions performed by DC are possible due to the division of labour between cellular DC subsets which are specialized to perform distinct functions. Myeloid DC (mDC) are key players in immunity against bacteria or tumours. They produce pro-inflammatory cytokines and perform antigen presentation [5]. In contrast, plasmacytoid DC (pDC) are the producers of type I interferons (IFN- α/β) in response to viral infection. On the one hand, pDC maintain the immune system by activation of NK cells, influencing the primary antibody response [6] and by causing bystander mDC activation [7]. On the other hand, pDC are less efficient in priming antigen specific T cells compared to mDC [8] and favour the generation of regulatory T cells (Tregs) [9].

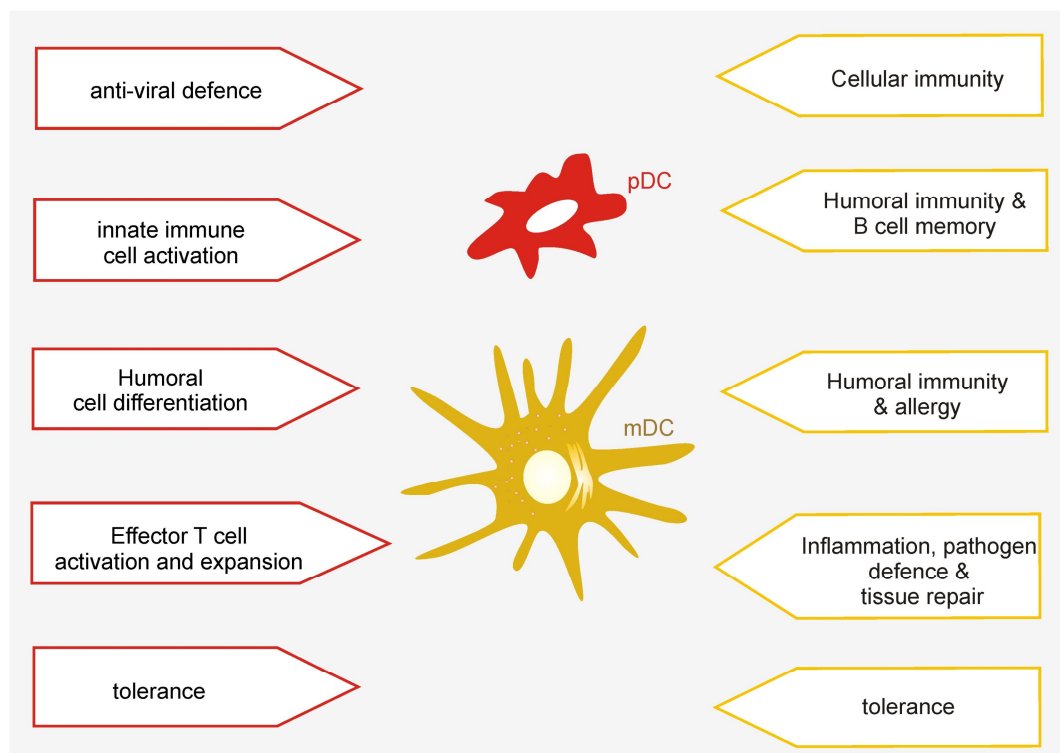


Figure 3: DC play multiple roles in immunity. These functions are shared between the DC subsets. Myeloid DC (yellow) have important functions (depicted as yellow-lined boxes) in cellular immunity, humoral immunity, allergy, tissue repair and tolerance. Plasmacytoid DC (red) play a role (depicted as red-lined boxes) principally in anti-viral defence but also aid in innate immune cell activation as well as humoral cell and effector T cell expansion.

3.4 Role of mDC in effector immunity

mDC play a plethora of roles in immunity that makes them the professional antigen-presenting cells that ideally participate in anti-tumour immunity. Most importantly, they are committed to all facets of effector immunity including T cell and B cell function (**Figure 4**).

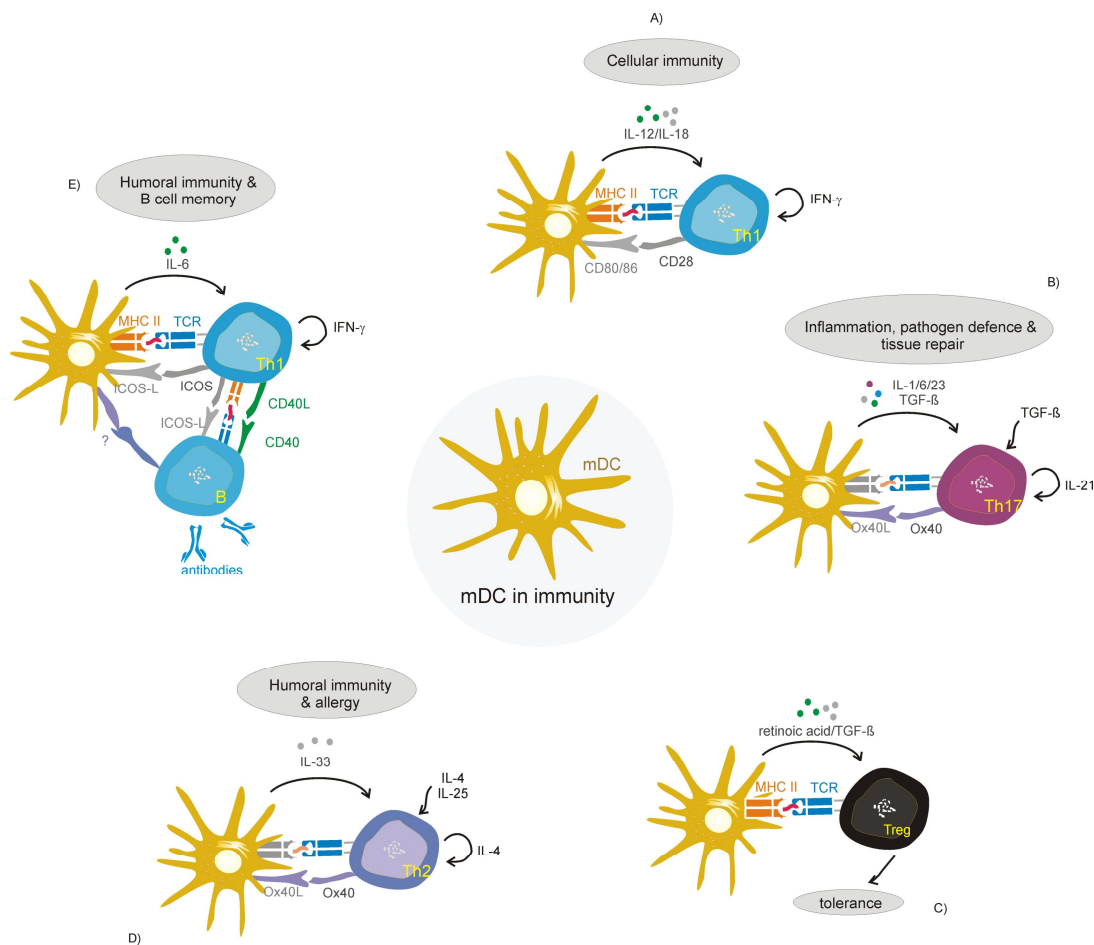


Figure 4: Role of mDC in effector Th immunity: The function of mDC in effector Th immunity can be outlined as follows. Clockwise from top: A) mDC participate in T cell immunity as follows: by means of MHC class II molecule interactions with T cells and CD80 molecules activated Th1 cells to produce IFN- γ . The IL-12/IL-18 produced by the mDC aids in activating the Th1 cells; B) mDC activate TH17 cells by means of Ox40L-Ox40 interactions and by means of IL-1/6/23 production. Th17 cells thus activated participate in tissue repair, pathogen defence and inflammation; C) mDC encourage differentiation of antigen-specific Treg; D) mDC produced IL-33 helps in differentiation of IL-4 producing Th2 cells. These T cells participate in mounting allergic responses; E) In addition to the role in T cell immunity, mDC also participates in humoral or B-cell immunity. mDC in co-operation with IFN- γ producing Th1 cells, induce antibody-production in B cells.

3.4.1 mDC in tumour tolerance induction

According to the theory of immunosurveillance, new cancer cells arise and these 'altered' cells are destroyed by the immune system, preventing the tumour outgrowth. To escape its elimination, a growing tumour activates the immune system in ways to ensure its own survival and further on, encourage its invasion to other areas of the body. Polarization to a tumour-supportive state can be principally observed for every immune cell population, including APC of the innate immune system such as macrophages [39] or DC [40]. These phagocytes program the cells of the adaptive immunity [41] to selectively induce immunosuppression and thereby dampen the inflammatory anti-tumour attack. This principle is exemplified for Treg cells in this study.

3.4.2 mDC and T cell interaction

DC undergo maturation, in order to be functionally active. Such mature DC present antigen to effector cells and produce cytokines to activate immune cells such as NK cells. Initially DC exist in an immature state in peripheral tissues. These immature DC have a capacity to phagocytose bacteria, viruses or tumour antigens or exosomes through pattern recognition receptors present on their surface. Once having phagocytosed, the DC undergo maturation. The maturation process is linked to changes in costimulatory molecules, cytokine production, changes in cytoskeleton, shutting down of the cell cycle and up-regulation of chemokine molecules [42]. During maturation, the changes in the cytoskeleton and chemokine receptor profiles induce DC to migrate to lymph node where they present antigens to T cells.

T cells are thymus-derived white blood cells that play a major role in effector immunity. They exhibit a specialized receptor called the T cell receptor (TCR) that allows them to communicate with phagocytes. Through the TCR, T cells establish contact with the major histocompatibility complex (MHC) molecules on DC. Antigens bound to MHC molecules are then recognized by T cells. Based on their functions T cells can be divided into several subtypes. The

helper T cells (Th) and cytotoxic T cells (Tc) recognize antigens presented by the DC through MHC II [43] or MHC I molecules [44] respectively. Th cells can be subdivided into Th1, Th2, Th17 and Treg depending on their functional profile [45]. They are also called CD4⁺ T cells since they express CD4 molecule on their surface, which is needed as a co-receptor in the TCR-MHC II complex. Th cells can produce cytokines that modulate the immune milieu but cannot kill pathogen-infected cells or aberrantly growing cancer cells. Th1 cells produce cytokines such as IFN- γ that facilitates cellular immunity [46] by activating other immune cells such as NK cells, cytotoxic CD8⁺ T-cells and macrophages. IFN- γ promotes antigen presentation in macrophages and increases expression of MHC molecules, leukocyte migration and expression of intrinsic anti-viral defense factors. Th2 cells participate in allergy and antibody production. Th2 cells produce IL-4 which activates B-cell class switching to IgE and induce their auto-proliferation. IFN- γ and IL-4 are cytokines that participate in T cell immunity by tilting the Th1/Th2 balance [47, 48]. Besides promoting Th1 immunity as described above, IFN- γ suppresses Th2 differentiation which would cause a humoral (antibody) response. IL-4 contributes to anti-inflammatory response by decreasing the production of macrophage and dendritic cell-derived IL-12. Th17 cells are another subtype of Th cells that mainly produce IL-17 and contribute to chronic inflammation and tissue repair. They cause autoimmune responses and in addition, Th17 cells produce IL-22 which is important for defence against pathogens such as *Candida* [49]. Regulatory T cells (Treg) are another subtype of Th cells that are central mediators of immune tolerance. Treg produce TGF- β or IL-10 which keep hyperinflammation in check [50]. Tc or cytotoxic T cells have the capacity to kill pathogen or viral infested cells and cancer cells. They are called CD8⁺ T cells since they express CD8 molecule on their surface, which is a co-receptor in the TCR-MHC I complex. Tc cells produce various molecules such as granzyme or perforin which cause lysis of pathogen-infected or tumour cells [51].

3.4.3 DC-Treg interaction in tumour-bearers

DC dampen anti-tumour immunity among other mechanisms, by generating tumour-specific Treg cells. The Treg cells have been demonstrated to be a major obstacle for anti-tumour immunity [52] due to their role in suppressing anti-tumour immunity. Treg can be primed and activated predominantly in the tumour-adjacent draining lymph nodes (TDLN), by factors shed from the tumour [53] or within the tumour bed itself [54]. Evidently Treg are often detected in the sentinel/regional lymph nodes (LNs) of tumour-bearing hosts that exhibit poor clinical prognosis [55]. Once primed in the TDLN, Treg travel to the tumour site, where they prevent effector T cells from eradicating the tumour and furthermore stimulate metastasis of tumour cells [56]. The aim of adoptive cellular immunotherapy against tumours is to generate tumour-directed cytotoxic T cells. However, the TDLN-derived suppressive Treg can potentially curb the benefit of an adoptive immunotherapy by suppressing the function of transferred or endogenous cytotoxic T cells. In addition, conventional cytotoxic therapy would need an active immune system to keep the residual tumour masses in check, which might be prevented by Treg [57]. Hence, the mechanisms of Treg generation within the TDLN have to be defined in order to design effective therapeutic strategies.

3.4.4 Different states of immunosuppressive DC in tumour-bearing animals

Generation/priming of tumour-specific Treg, requires antigen uptake and presentation by professional APC, i.e, DC. To exhibit their regulatory function, DC probably undergo tumour-dependent phenotypical alterations that enables them to foster immune escape [40, 58]. Initially, DC were thought to promote T cell tolerance due to being trapped in an immature state in tumour-bearing animals. However, it emerges that depending on the tumour microenvironment they are exposed to, DC may exist in different states of maturation, activation, i.e immunostimulatory capacity [59, 60]. Thus, even DC within the tumour might be capable of presenting tumour-derived antigens. Tumour-derived antigens are acquired by DC directly at the tumour site [61],

from metastasing tumour cells [60], or through tumour-released exosomes/microvesicles [62, 63], which are primarily drained to the TDLN.

3.4.5 Uptake of dying tumour cell-derived factors by DC

In addition to antigens, DC receive other tumour-derived signals that shape their phenotype and the subsequent profiling of T cells. A prominent source of such signals are dying tumour or stromal cells that are continuously produced during tumour growth [64] or by conventional cancer-ablation methods such as chemotherapy or radiotherapy. With regard to the immunological outcome, the two extremes are: 1) effective antigen cross-presentation and induction of an inflammatory response elicited by DC that eventually prepares immune effectors to eradicate malfunctioning cells or 2) tolerance to dampen an over-activated immune reaction [65, 66]. The decision towards inflammation *versus* tolerance depends on the surface protein/lipid signatures as well as immune-modulating factors released by dying cells, which are primarily determined by the mode of cell death [67].

3.4.6 Types of cell death

There are two broad classifications of how cells may undergo death. This includes: 1) necrosis, which occurs when a cell is exposed to extreme physiological conditions such as hypoxia/anoxia or hypothermia that leads to rupture of the plasma membrane and release of contents that elicit an immune response; or 2) apoptosis, which occurs under normal physiological conditions ensuring cell turnover and tissue homeostasis (**Figure 5**).

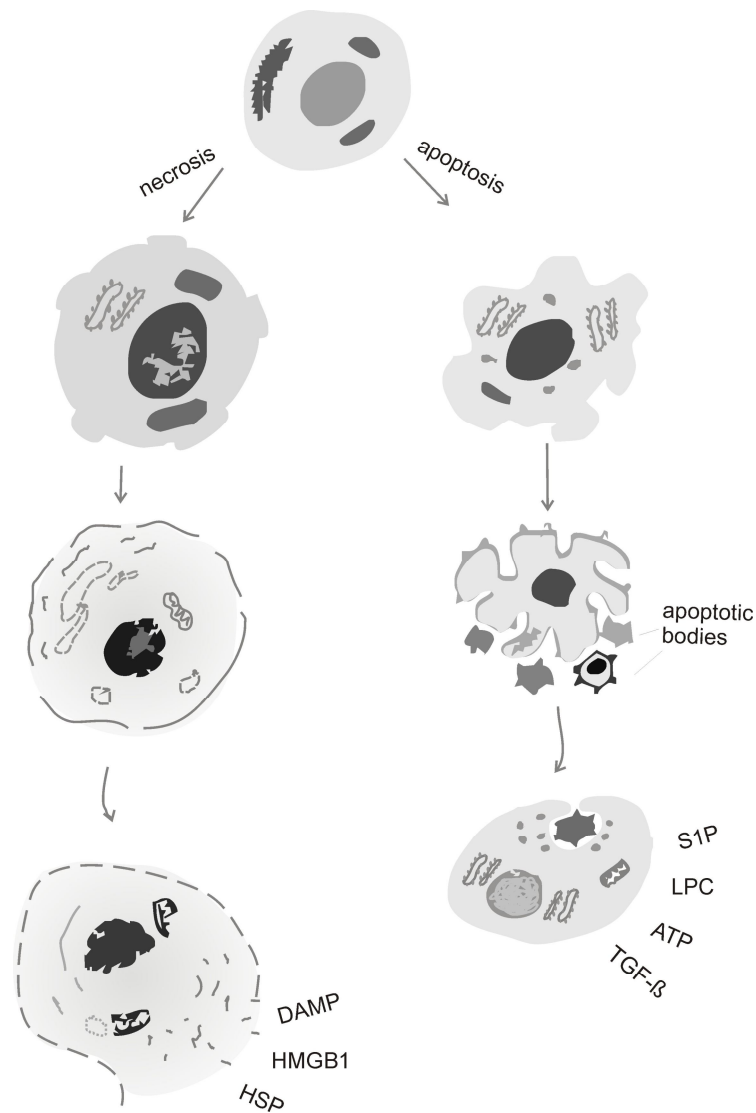


Figure 5: Modes of cell death and the factors released: Cell death can occur in two modes. 1) On left: Necrosis refers to cell death following the introduction of an intense physiological stressor such as hypoxia or hypothermia. Following this the cells undergo necrotic cell death. The characteristic feature of necrotic cell death includes swelling of cells, rupture of plasma membrane, rupture of internal organelles and the release of the cellular contents. Factors released during necrotic cell death may include molecules classified as danger-associated molecular patterns (DAMP) among them heat shock proteins (HSP) or high-mobility group protein B1 (HMGB) or large amounts of ATP. On the other hand cells might also undergo 'physiological' apoptotic cell death as a part of maintaining cell turnover and tissue homeostasis. 2) On right: In this case cells do not swell, but rather shrink. Further the cell blebs, forming apoptotic bodies. The cell undergoes changes in the genetic material such as chromatin condensation, DNA degradation and nuclear fragmentation through activation of specific proteases. This further results in release of lipids such as lysophosphatidylcholine (LPC) or sphingosine-1-phosphate (S1P), anti-inflammatory proteins such as transforming growth factor (TGF)- β as well as nucleotides such as UTP/ATP.

3.4.7 Cell death-induced immune responses

Necrosis induces shedding of danger-associated molecular patterns (DAMPs), which activate corresponding TLRs on DC. For example high-mobility group box 1 (HMGB1) is recognized by TLR2, TLR4 or the receptor for advanced glycation end products (RAGE) on the surface of APC [68]. In contrast, heat shock proteins (HSP) are taken up through scavenger receptors. For apoptosis, the immunological outcome is ambiguous, because of the varying nature of the apoptotic cell surface proteome. These may include ligand-receptor interactions such as phosphatidylserine (PtdSer)-MER/BAI1/ T-cell immunoglobulin- and mucin-domain-containing molecule-4 (TIM-4), intercellular adhesion molecule-3 (ICAM-3)-CD14 or milk fat globule-EGF factor 8 (MFG-E8)-lipid rafts between apoptotic cells and phagocytes respectively. In addition, apoptotic cells shed lipids, nucleotides and other immunomodulating factors that interact with the DC by means of appropriate receptors [69]. Apoptosis can be immunogenic as demonstrated by an increase in antigen-cross-presentation and the induction of cytotoxic T cells upon priming with AC *in vivo* [70]. On the other hand, triggering of multiple immunosuppressive pathways upon priming with AC has been recognized [71]. In case of cancer-ablation treatments such as chemotherapy, the decision towards generating an anti-tumour response or tolerance might be determined by the drug being used, as recent evidence suggests that certain chemotherapeutic drugs such as oxaliplatin trigger immunogenic cancer cell death [72]. However, cross-presentation of AC-derived antigens after chemotherapy does not necessarily culminate in anti-tumour immunity [73]. Interestingly, forced expression of (heat shock proteins) HSP, which are usually present on necrotic cells, can render AC immunogenic [74].

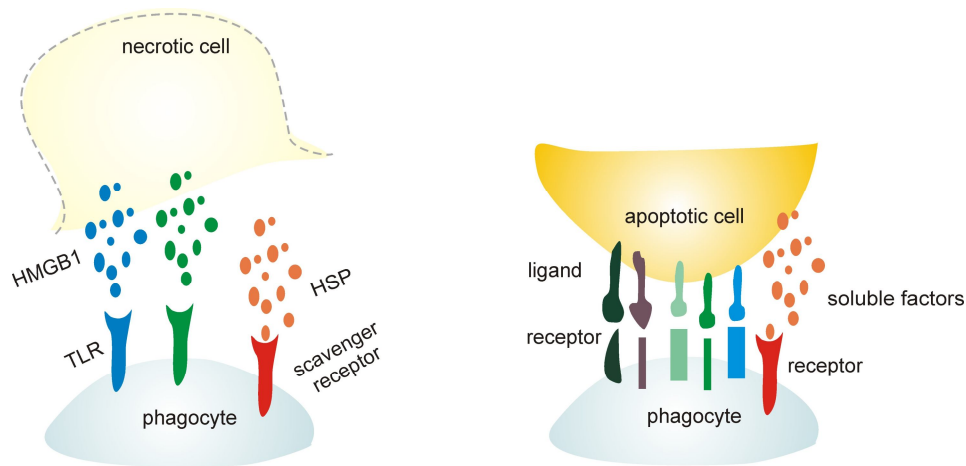


Figure 6: Exposure of phagocytes to NC or AC-derived signals. Left: The signals released from necrotic cells (NC) are usually factors such as HSP, HMGB1 or DAMP those are sensed by DC. Right: Apoptotic cells expose ligands such as PtdSer, ICAM-3, MFG-E8, between which interact with receptors TIM-4, CD14 or rafts on the surface phagocytes. In addition apoptotic cells may shed soluble factors such as lipids LPC or S1P that are taken up by the phagocytes.

Studies have focused on immunogenicity of surface alterations on dying cells. However, the signalling molecules secreted from dying cells that drain the adjacent lymph nodes together with tumour antigens may also be important for inducing tolerance and possibly favour relapse [53]. AC secrete immunomodulators in a regulated manner, among them lipids such as lysophosphatidylcholine (LPC) or sphingosine-1-phosphate (S1P), anti-inflammatory proteins such as transforming growth factor (TGF)- β as well as nucleotides, which have the capacity to modify DC-dependent immunity [67] (Figure 6).

3.5 pDC roles in immunotherapy

Myeloid DC have been widely used in immunotherapy against cancer at least in model systems [10]. Furthermore, the use of the viral mimetic CpG that activates pDC or using pDC themselves along with mDC in cancer therapy resulted in favourable outcomes [11, 12]. In addition, IFN- α production by pDC was required to cause tumour rejection by the immune system [13]. On the other hand, pDC might also have a tumour-inducing capacity, which could

offset promising therapeutic implications [14]. On the contrary, the ‘tolerance-inducing’ properties of pDC (**Figure 7**) were harnessed for therapy in diseases such as allograft rejection [15] or rheumatoid arthritis [16].

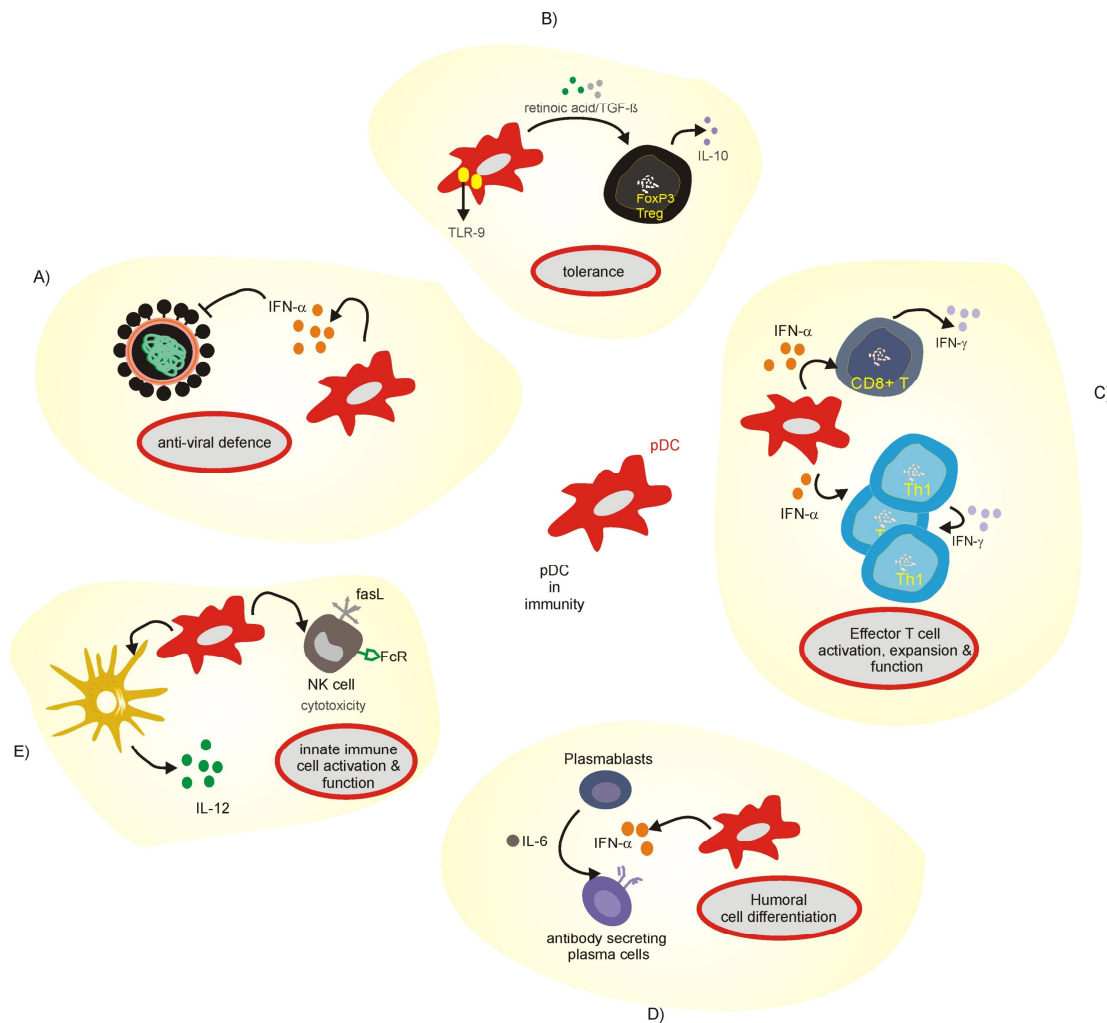


Figure 7: pDC roles in immunity: The functions of pDC in modulating immunity can be viewed in detail as follows: (clockwise from left) A) pDC are the vital immune cells in the body that are involved in anti-viral defence. Upon virus instigated TLR-9 activation, pDC drive IFN- α -dependent inflammation. pDC are the principal producers of IFN- α and together with production of IL-12 they activate Th1 immunity; B) pDC produce TGF- β or retinoic acid which help in differentiation of FoxP3-expressing regulatory-T cells (Treg). These Treg in turn produce immunosuppressive IL-10 thereby encouraging tolerance; C) The IFN- α produced by pDC can activate CD8⁺ T cells and likewise Th1 cells to produce IFN- γ . Thus pDC play a vital role in expanding and/or, activating T cells; D) In addition pDC-produced IFN- α helps in differentiation of antibody-secreting plasma cells from precursor plasmablasts; E) finally pDC are crucial for innate immune cell activation. pDC encourage IL-12 production by mDC and enhance the cytotoxic function of NK cells.

The importance of pDC in research and therapy necessitates a system to generate pDC equivalents from easily available sources in humans. In

addition, these cells are rare in human blood forming up to 0.32% of all immune cells in peripheral blood [17]. In addition, if such pDC-like cells could be manipulated during their development, they might be engineered according to specific therapeutic needs.

3.6 DC development

3.6.1 Precursors involved in DC subset development

In order to understand DC function or to generate functional subsets for cellular therapy *in vitro*, it is necessary to understand the biology and classification of DC precursor development. Hematopoiesis is the process responsible for generation of the various cells that make up the blood. The principal precursors are called hematopoietic stem cells (HSC). They have an innate capacity to give rise to different progenitor cells which include common myeloid progenitors (CMP) or common lymphoid progenitors (CLP). These ultimately give rise to the different immune cell populations. For example downstream of CMP, 1) erythropoiesis gives rise to reticulocytes and erythrocytes, 2) thrombopoiesis gives rise to thrombocytes, 3) granulopoiesis gives rise to basophils, neutrophils and eosinophils, 4) Mast cells form directly from CMP and 5) monocytopoiesis gives rise to monocytes and myeloid DC. Downstream of CLP, lymphopoiesis takes place giving rise to: 1) B lymphocytes or plasma cells, 2) T lymphocytes and 3) lymphoid DC. Thus, DC precursors are also formed as a result of hematopoiesis in the bone marrow.

Classically, the development of DC subsets was assumed to result from radically different precursor sources. mDC were reported to develop from myeloid precursors and the development of pDC was assumed to be entirely lymphoid. However, recently common progenitors were identified for both mDC and pDC. Whereas HSC-derived multipotent progenitors give rise to either CMP or CLP, both these progenitors were able to generate pDC [18]. Interestingly, at least in the mouse, the functions of common myeloid progenitor (CMP)-derived and common lymphoid progenitor (CLP)-derived

pDC were found to be distinct. Whereas CLP were prone to pDC generation, thus yielding higher numbers of pDC, MP developed faster into pDC which also produced higher levels of IFN- α [19]. In addition following another, more recent hypothesis, the common precursor of DC subtypes can be a myeloid progenitor-monocyte/DC progenitor (MP-MDP) or yet another unidentified progenitor further downstream of MP-MDP. Following the current perception, the MP-MDP then give rise to respective mDC or pDC precursors [20] (**Figure 8**). To add further complication to the whole scenario, the above described theories may be true for DC development only in mice. DC development in humans may operate independently of conventional myeloid or lymphoid pathways [21].

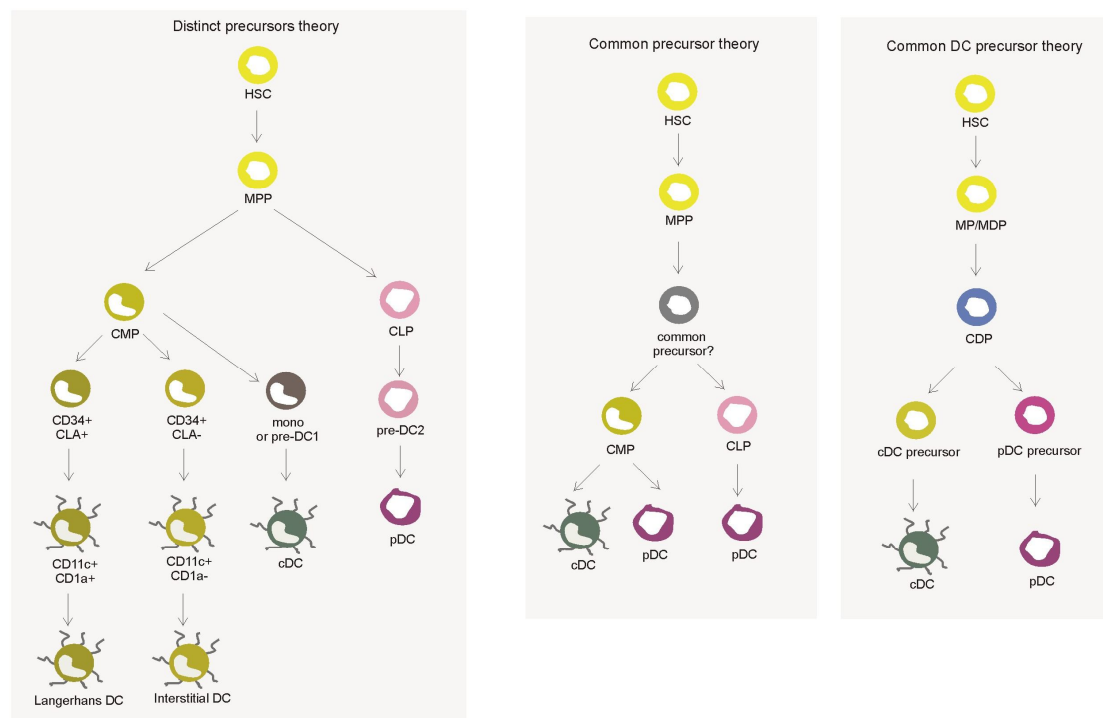


Figure 8: DC subset development theories: (Left) Distinct precursor theory: This classical theory suggests that the DC subsets arise from distinct precursors. Hematopoietic stem cells (HSC) give rise to multipotent progenitor (MPP) which forks into two distinct precursors - the common myeloid precursor (CMP) and the common lymphoid precursor (CLP). The CMP gives rise to Langerhans DC, interstitial DC or cDC through a series of steps involving one or two precursors. In detail, cDC arise from pre-DC1 or monocytes under the CMP precursor pathway. pDC arise from the CLP arm through a pre-DC2 precursor. (Middle) The common precursor theory suggests that a common precursor downstream of the HSC-MPP pathway differentiates to either CMP or CLP. cDC arise from CMP, whereas pDC arise from both CMP and CLP. (Right) The common DC precursor theory suggests that a common DC progenitor (CDP) differentiating along the myeloid progenitor-monocyte/DC progenitor (MP)-(MDP) pathway is responsible for cDC or pDC differentiation from respective precursors.

3.6.2 Cytokines that shape pDC development and the myeloid progenitor hypothesis

A crucial determinant for pDC generation is the Fms-related tyrosine kinase 3 ligand (Flt3-L). Flt3-L overexpressing transgenic mice had increased numbers of pDC, whereas Flt3-L deficient mice had less [18]. Importantly, the administration of Flt3-L to humans led to increased numbers of peripheral pDC [22]. Common precursors for mDC and pDC were identified as common pro-DCs in the mouse bone marrow [18]. Also, Flt3^{high} and Flt3^{low} CD34⁺ progenitor cells, isolated from human bone marrow, were described. CD14⁺ monocytes were the major cell type generated from Flt3^{high} cells, whereas cells generated from Flt3^{low} cells were mainly erythroid cells [23]. Furthermore, Flt3 was detected on a subset of CD34⁺ CD14⁺ CD64⁺ monocytic precursors in addition to being detected on a subset of CD34⁺ CD38⁻ bone marrow cells and CD34⁺ CD19⁺ B lymphoid progenitors. Thus, it is tempting to speculate that administration of Flt3-L to humans results in high pDC numbers which are mobilized to differentiate along the myeloid lineage. Interestingly, monocytes are easily available myeloid-derived cells in human peripheral blood. This opens the possibility to employ them for pDC generation. Besides Flt3-L, GM-CSF might be important for pDC generation. pDC progenitors were less in Flt3-L-deficient mice as compared to GM-CSF-deficient mice, and interestingly the latter had less pDC progenitors than wildtype mice [24].

3.6.3 Transcriptional machinery involved in pDC development

The basic helix-loop-helix transcription factor E2-2 was recently defined as the critical pDC lineage-determining transcription factor in humans and mice [25]. E2-2 haploinsufficiency in humans leads to the development of a condition called the Pitt-Hopkins syndrome characterized by cranio-facial/neural abnormalities, mental retardation and motor dysfunction. In addition, such individuals exhibit a reduced capacity to fight viral diseases due to decreased number of pDCs and an impaired type I IFN production/response of these

cells [25]. E2-2 is inhibited by ID proteins (inhibitor of differentiation/DNA binding) [26]. Of this protein family, ID2 was found to be essential for mDC development, but loss of ID2 did not affect pDC development [27]. In addition, genes that are enriched in pDC such as SpiB, Irf7 and Irf8 are under the transcriptional control of E2-2 [25] (**Figure 9**). SpiB, which was considered to be the crucial pDC determining factor, serves to suppress ID proteins and additionally requires E2-2 to determine pDC development [28]. Importantly, E2-2 is also required to maintain the function of pDC after they are generated [29].

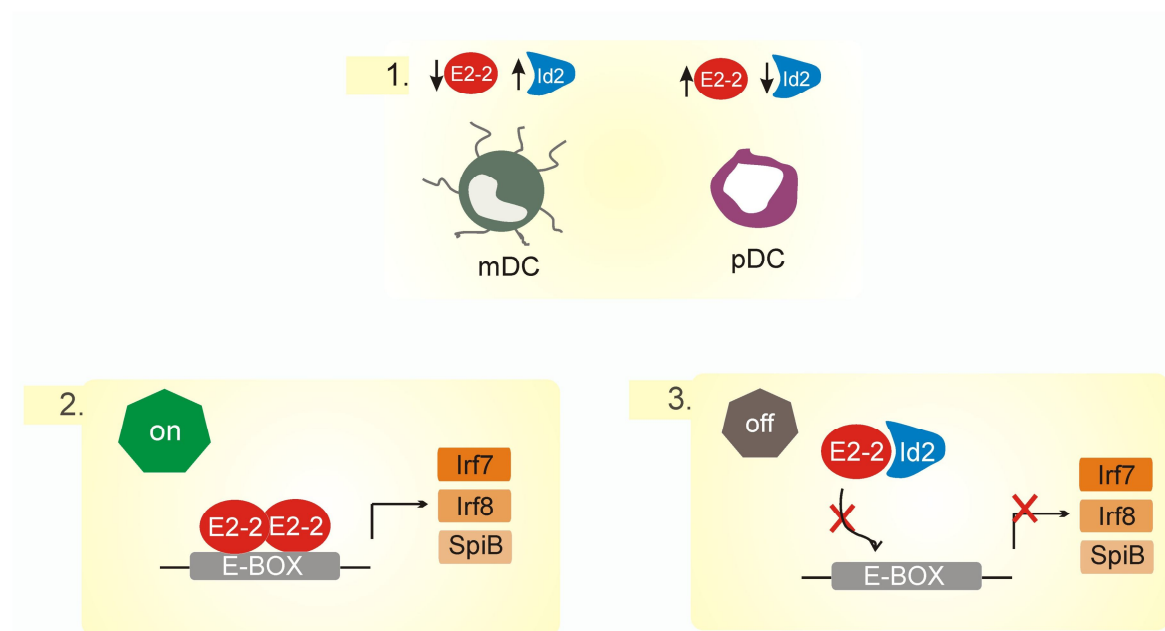


Figure 9: Transcription factors (TF) involved in pDC development. A) TF profile in DC subsets: mDC express high levels of ID2 and do not express E2-2. This is in contrast to pDC which express high levels of E2-2 but a low ID2; B) E2-2 is a TF that is crucial for pDC development. The TF is active as a dimer. An active E2-2 dimer binds to E-Box element in genes such as Irf-7/8, Spi-B and activates their transcription; C) In the presence of E2-2 inhibiting protein ID2, E2-2 monomers are not able to dimerize, which is required to initiate transcription. In this case the E-Box is not occupied by the E2-2 dimer and gene expression is switched off. Therefore in the presence of high levels of ID2, the E2-2 dependent transcription of pDC-defining genes is shut down, thereby inhibiting pDC function and differentiation.

3.6.4 Hypoxia as a microenvironmental factor in hematopoiesis

In addition to its effects regarding angiogenesis and modulation of immune responses, hypoxia may also participate in hematopoiesis in the bone marrow. The oxygen content (O_2) in the bone marrow may range from close to anoxia (0%) to 6% as opposed to a well oxygenated tissue such as the blood, where O_2 levels range from 4% to 14% [30, 31]. The O_2 -gradient within the bone marrow is a determining factor for either keeping hematopoietic stem cells (HSC) in a low-replicating pluripotent state or to induce differentiation along the hematopoietic lineage. HSC are located in an extremely hypoxic niche as demonstrated by dye-perfusion and engraftment studies [32, 33]. The primary hypoxia-induced transcription factors, the hypoxia-inducible factors (HIF)-1 to 3 are stabilized under low O_2 concentrations. They are heterodimers consisting of a variable O_2 -sensitive α subunit and a stable common β subunit, also known as aryl hydrocarbon receptor nuclear translocator (ARNT) [34]. Both HIF-1 and HIF-2 were recently connected to HSC biology. HIF-1 is needed for HSC quiescence in their hypoxic niche [35], whereas HIF-2 is activated downstream of STAT5 in HSC to maintain their self-renewing capacity [36]. Beside HSC maintenance, HIF-1 plays a major role in hematopoiesis in embryos [37] and in the adult organism [38]. However, whether HIFs affect myeloid cell development in the adult bone marrow of mammals was unknown.

3.7 Aims of this study

Tumour antigens are recognized by APC, which take up and present the antigens to effector cells. These effector cells then ideally eradicate the tumour. In patients that develop a clinically detectable tumour, the immune status is dysregulated. Most often they exhibit increased levels of alternatively activated APC such as DC and regulatory T cells. These together suppress anti-tumour immunity.

Dendritic cells act as professional APC that are central in regulating various immune processes including tumour immunity. The ability of DC to perform opposing functions spans across the whole immune spectrum, including antigen presentation and immune cell activation, anti-viral immunity, tolerance induction or tissue repair. These functions are met by at least two distinct DC subsets. The unique property of mDC to activate effector T cells towards tumour killing made them likely candidates for use in cancer immunotherapy. Whereas the generation of mDC generation *in vitro* has been long established, a similar protocol to generate pDC was lacking. Hence, the first part of the thesis, addresses the aim of establishing a protocol to generate pDC equivalents from an easily and abundantly available source, so that they might be studied under the influence of tumour microenvironmental factors such as hypoxia or dying tumour cells. Since monocytes meet the criteria for the latter, we asked if they could be harnessed for generation of pDC-like cells. Further on, the mo-pDC thus generated had to be characterized in detail to identify similarities to their physiological counterparts or to check in which features these cells behaved differently to primary pDC. Therefore, mo-pDC were characterized along these levels: 1) lineage-determining transcription factor profile, 2) specific surface markers and 3) functional profile. The mo-pDC differentiation was also studied under the tumour stress factor hypoxia. Interestingly, the bone marrow exhibits a low-oxygen environment as opposed to other tissues. Therefore, we also asked for the impact of hypoxia on pDC generation from mouse bone marrow precursors to support findings in from the studies with human cells as outlined above. Of particular interest was the

impact of the hypoxia-induced transcription factor HIF-1, which we investigated by using bone marrow from conditional HIF-1 α -deficient mice.

In order to keep immune hyperinflammation in check, the immune system has evolved a regulatory network that shuts down its over-activation. This includes the APC that produce regulatory cytokines such as IL-10 or TGF- β to limit inflammation. In addition, these alternatively activated APC modulate effector immunity to mount tolerance. By way of producing tolerance-inducing factors, cancer cells use this APC-effector regulatory network to their benefit. At the top of the trigger of this regulatory network lie tumour microenvironmental stress factors such as hypoxia or the presence of dying cells. Therefore, in the second part of the thesis we focused on elucidating the influence of apoptotic tumour cells on the mDC phenotype with a focus on their ability to shape T cell responses. Since tumour cells are thought to evade immunity by shedding certain factors that mount tolerance, we specifically asked if supernatant of apoptotic tumour cells can prime DC to trigger T cell differentiation that borders along tolerance. T cells were characterized along these levels: 1) cytotoxic function, 2) surface marker profile and 3) secreted cytokines. Indeed, apoptotic tumour cells induced tolerogenic DC that expanded a certain subpopulation of Treg cells. Hence, we investigated the factor released from apoptotic tumour cells that was responsible for this shift in the T cell profile. Also we checked mechanisms how DC achieved Treg generation. Last, we wanted to know how the specific Treg in our system suppressed CD8⁺ T cells from eradicating tumour cells. The impact of adenosine generation was investigated as a candidate responsible for the suppression of cytotoxicity.

4 Materials

4.1 Chemicals and Reagents

The commercially purchased chemicals used were of the highest grade of purity:

β -mercaptoethanol	Sigma-Aldrich Chemie GmbH, Deisenhofen
40% Acrylamide/Bis-acrylamide (37.5% : 1.0% w/v)	Roth GmbH, Karlsruhe
Accutase	PAA Laboratories GmbH, Cölbe
Acrylamide/Bis-acrylamide	Bio-Rad Laboratories GmbH, München
Ammonium chloride (NH ₄ Cl)	Sigma-Aldrich Chemie GmbH, Deisenhofen
Ammonium persulfate (APS)	Sigma-Aldrich Chemie GmbH, Deisenhofen
Brefeldin A	Sigma-Aldrich Chemie GmbH, Deisenhofen
Blocking buffer	Rockland Immunochemicals Inc, Gilbertsville (USA)
Bovine Serum Albumin (BSA)	Sigma-Aldrich Chemie GmbH, Deisenhofen
Bromophenol blue	Fluka GmbH, Buchs
Caspase-3 substrate (Ac-DEVD- AMC)	Alexis Biochemicals, Grünberg
Chloroform	Merk Eurolab GmbH, Darmstadt
Collagenase IA	Sigma, Steinheim, Germany
Dimethylsulfoxide (DMSO)	Roth GmbH, Karlsruhe
Disodium hydrogen phosphate (Na ₂ HPO ₄)	Merck EuroLab GmbH, Darmstadt
Dithiothreitol (DTT)	Roth GmbH, Karlsruhe
DNase I	Promega, Mannheim Germany

Ethanol	Roth GmbH, Karlsruhe
Ethylenediaminetetraacetic acid (EDTA)	Sigma-Aldrich Chemie GmbH, Deisenhofen
HEPES	Roth GmbH, Karlsruhe
Isopropanol	Merck EuroLab GmbH, Darmstadt
L-glutamine	PAA Laboratories GmbH, Cölbe
Lymphocyte separation medium (Ficoll)	PAA Laboratories GmbH, Cölbe
Magnesium chloride (MgCl ₂)	Roth GmbH, Karlsruhe
Magnesium sulfate (MgSO ₄)	Roth GmbH, Karlsruhe
Methanol (MeOH)	Roth GmbH, Karlsruhe
1-Methyl-tryptophan (L/D-1MT)	Sigma-Aldrich Chemie GmbH, Deisenhofen
Milk powder	Merck EuroLab GmbH, Darmstadt
Monopotassium phosphate KH ₂ PO ₄	Sigma-Aldrich Chemie GmbH, Deisenhofen
Neomycin (G 418)	PAA Laboratories GmbH, Cölbe
Nonidet P-40	Sigma, Steinheim, Germany
Oxaliplatin	Sigma, Steinheim, Germany
Paraformaldehyde (PFA)	Sigma-Aldrich Chemie GmbH, Deisenhofen
Phenylmethanesulfonylfluoride (PMSF)	Sigma-Aldrich Chemie GmbH, Deisenhofen
Potassium bicarbonate (KHCO ₃)	Sigma-Aldrich Chemie GmbH, Deisenhofen
Potassium chloride (KCl)	Merck EuroLab GmbH, Darmstadt
Protease inhibitor mix	Roche Diagnostics GmbH, Mannheim
Tetramethylethylenediamine (TEMED)	Sigma-Aldrich Chemie GmbH, Deisenhofen
Tris	Sigma-Aldrich Chemie GmbH, Deisenhofen
Tris buffered saline (TBS)	Sigma-Aldrich Chemie GmbH,

	Deisenhofen
Triton X-100	Sigma-Aldrich Chemie GmbH, Deisenhofen
Trypsin	Sigma-Aldrich Chemie GmbH, Deisenhofen
Tween 20	Sigma-Aldrich Chemie GmbH, Deisenhofen
Sodium chloride (NaCl)	Merck EuroLab GmbH, Darmstadt
Tetraethylendiamine (TEMED)	Roth GmbH, Karlsruhe
Tris-HCl	Roth GmbH, Karlsruhe
Triton X-100	Roth GmbH, Karlsruhe
Tryptone	Sigma-Aldrich Chemie GmbH, Deisenhofen
Tween 20	Roth GmbH, Karlsruhe
Yeast extract	Life Technologies, Scotland

4.2 Buffers and Solutions

Rinsing buffer: (for cell separation) (in PBS)

EDTA	0.5 M
------	-------

Running buffer: (for cell separation) (in PBS)

BSA	0.5%
-----	------

EDTA	0.5 M
------	-------

FACS wash buffer (in PBS)

BSA	0.2%
-----	------

Antibody solution

TBS	50% (v/v)
-----	-----------

Blocking Buffer	50% (v/v)
-----------------	-----------

Tween 20	0.06% (v/v)
----------	-------------

Blocking solution (in PBS)

Triton X-100	0.1%
BSA	3%

10 x blotting buffer (pH 7.4) (in PBS)

Tris-HCl	250 mM
Glycine	1.9 M
pH	8.3
NaCl	137 mM
KCl	2.7 mM
Na ₂ HPO ₄	8.1 mM
KH ₂ PO ₄	1.5 mM

Potassium phosphate buffer (pH 8.5)

KH ₂ PO ₄	1 M
---------------------------------	-----

Lower Tris Buffer (pH 8.8)

Tris/HCl	1.5 M
----------	-------

HIF lysis buffer (pH 8.0)

Tris/HCl	50 mM
EDTA	5 mM
NaCl	150 mM
Nonidet P-40	150 mM
PMSF	0.5 mM
DTT	1 mM
Protease inhibitor mix	1 x

4 x SDS-PAGE sample buffer (pH 6.9)

Tris/HCl	125 mM
10% SDS	2% (v/v)
Glycerol	20% (v/v)
Bromophenol blue	0.002% (w/v)
DTT	5 mM

SDS separating gel (10%)

H ₂ O distilled	4.9 ml
Lower Tris buffer	2.5 ml
40% Acrylamide/Bis-acrylamide (37.5% : 1.0% w/v)	2.5 ml
SDS 10% (w/v)	100 µl
Ammonium persulfate 10% (w/v)	50 µl
TEMED	5 µl

SDS stacking gel (4%) (pH 7.1)

H ₂ O distilled	6.4 ml
Upper Tris buffer	2.5 ml
40% Acrylamide/Bis-acrylamide (37.5% : 1.0% w/v)	1 ml
SDS 10% (w/v)	100 µl
Ammonium persulfate 10% (w/v)	50 µl
TEMED	5 µl
10 x SDS running buffer:	
Tris/HCl	250 mM
Glycine	1.9 M
SDS	7 mM

10 x TBS (pH 7.4)

Tris/HCl	500 mM
NaCl	1.5 M

TE (Trypsin/EDTA in PBS)

Trypsin	0.5 g/l
EDTA	0.2 g/l

1 x TTBS

TBS	1 x
Tween 20	0.06% (v/v)

Upper Tris Buffer pH 6.8

Tris/HCl	0.5 M
----------	-------

Erythrocyte lysis buffer (in 1L distilled H₂O)

NH ₄ Cl	8.26g
KHCO ₃	1 g
EDTA	0.037 g

4.3 Pre-made Buffers

autoMACS running buffer	Miltenyi Biotec, Bergisch Gladbach, Germany
BD Cytotfix/Cytoperm Buffer	BD Pharmingen, San Jose, CA USA
BD perm/wash buffer	BD Pharmingen, San Jose, CA USA
FACS wash buffer	Miltenyi Biotec, Bergisch Gladbach, Germany
FoxP3 buffer set	BD Biosciences, Heidelberg

4.4 Dye and beads

CFSE (carboxyfluorescein succinimidyl ester)	Molecular probes, Invitrogen, Karlsruhe, Germany
CMAC (CellTracker Blue - amino-4-chloromethylcoumarin)	Invitrogen, CA, USA
CompBeads	BD Biosciences, Heidelberg
Cytometer Setup and Tracking (CST) beads	BD Biosciences, Heidelberg
Flow-Count Fluorospheres	Beckman-Coulter, Krefeld, Germany
Propidium iodide (PI)	Sigma-Aldrich Chemie GmbH, Deisenhofen

4.5 Kits

Annexin V-FITC/PI Apoptosis Kit	Coulter-Immunotech GmbH, Hamburg
BD Cytometric Bead Array	BD Biosciences, Heidelberg
Human Inflammation Kit	
BD Human Th1/TH2/TH17 kit	BD Biosciences, Heidelberg
iLite human IFN- α kit	PBL InterferonSource, Piscataway, NJ, USA
Peq Gold	Peqlab, Erlangen, Germany
RNeasy micro kit	Qiagen, Hilden, Germany
Sensiscript RT kits	Qiagen, Hilden, Germany
Standard DC Protein Assay Kit	Bio-Rad Laboratories GmbH, Munich
VeriKine ELISA kit	PBL InterferonSource, Piscataway, NJ, USA

4.6 Antibodies

4.6.1 Human FACS antibodies:

anti-IFN- α -PE	BD Pharmingen, San Jose, CA USA
anti-CD14-APC	Immunotools, Friesoythe, Germany
anti-CD45RA-APC	Immunotools, Friesoythe, Germany
anti-CD123-APC	Immunotools, Friesoythe, Germany
anti-CD86-FITC	Immunotools, Friesoythe, Germany
anti-CD135-FITC	Immunotools, Friesoythe, Germany
anti-CD1a-FITC	Immunotools, Friesoythe, Germany
anti-BDCA2-PE	Miltenyi Biotec, Bergisch Gladbach, Germany
anti-CD11b-APC	Miltenyi Biotec, Bergisch Gladbach, Germany
anti-HLA-ABC (MHC I)-FITC	Miltenyi Biotec, Bergisch Gladbach, Germany
anti-HLA-DR (MHC II)-PE-Cy7	BD Biosciences, Heidelberg,

	Germany
Anti-TLR4-PE	Imgenex, San Diego, CA, USA
Human Fc Receptor Binding Inhibitor	eBioscience, San Diego, CA USA
Anti-CD3-V450	BD Biosciences, Heidelberg, Germany
Anti-CD4-V500	BD Biosciences, Heidelberg, Germany
Anti-CD8-APC-H7	BD Biosciences, Heidelberg, Germany
Anti-CD25-PE-Cy7	BD Biosciences, Heidelberg, Germany
Anti-CD69-AlexaFlour 700	BD Biosciences, Heidelberg, Germany
Anti-CD73-PE	BD Biosciences, Heidelberg, Germany
Anti-CD39-FITC	Miltenyi Biotec, Bergisch Gladbach, Germany
Anti-CD19-Qdot 655	Invitrogen, Carlsbad, CA, USA
Anti-FoxP3-APC	BD Biosciences, Heidelberg, Germany
Anti-TGF- β 1-PE	IQ products, Groningen, Netherlands
Anti-CD80-PE	Biolegend, Fell, Germany
Anti-CD83-APC	Biolegend, Fell, Germany
Anti-CD40-FITC	Biolegend, Fell, Germany

4.6.2 Human Neutralizing antibodies

IL-27 neutralizing antibody	R&D Systems, Wiesbaden-Nordernstadt, Germany
IgG1 isotype control	R&D Systems, Wiesbaden-Nordernstadt, Germany

TGF- β neutralizing antibody R&D Systems, Wiesbaden-Nordernstadt, Germany

4.6.3 Murine FACS antibodies

CD19-APC-Cy7-PE	BD Biosciences, Heidelberg, Germany
CD115-PE	BD Biosciences, Heidelberg, Germany
CD45-V450	BD Biosciences, Heidelberg, Germany
B220-V450	BD Biosciences, Heidelberg, Germany
CD11c-AlexaFluor700	BD Biosciences, Heidelberg, Germany
Ly6C-PerCP-Cy5.5	BD Biosciences, Heidelberg, Germany
CD11b-eFluor605	ebioscience, San Diego, CA, USA
CD8-eFluor650	ebioscience, San Diego, CA, USA
HLA-DR-APC	Miltenyi, Bergisch Gladbach, Germany
CD11b-APC	Miltenyi, Bergisch Gladbach, Germany
SiglecH-PerCP-Cy5.5	Biolegend, Fell, Germany
CD317/120G8	Dendritics, Lyon, France
Mouse BD Fc Block	BD Biosciences, Heidelberg, Germany

4.6.4 Primary human antibodies:

Anti-E2-2 (rabbit polyclonal) ABCAM, Cambridge, UK

Anti-IDO (mouse monoclonal) ABCAM, Cambridge, UK

4.6.5 Secondary human antibodies:

IRDye680-labelled anti-rabbit Li-COR Biosciences GmbH, Bad
Homburg

IRDye800-labelled anti-rabbit Li-COR Biosciences GmbH, Bad
Homburg

4.7 Microbeads:

Human CD14 microbeads Miltenyi, Bergisch Gladbach,
Germany

Human CD4⁺ CD25⁺ regulatory Miltenyi, Bergisch Gladbach,
T cell isolation kit Germany

Anti-FITC microbeads Miltenyi, Bergisch Gladbach,
Germany

4.8 Media and reagents for cell culture

Bovine insulin Sigma-Aldrich Chemie GmbH,
Deisenhofen

Dulbecco's Modified Eagle PAA Laboratories GmbH, Cölbe
Medium (DMEM)

FCS PAA Laboratories GmbH, Cölbe

L-glutamine PAA Laboratories GmbH, Cölbe

Lymphocyte separation medium PAA Laboratories GmbH, Cölbe

Non essential amino acids PAA Laboratories GmbH, Cölbe

PBS (Instamed 9.55 g/ml)	Biochrom AG, Berlin
Penicillin/Streptomycin	PAA Laboratories GmbH, Cölbe
Roswell Park Memorial Institute (RPMI) 1640	PAA Laboratories GmbH, Cölbe
Sodium pyruvate	PAA Laboratories GmbH, Cölbe

4.9 Cytokines

Human Flt3-L	Immunotools, Friesoythe, Germany
Murine Flt3-L	PeptoTech, London, UK
Human GM-CSF	Miltenyi, Bergisch Gladbach, Germany
Human IL-2	Immunotools, Friesoythe, Germany
Human IL-4	Immunotools, Friesoythe, Germany
Human TNF- α	Peptotech Inc. NJ, USA

4.10 ELISA

IL-27 sandwich ELISA	Biologend, San Diego, CA USA
VeriKine™ Mouse Interferon-Alpha ELISA Kit	PBL interferon source, NJ, USA

4.11 Stimulators and Inhibitors

APCP (CD73 inhibitor 5'-[$\alpha\beta$ -methylene] diphosphate)	Sigma, Steinheim, Germany
ARL67156	Sigma, Steinheim, Germany
all-trans retinoic acid (ATRA)	Sigma-Aldrich, St. Louis, MO, USA
1x Brefeldin A (BFA)	BD fastimmune, San Jose, CA USA
CpG-A (2336) oligonucleotides	InvivoGen, San Diego, CA, USA

(ODN)

CSC (Adenosine receptor A2a antagonist 8 (3-chlorostyryl) caffeine)

CYM50358 Courtesy: E. Roberts, The Scripps Institute, La Jolla, CA, USA

CYM50374 Courtesy: E. Roberts, The Scripps Institute, La Jolla, CA, USA

JTE-013 Biomol, Hamburg Germany

Lipopolysaccharide Sigma, Steinheim, Germany,

Staurosporine Sigma, Steinheim, Germany

Vitamin D3 Fluka, Biochemica, St. Louis, MO, USA

VPC23019 Avanti Polar Lipids, Alabaster, AL, USA

4.12 Oligonucleotides

The below given oligonucleotides were from biomers.net GmbH (Ulm):

p35: sense 5'-AGATAAAACCAGCACAGT-GGAGGC-3', antisense: 5'-GCCAGGCAACTCCCATTAGTTAT-3';

p28 sense: 5'-AGGA-GCTGCGGAGGGAGTT-3', antisense: 5'-AGGGGCAGGAGGTACAGGTTTC-3';

IL-10 sense: 5'-AAGCCTGACCACGCTTTCTA3-', antisense: 5'-TAGCAGTTAGGAAGCCCC-AA-3'.

The below given oligonucleotides were from Qiagen, Hilden, Germany:

Human E2-2 (QT00031829), human ID2 (QT00210637), human IFN- α 1 (QT00201964), IFN- α 2 (QT00212527), IFN- α 16 (QT00202671), and human IRF7 (QT00210595). Actin (QT01680476) and 18S (QF00530467) served as the internal controls.

4.13 Cells and cell lines

Primary human monocytes: Primary human monocytes were isolated from Buffy Coats, which were obtained from DRK-Blutspendedienst Baden-Württemberg-Hessen, Frankfurt.

MCF-7 cells: MCF-7 human breast adenocarcinoma cells were established from the pleural effusion of a 69-year-old Caucasian woman with metastatic mammary carcinoma (after radio- and hormone therapy) in 1970 [75].

Mouse pDC: Mouse bone marrow cells were used as a precursor source for generating pDC. Bone marrow cells were obtained from hindlimbs of HIF-1 α ^{fl/fl} LysM-Cre mice under sterile conditions followed by erythrocyte lysis. The bone marrow cells were cultured in low adhesion plates with appropriate cytokines such as murine FLT3-L to obtain mouse pDC.

4.14 Instruments

Autoclave HV 85	BPW GmbH, Süssen
autoMACS™ Separator	(Miltenyi Biotec, Bergisch Gladbach, Germany)
AxioScope fluorescence microscope	Carl Zeiss MicroImaging, Jena, Germany
B250 Sonifier	Branson Ultrasonics, Danbury (USA)
Bioanalyzer	Agilent, Böblingen, Germany
CASY®	Schärfe System, Reutlingen
Centrifuge 5415 R	Eppendorf GmbH, Hamburg

Centrifuge CR 3.22	Jouan GmbH, Unterhaching
Centrifuge MR 23i	Jouan GmbH, Unterhaching
Centrifuge ZK380	Hermle GmbH, Wehingen
FACSCanto flow cytometer	BD Biosciences GmbH, Heidelberg
Fluorescence microscope Axiovert 200M	Carl Zeiss MicroImaging Inc, Göttingen
Holten LaminAir clean bench	Jouan GmbH, Unterhaching
Hypoxia workstation incubator	<i>In vivo</i> 400, Ruskin Technology, UK
IG 150 (cell culture incubator)	Jouan GmbH, Unterhaching
LabLine Orbit Shaker	Uniequip GmbH, Martinsried
LSRII/Fortessa flow cytometer	BD Biosciences
Magnetic stirrer Combimag RCH	IKA Labortechnik GmbH & Co. KG, Staufen
Mastercycler Thermocycler	Eppendorf GmbH, Hamburg
MediMachine	BD Biosciences GmbH, Heidelberg
Mini-PROTEAN 3 System (SDS- PAGE)	Bio-Rad Laboratories GmbH, München
Mithras LB940 multimode reader	Berthold Technologies, Bad Wildbad
NanoDrop spectrophotometer	NanoDrop, Wilmington, USA
Odyssey infrared imaging system	Li-COR Biosciences GmbH, Bad Homburg
Pure water system Purelab Plus	ELGA LabWater GmbH, Siershahn
Sub-Cell® GT electrophoresis system	Bio-Rad Laboratories GmbH, München
Thermomixer 5436	Eppendorf GmbH, Hamburg
Ultra-Sonifier	MSE, Loughborough (England)
UV-Transilluminator documentation system	Raytest GmbH, Straubenhardt

4.15 Plastic material

12-well Ultra-Low attachment plates	Corning, Amsterdam, Netherlands
Nylon mesh	BD Biosciences GmbH, Heidelberg
Pipettes (10 μ l, 100 μ l, 1.000 μ l)	Eppendorf GmbH, Hamburg
Cell culture dishes)	Greiner Bio-One GmbH, Frickenhausen

4.16 Software

Aida Image Analyzer v 3.11	Raytest GmbH, Straubenhardt
AxioVision Software	Carl Zeiss MicroImaging Inc, Göttingen
BD FACSDiva™ Software	BD Biosciences GmbH, Heidelberg
FCAP software	BD Biosciences, San Jose, CA USA
FlowJo software 7.6.1	Treestar, Ashland, OR, USA
Gene Expression Macro	Bio-Rad, München, Germany
GraphPad Prism 5.0	GraphPad Software, San Diego, CA, USA
MikroWin 2000	Berthold Technologies Bad Wildbad

5 Methods

5.1 Cell culture

MCF-7 breast carcinoma cells were maintained in RPMI 1640 supplemented with 5 mM glutamine, 100 U/ml penicillin, 100 µg/ml streptomycin and 10% heat-inactivated FCS supplemented with 1mM sodium pyruvate, 1 x non essential amino acids and 10 µg/ml bovine insulin. Cells were kept in a humidified atmosphere of 5% CO₂ in air at 37°C and were transferred twice a week.

5.2 Primary human immune cell isolation and expansion

Primary human blood cells were obtained from Buffy Coats (DRK-Blutspendedienst Baden-Württemberg-Hessen, Institut für Transfusionsmedizin und Immunhämatologie, Frankfurt, Germany) using Ficoll-Hypaque gradients. For isolation of CD14⁺ human monocytes, total Buffy Coats were layered on a Ficoll-Isopaque gradients ($\rho=1077$ g/ml) and the interphase containing PBMC was obtained by centrifugation (440 g, 35 min). PBMC were washed with PBS/2 mM EDTA/0.5% BSA and CD14⁺ monocytes were isolated by magnetic cell sorting using human CD14 microbeads in the autoMACS™ Separator. The negative fraction consisting of CD14⁻ PBMC was used for T cell enrichment. Therefore, cells were cultured in T cell medium [76] containing IL-2 (100 U/ml) for 6 days. Every two days, cells adhering to the culture flask were depleted and expanding lymphocytes were split 1:2. Or using a similar protocol, the negative fraction was used to separate CD3⁺ lymphocytes from the same donor using human CD3 microbeads. CD3⁺ T lymphocytes were cultured with IL-2 (100 U/ml) for up to 6 days [77].

5.3 Animals

Animal handling followed the guidelines of the Hessian animal care and use committee. Mice carrying loxP-flanked alleles of HIF-1 α [78] were bred with

LysM-Cre transgenic mice [79] in the C57BL/6 background. Age-matched C57BL/6 wildtype mice were controls.

5.4 Generation and maturation of plasmacytoid and myeloid DC

Human primary monocytes were cultured in 12 well cell culture plates in RPMI 1640 containing 10% FCS for 5 days with GM-CSF (100 ng/ml) and IL-4 (5 ng/ml) to generate myeloid DCs and Flt3-L (100 ng/ml) to generate mo-pDC. On day 5, Lipopolysaccharide (LPS) (1 µg/ml) was added to mDC cultures and 5 µg/ml CpG-A (2336) oligonucleotides (ODN) were added to mo-pDC cultures to induce maturation. In some experiments immature mo-pDC were used or mo-pDC were allowed to differentiate for 10 days. To investigate the impact of vitamins on mo-pDC development, monocytes were cultured with Flt3-L in combination with 3 nM all-trans retinoic acid (ATRA) or 3 µM Vitamin D3. In some experiments mo-pDC were prestimulated overnight with 10 ng/ml TNF-α prior to addition of CpG-A oligonucleotides. Also, human peripheral CD14⁺ human monocytes were differentiated with Flt3-L under hypoxia (1% O₂, 5% CO₂) in a hypoxia workstation incubator. The resulting mo-pDC cultured under hypoxia were then compared with mo-pDC differentiated under normoxia (20% O₂, 5% CO₂). Morphology of mo-pDC and mDC was routinely analyzed using an AxioScope fluorescence microscope at room temperature, using a charge-coupled device camera and the AxioVision Software.

5.5 Isolation of primary pDC

Primary untouched pDC were isolated from human PBMC using a Plasmacytoid DC Isolation Kit that employs an indirect magnetic labeling system.

5.6 Murine pDC generation from bone marrow and hypoxic culture

pDC were differentiated from bone marrow as described [80]. Briefly, mouse bone marrow cells were obtained from the hindlimbs after disinfection with 70% ethanol. The limb was dissected at the knee to obtain upper and lower

limb. A 26-gauge needle filled with PBS was used to flush out the bone marrow contents. The elution was passed through a 76 μ M nylon mesh in order to obtain a single cell suspension. Cells were centrifuged at 500xg for 5 minutes. Erythrocyte lysis was performed on the pellet using an hypotonic solution. The resulting erythrocyte-free cell suspension was seeded in a concentration of 2×10^6 total bone marrow cells/ml in RPMI1640 supplemented with 10% FCS and 200 ng/ml recombinant murine Flt3-L were seeded to 12-well Ultra-Low attachment plates. Culture was maintained for up to 9 d, with medium change every 3rd day. Cells were cultured either under high (20%) or low (1-5%) O₂ levels as indicated using a InVivo2 400 hypoxia workstation.

5.7 Preparation of tumour cell supernatants

MCF-7 human breast carcinoma cells were grown in RPMI 1640 medium plus 10% FCS. Generation of supernatants of living (VCM), apoptotic (ACM) or necrotic (NCM) MCF-7 cells was performed essentially as described. To produce apoptotic cell conditioned medium (ACM), cells were exposed to 1 μ g/ml staurosporine (Sts) 1 h to induce apoptosis). Cells were washed twice with PBS subsequent to apoptosis-induction, followed by an incubation for another 4 h in appropriate medium (1.2.1). Alternatively, [81]. MCF-7 cells remained untreated (living), or 30 μ M oxaliplatin for 16 h (immunogenic cell death) or were incubated at 56°C for 30 min (necrosis), followed by washing and further incubating for at least another 5 h in full medium. The resulting conditioned medium were called viable condition medium (VCM) or Oxaliplatin-ACM (OXA-ACM) or necrotic condition medium (NCM) respectively. Thereafter, conditioned media were harvested by centrifugation (13.000 x g, 5 min) and filtration through 0.2 μ m pore filters, to remove apoptotic bodies (incase of ACM or OXA-ACM) [82], [83] or residual cellular particles (in case of NCM or VCM).

5.8 DC-T cell co-culture

Tumour cell supernatants were added to 2×10^5 human monocyte-derived DC at ratios of 1:1 for 16 h, followed by washing. Afterwards 2×10^6 T cell-enriched PBMC were added and co-cultures were maintained for another 3 days without changing media.

5.9 Treg isolation and CD39⁺ cell isolation

Treg were isolated from DC-T cell co-cultures using the CD4⁺CD25⁺ Regulatory T Cell isolation Kit by magnetic separation. Treg-depleted populations were added back to the respective co-cultures. Isolated Treg (controlled via FACS, **Figure 26**) were either used for RNA isolation or were interchanged between ACM and VCM groups at ratios reconstituting mean FoxP3-expressing cells (0.5%) to monitor their specific suppressive potential. CD39-expressing T cells from IL-2 enriched T cell cultures were removed by staining with CD39-FITC antibody and magnetic separation using anti-FITC microbeads. The CD39-depleted populations were then used for co-cultures.

5.10 Stimulation of human monocyte-derived DC

S1P and the S1PR1/3 inhibitor VPC23019 (1 μ M) were dissolved according to the manufacturer's instructions. The S1PR2/4 antagonist JTE-013 (15 μ M) and the S1PR4 antagonists CYM50358 and CYM50374 (each 200 nM) [84] were dissolved in DMSO. These reagents were pre-incubated for 30 min with DC prior to addition of tumour cell supernatants. The indolamine-2,3-dioxygenase (IDO) inhibitors L-1MT or D-1MT (1 mM) [85] were added to DC 2 h prior to T cell addition. IL-27 neutralizing pab and the isotype control were added at 1 μ g/ml to DC 30 min before addition of T cells. The CD39 inhibitor ARL67156 (250 μ M), the CD73 inhibitor 5'-[α β -methylene] diphosphate (APCP) [86] (100 μ M) dissolved in ddH₂O and the adenosine receptor A2a antagonist 8 (3-chlorostyryl) caffeine (CSC) [87] (10 mM) dissolved in DMSO as well as the CD69 antibody, TGF- β neutralizing antibody [88] and the respective isotype controls were added to DC-T cell co-cultures at day 2.

5.11 Cytotoxicity assay

Cytotoxicity was quantified using a slightly modified established assay [89] (**Figure 10**). The T cells from DC-T cell coculture was harvested into FACS tubes. These were pelleted at 500 xg for 5 minutes. The pellet was resuspended in 500µl FACS buffer (PBS + 0.2% BSA). 20µl of this suspension was pipetted into FACS tubes along with 80µl FACS buffer. These cells were stained with propidium iodide (PI) for 10 min.

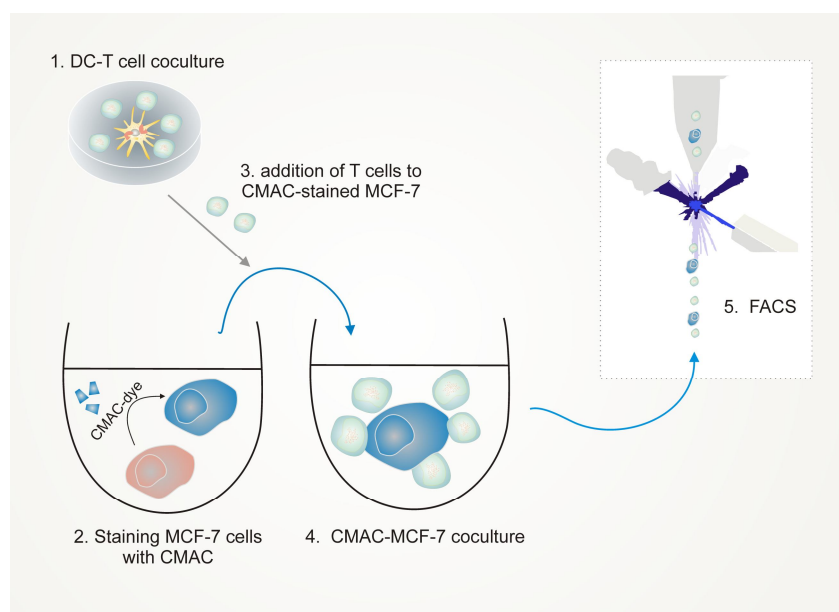


Figure 10: Cytotoxicity assay was performed as depicted: 1. DC were cocultured for 3 days with T cell-enriched PBMC, here depicted as DC-T cell coculture; 2. Live MCF-7 cells were stained with Cell Tracker Blue (CMAC) dye for 45 minutes. The resulting cells were called CMAC-MCF-7 cells. 3. T cells were stained with flourospheres and absolute cell counting was done using flow cytometry; 4. T cells were added to CMAC-MCF-7 cells at different ratios and cocultured for 4h; 5. The CMAC-MCF-7-T cell coculture was stained with PI and flourospheres. The number of living MCF-7 cells and their absolute count was determined by comparing PI and flourocount flouresence respectively with that of the non co-cultured MCF-7 control.

Directly before sample acquisition, Flow-Count Fluorospheres (Beckman-Coulter, Krefeld, Germany) were added as an internal cell counting standard. 10^3 events of living lymphocytes were recorded. The value of flourospheres required to attain the number was used to calculate the absolute number of lymphocytes. Human breast carcinoma cells (MCF-7 and T47D), 2×10^6 each

were suspended in FACS buffer. The cells were stained with 100 μ M CellTracker Blue (7-amino-4-chloromethylcoumarin, CMAC) (Invitrogen, CA, USA) according to manufacturer's instructions for 45 min. This was followed by washing with FACS buffer and the cells were centrifuged at 500 xg for 5 minutes. Afterwards, 5×10^4 breast cancer cells were seeded in FACS tubes together with T cells from DC co-cultures in ratios as indicated for 4 h. The reaction mix was then stained with propidium iodide (PI) for 10 min. Directly before sample acquisition, Flow-Count Fluorospheres (Beckman-Coulter, Krefeld, Germany) were added as an internal cell counting standard and 2×10^3 living (PI⁻, CMAC⁺, FSC^{high}) breast cancer cells were recorded for each sample in comparison to unstimulated breast cancer cells. Cytotoxicity was calculated as described [89]. In some experiments, blocking of CD8 in T cells was triggered using CD8 antibody [90] or the respective isotype control (BD Biosciences) 1 h before performing cytotoxicity experiments.

5.12 Flow cytometry of human DC

Antibodies used for mo-pDC staining in comparison to mDC; monocytes or primary pDC were APC-labelled CD14, CD45RA, CD123, FITC-labelled CD86, CD1a, Alexa 488-labelled CXCR3, PE-labelled CD135, BDCA2, APC-labelled BDCA4 and CD11b, HLA-ABC (MHC I)-FITC, FITC-labelled TLR7, PE-labelled TLR9 and TLR4 and respective isotype controls. For analysis of surface marker expression, monocytes or DC were detached from the dishes by treatment with accutase [91] and washed with ice-cold PBS. Cells were then stained with respective antibodies, incubated on ice for 30 min and analyzed by flow cytometry. Appropriate isotype controls or monocytes stained with respective antibodies were used as controls.

For analysis of DC maturation, DC were detached from the wells by treatment with accutase [91] (PAA), washed with ice-cold PBS/0.2% BSA and incubated on ice for 20 min with CD86-FITC, HLA-DR (MHC II)-PE-Cy7 or HLA-ABC (MHC I)-FITC or CD80-PE, CD83-APC and CD40-FITC. For polychromatic flow cytometry analysis of T cells from DC co-cultures, cells were harvested using a pipette, transferred to FACS tubes and washed with ice-cold PBS.

Next, non-specific antibody binding to FC- γ receptors was blocked using Human Fc Receptor Binding Inhibitor for 20 min, cells were resuspended in FACS staining buffer and incubated with a pre-mixed antibody cocktail consisting of CD3-V450, CD4-V500, CD8-APC-H7, CD25-PE-Cy7, CD69-AlexaFlour 700 and CD73-PE, CD39-FITC, CD19-Qdot 655 on ice for 30 min. Then, cells were fixed and permeabilized using the FoxP3 buffer set from BD Biosciences according to manufacturer's instructions, washed with PBS/0.2% BSA and incubated with FoxP3-APC antibody for 60 min at RT. For analysis of TGF- β expression, cells were pre-treated with 500 ng/ml Brefeldin A and TGF- β 1-PE antibody was used alongside with the FoxP3 antibody. Samples were acquired using a LSRII/Fortessa flow cytometer and analyzed using FlowJo software 7.6.1. All antibodies were titrated to determine optimal concentrations. Antibody-capturing CompBeads were used for single-color compensation to create the multi-color panel compensation matrix. For gating, fluorescence minus one (FMO) controls and/or isotype controls were used. The instrument calibration was controlled and adjusted daily using Cytometer Setup and Tracking (CST) beads.

5.13 Murine Polychromatic flow cytometry

pDC were identified from *in vitro* bone marrow cultures, whole bone marrow, spleen or whole blood using the following antibodies: CD19-APC-Cy7, CD115-PE, CD45-V450, B220-V450, CD11c-AlexaFluor700, (CD11b-eFluor605, CD8-eFluor650 ; HLA-DR-APC, CD11b-APC; SiglecH-PerCP-Cy5.5; CD317/120G8. Single cell suspensions were generated from solid tissues by digestion with 3 mg/ml Collagenase IA, 1 U/ml DNase I in 50% DMEM for 30 min at 37°C, followed by processing with MediMachine, RBC lysis and filtering through a 70 μ m nylon mesh. Cells were transferred to FACS tubes, non-specific antibody binding to FC- γ receptors was blocked with Mouse BD Fc Block for 20 min on ice. This was followed by incubation with individual antibody cocktails for 30 min on ice. Samples were acquired with a LSRII/Fortessa flow cytometer and analyzed using FlowJo software 7.6.1. All antibodies were titrated to determine optimal concentrations. Antibody-capturing CompBeads were used for single-color compensation to create

multi-color compensation matrices. For gating, fluorescence minus one (FMO) controls were used. The instrument calibration was controlled daily using Cytometer Setup and Tracking beads.

5.14 RNA isolation, cDNA synthesis and qPCR

RNA from mo-pDC was extracted using peqGold RNAPure. RNA concentrations were determined using the NanoDrop spectrophotometer and 1 µg RNA was used for cDNA synthesis. Total RNA (1 µg) was transcribed with the iScript cDNA synthesis kit. Quantitative real-time PCR was performed using MyIQ real-time PCR system (and Absolute Blue QPCR SYBR Green fluorescein mix. The following primers were used for quantitative real-time-PCR of mo-pDC: human E2-2; human ID2; human IFN alpha 1 , IFN alpha 2, IFN alpha 16, human IRF-7. 18S RNA levels were employed for normalization. Real-time PCR results were quantified using Gene Expression Macro.

RNA from $< 10^5$ Treg was isolated using the RNeasy micro kit according to the manufacturer's instructions. The resulting RNA was quantitated using the Bioanalyzer from Agilent and was transcribed to cDNA using sensiscript RT kits. Quantitative PCR was performed as described [92]. Human ebi3, actin and 18S rRNA were amplified using QuantiTect Primer Assays. Results were analyzed using Gene Expression Macro (Bio-Rad, München, Germany). Actin and 18S served as the internal controls. For amplifying murine E2-2/TCF4, ID2, CXCL12, actin or TBP, QuantiTect Primer Assays were used. Results were analyzed using Gene Expression Macro. Actin and TBP served as the internal controls.

5.15 Cytokine quantitation

The amount of TNF- α , IL-10, IL-6, IL-12 in DC supernatants and the cytokines IFN- γ , IL-10, IL-4, IL-17, IL-2 from DC/T cell co-cultures were measured using Human Inflammatory Cytokine or Human Th1/TH2/TH17 kits according to the manufacturer's protocol. TLR agonists were added to DC to induce

maturation. After 24h, the supernatants were harvested and centrifuged. The amount of TNF- α , IL-10, IL-6, IL-1 β in the supernatants of mature DC and the amounts of TNF- α in the supernatants from immature DC were measured using human inflammation kits according to manufacturer. Samples were analyzed by FACS and processed with BD Biosciences' FCAP software. Samples were acquired in the flow cytometer and processed with BD Biosciences FCAP software. An IL-27 sandwich ELISA was used to quantify IL-27 levels in treated DC supernatants following the manufacturer's instructions. Measurement of murine IFN- α in supernatants of 5 μ g/ml CpG-A-stimulated pDC was performed using VeriKine ELISA kit.

5.16 T lymphocyte proliferation assay

CD3⁺ T lymphocytes were loaded with 0.5 μ M carboxyfluorescein succinimidyl ester (CFSE) according to manufacturer's protocol. CFSE loaded CD3⁺ T lymphocytes were cocultured with autologous mature DC subsets at a 5:1 ratio for 5 days. Afterwards, the supernatant from the cocultures was harvested. DC were gated from the CD3⁺ T lymphocyte population, following which, CFSE-dependent green fluorescence was quantitated using FACS analysis.

5.17 Apoptotic cell phagocytosis assay

Jurkat cells were stained with CFSE according to the manufacturer's protocol. CFSE-labelled Jurkat cells were treated with 1 μ g/ml staurosporine for 2.5 h in RPMI 1640 without serum. The resulting apoptotic Jurkat cells were added to mDC and mo-pDC in a 50:1 ratio and cultures were incubated at 37 °C for 3.5 h. Then, the cells were harvested and placed on ice to arrest phagocytosis. Cells were incubated for 30 min with APC labelled anti-CD11b antibody and the fluorescence was quantitated using FACS analysis. CD11b⁺ cells, which were double-positive for CFSE were considered to be phagocytic. Apoptotic Jurkat cells (only CFSE⁺) served as negative control.

5.18 Western blot analysis

Generally, immature mo-pDC were used for Western analysis, which was performed as described [81]. A Rabbit polyclonal antibody to E2-2 was used. Blots were counterstained with IRDye infrared secondary antibodies, which were visualized with the Odyssey infrared imaging system.

5.19 IFN- α intracellular staining (ICS)

DC or PBMC were suspended in 500 μ l culture medium. Cells were treated with CpG ODN for 2 h and incubated with 10 μ l of 1x Brefeldin A (BFA) to block anterograde protein transport. After 2 h, 50 μ l of 20 mM EDTA was added and cells were incubated overnight at 4°C. Thereafter, cells were washed with FACS wash buffer) and stained with anti-CD123 or anti-CD45RA antibody for 30 min. Subsequently, cells were fixed and permeabilized using BD Cytofix/Cytoperm Buffer and washed with BD perm/wash buffer, followed by staining for 60 min with anti-IFN- α PE antibody, that is described by the manufacturers to react with human IFN- α 2b and to lesser extent with IFN- α 7. After subsequent washing steps, staining was analyzed in FACS.

5.20 IFN- α bioassay

TLR agonists were added to DC to induce maturation or immature DC were used. Supernatants were harvested 24 h after stimulation. In order to quantitatively determine bioactivity of IFN- α in the supernatants, the iLite Human interferon alpha kit was used according to the manufacturer's instructions.

5.21 Statistical analysis

FlowJo 7.5 software was used for generating FACS traces and for quantifying the mean fluorescence intensities. p-values were calculated by ANOVA with Bonferroni's correction or paired Student's t-test. Differences were considered significant at $p < 0.05$. Data were analyzed using GraphPad Prism 5.0 for Windows (GraphPad Software, San Diego, CA, USA)

6 Results

6.1 Ex-vivo mo-pDC generation and study under hypoxia

The study of dendritic cell populations under the influence of tumour microenvironmental factors required easily available cell sources for *in vitro* analysis of their function. Since pDC are rare in human blood and suitable cell lines do not exist, we wondered if these cells could be generated *in vitro* in a comparable manner as described for mDC [93]. Therefore, in this study, monocytes present in human peripheral blood were exploited for the generation of pDC-like cells using Flt3-L. The mo-pDC thus obtained were analyzed for expression of surface markers, which are known to be differentially expressed on pDC compared to mDC. Mo-pDC mimicked pDC characteristics but retained some properties of monocytes from which they were differentiated. In addition, the functional behaviour of mo-pDC, such as the ability to cause autologous lymphocyte proliferation and the capacity of mo-pDC to phagocytose apoptotic cells were determined. Mo-pDC expressed E2-2 as well as markers, which are under the transcriptional control of E2-2. Further, functional human pDC equivalents were generated by standardizing appropriate cytokine or agonist combinations that accentuate IFN- α production. Finally, the influence of hypoxia on pDC generation and the resulting mo-pDC phenotype was investigated.

6.1.1 Generation and characterization of mo-pDC from human monocytes using Flt3-L

Though the developmental origin of pDC was long considered to be entirely lymphoid, recently common myeloid progenitors were identified for both mDC and pDC [18]. Besides, Flt3-L was identified as a vital determinant for pDC generation in humans [22] and mice [18]. Therefore, we questioned whether pDC equivalents could be generated from monocytes using Flt3-L.

First, we checked for the expression of Flt3 to justify an attempt to generate pDC equivalents using Flt3-L. CD14⁺ monocytes isolated from human peripheral blood were stained with anti-Flt3 antibody and found to be positive for Flt3 by using FACS analysis (**Figure 11A**).

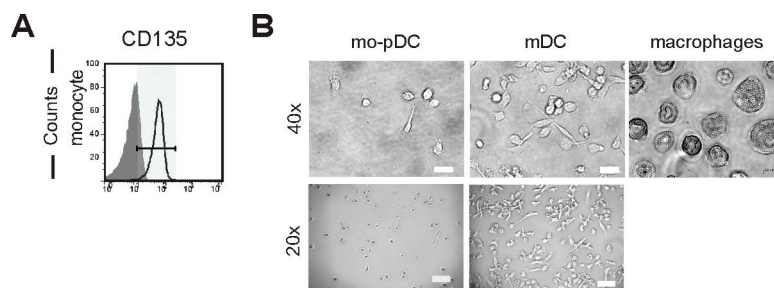


Figure 11. Morphology of mo-pDC compared to mDC and macrophages (A) Human peripheral blood CD14⁺ monocytes were stained with anti-Flt3 (CD135)-PE and its expression was quantitated by FACS. Isotype antibody stained monocytes served as a negative control, indicated as shaded. (B) Phase contrast images indicate the morphology of mo-pDC, compared to mDC or macrophages (upper panels: 40x magnification, bars indicate 100 μ m; lower panels: 20x magnification, bars indicate 20 μ m). Representative FACS traces are shown. Experiments were repeated at least four times using monocytes of different donors.

Subsequently, monocytes were cultured in the presence of Flt3-L for 5 days to generate pDC-like cells. The resulting monocyte-differentiated cells were called mo-pDC. These immature mo-pDC were matured with CpG ODN, which is a viral mimetic TLR9 ligand, while mDC were matured with the TLR4 ligand LPS. The numbers of DC subsets obtained from monocytes were routinely determined. From 10⁶ monocytes, $1.34 \pm 0.63 \times 10^5$ mo-pDC were obtained, whereas the number of mDC was $4.18 \pm 1.73 \times 10^5$. Furthermore, differences in morphology of mo-pDC *versus* mDC were routinely monitored using phase-contrast microscopy (**Figure 11B**).

pDC were reported to differ in their expression of surface markers when compared to mDC [18, 94]. Immature myeloid CD11c⁺ DC express TLR1-4 and TLR6-8 while pDC express TLR1, TLR6, TLR7, TLR9, and TLR10 [94]. Therefore, we checked for differences in expression of surface markers between the resulting mo-pDC and mDC. As a reference, we compared expression of important surface markers on mo-pDC with their expression on primary pDC isolated from human blood.

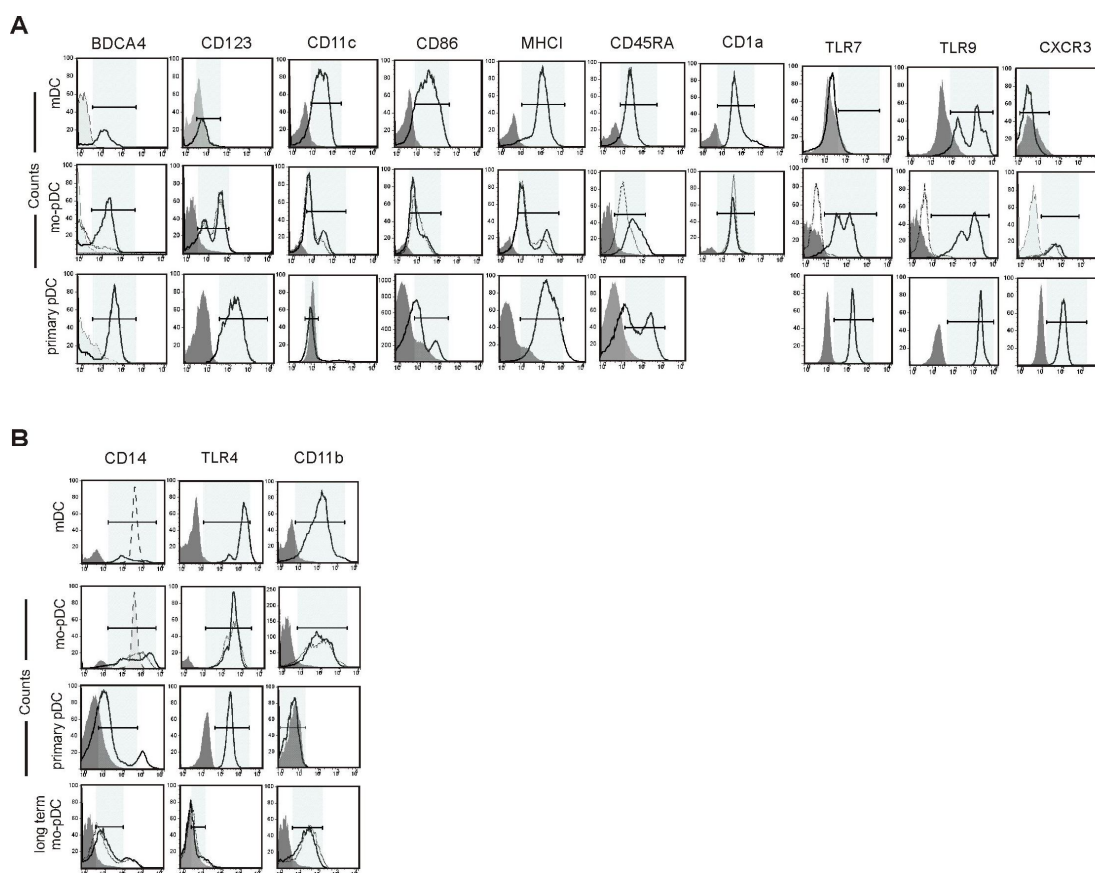


Figure 12. Mo-pDC differ in surface marker expression compared to mDC. (A) *Ex-vivo* untouched human pDC were isolated from different donors and activated for 24 hours with 5 μ g/ml CpG-A 2336. Monocytes were differentiated with GM-CSF (100 ng/ml)/IL-4 (5 ng/ml) for 5 days and resulting mDC were matured with LPS. Monocytes were differentiated with Flt3-L (100 ng/ml) for 5 days and resulting immature mo-pDC were analyzed (dotted FACS traces) or matured with CpG ODN or LPS prior to analysis. The mo-pDC or mDC and primary pDC were stained with anti-BDCA4, CD123, CD11c, CD86, MHCI, CD45RA, CD1a, TLR7, TLR9, CXCR3 antibodies; (B) For some surface marker analysis mo-pDC were differentiated for up to 10 days (long-term mo-pDC). The mo-pDC or mDC, primary pDC and long-term mo-pDC were stained with anti-TLR4, CD14 (here CD14 stained monocyte served as positive control indicated by dashed-line), CD11b antibodies. Expression of the surface markers was quantitated by FACS. Isotype antibody-stained mDC or mo-pDC or primary pDC or long-term mo-pDC respectively served as appropriate negative controls (shaded FACS traces). Representative FACS traces are shown. Experiments were repeated at least four times using monocytes of different donors.

In human blood and bone marrow, BDCA4 is exclusively expressed on pDC [95], while CD123 is also a prominent pDC marker [94]. Indeed BDCA4 and CD123 surface expression was higher in mo-pDC compared to mDC, and similar to primary pDC (**Figure 12A**). In contrast, CD11c and CD86 which are co-stimulatory molecules for T cell activation were lower in mo-pDC and primary pDC (**Figure 12A**). In addition mo-pDC generated with Flt3-L expressed MHCI, CD1a and higher CD45RA compared to mDC (**Figure 12A**).

Table 1: Quantification of surface marker expression

Surface markers	Monocytes				
Surface markers	mDC	Immature mo-pDC	Mature mo-pDC	Primary pDC	Long-term mo-pDC
CD135	68±11				
BDCA4	40±9	64±0.4	45±6	51±2	
CD123	28±5	58±4	57±22	77±5	
CD11c	48±9	24±16	5±7	26±10	
CD86	55±14	9±0.7	10±1	4±2	
MHCI	189±45	72±51	113±83	84±3	
CD45RA	66±3	59±8	74±4	88±7	
CD1a	113±22	37±4	39±2		
CD14	165±36	640±74	390±87	77±4	40±15.8
TLR4	1440±101	341±14	327±19	84±3	5±1.6
CD11b	80±3	69±13	62±4	5±0.2	41±16.2
TLR7	9±14	1±2	45±6	99±12	
TLR9	92±3	3±2.5	84±2.2	85±4	
CXCR3	7.2±4	10±1.2	14±1.2	60±6	
BDCA2	37±12.6		51±3.5	79±2	

MFI ± S.D of surface marker expression displayed in **Figure 11A, 12A, 12B, 13D**

In addition mo-pDC expressed CD14, a monocytic marker and TLR4, a prominent mDC marker, which were however lost upon long-term culture for 10 days. Mo-pDC expressed slightly lowered CD11b which was retained even through long-term culturing (**Figure 12B**). Primary pDC are reported to express TLR7 and TLR9 as opposed to myeloid DC [94]. Mo-pDC expressed high TLR7 compared to mDC and similar to primary pDC, whereas TLR9 was highly expressed on mo-pDC, but surprisingly also on mDC. Plasmacytoid DC

were characterized by CXCR3 expression [96]. Mo-pDC were slightly CXCR3 positive compared to primary pDC, but CXCR3 was not expressed on mDC (**Figure 12A**). Quantification of the expression data is shown in **Table 1**.

6.1.2 Expression of pDC developmental transcription factors by mo-pDC

E2-2, a specific transcriptional regulator of the pDC lineage, was shown to be absent in monocytes, macrophages and CD11c^{high} CD11b⁺ mDC [25]. Therefore, we compared E2-2 protein expression in monocytes, which were frozen directly after isolation vs. mo-pDC generated from monocytes of the same donor.

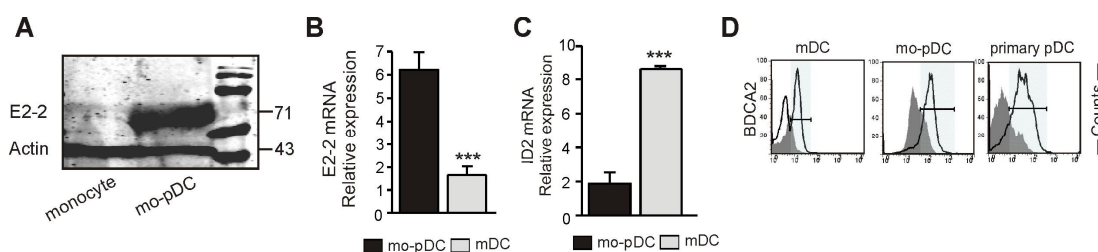


Figure 13. Expression of pDC lineage determining transcription factor E2-2 and E2-2-controlled BDCA2. (A) E2-2 protein expression in monocytes and immature mo-pDC from the same donor was analyzed by Western blotting. Actin serves as a loading control. A representative blot of three independent experiments using different donors is shown. (B) E2-2 mRNA expression in mo-pDC and mDC was quantitated by qPCR. Asterisks marks statistically significant differences ($p < 0.05$). (C) ID2 mRNA expression in mo-pDC and mDC was quantitated by qPCR. Asterisk marks statistically significant differences ($p < 0.05$). (D) Monocytes were differentiated with Flt3-L or GM-CSF/IL-4 for 5 days and matured with CpG ODN or LPS. Resulting mo-pDC or mDC and primary pDC, immature mo-pDC (dotted FACS trace) were stained with the anti-BDCA2 antibody. BDCA2 expression was quantitated by FACS along with isotype controls. Representative FACS traces are shown. Experiments were repeated at least four times using monocytes of different donors.

Mo-pDC showed strong E2-2 protein expression, while it was absent in monocytes (**Figure 13A**). Furthermore, on mRNA level, mo-pDC expressed significantly higher E2-2 compared to mDC (**Figure 13B**), whereas mRNA levels of ID2, the functional inhibitor of E2-2 [26] were significantly lower (**Figure 13C**). E2-2 regulates the synthesis of BDCA2 [97], which is specifically expressed by pDC and internalizes antigen for presentation to T

cells. Mo-pDC expressed high BDCA2 similar to primary pDC, whereas mDC were BDCA2 low (**Figure 13D**).

6.1.3 Functional validation of mo-pDC

Plasmacytoid DC were reported to be poor inducers of T cell proliferation, since they do not capture, process and load antigen as effectively as mDC [98]. Thus, we checked for the ability of mo-pDC to induce proliferation of autologous CD3⁺ lymphocytes.

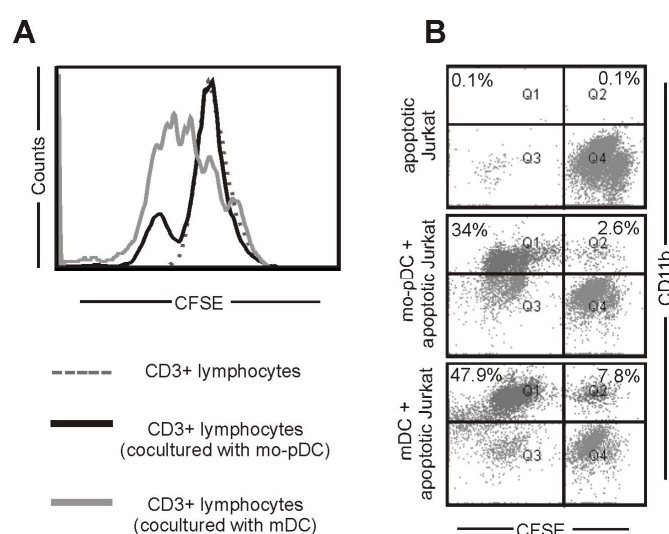


Figure 14. Functional validation of mo-pDC versus mDC. (A) Human peripheral blood CD3⁺ lymphocytes were stained with 0.5 μ M CFSE and then cocultured with mature mo-pDC or mDC from the same donor for 5 days. Supernatants were harvested and the CFSE fluorescence was quantitated by FACS. The dotted line denotes CD3⁺ lymphocytes alone, the black line denotes CD3⁺ lymphocytes cocultured with Mo-pDC and the gray line denotes CD3⁺ lymphocytes cocultured with mDC. Representative FACS traces of three independent experiments from different donors are shown. (B) Jurkat cells were labeled with 0.5 μ M CFSE and killed with staurosporine for 2.5 h. Apoptotic Jurkat cells were then cocultured with mo-pDC or mDC for 3.5 h. The cocultures were harvested, stained with anti-CD11b-APC and analyzed by FACS. Q4 denotes CD11b⁻ CFSE⁺ apoptotic Jurkat cells; Q1 denotes non-phagocytic CD11b⁺ CFSE⁻ DC and Q2 denotes phagocytic CD11b⁺ DC that have taken up CFSE⁺ Jurkat cells. Representative FACS traces of four independent experiments from different donors are shown.

Therefore, autologous CD3⁺ lymphocytes were labelled with CFSE, which can be used to monitor lymphocyte proliferation, due to the progressive halving of CFSE fluorescence within daughter cells following each cell division. CFSE labelled CD3⁺ lymphocytes were cocultured with DC subsets for 5 days and CFSE fluorescence was quantitated using FACS. We found that CD3⁺

lymphocytes cocultured with mo-pDC proliferated less, whereas CD3⁺ lymphocytes from a mDC coculture proliferated for many generations (**Figure 14A**). CD3⁺ lymphocytes without DC coculture served as a control.

We also compared the capability of the DC subsets to phagocytose apoptotic cells. Jurkat T cells were labelled with CFSE and treated with staurosporine for 2.5 h to undergo apoptosis. Apoptotic CFSE-Jurkat were then cocultured with mo-pDC or mDC for 3.5 h at 37 °C to allow phagocytosis. Cocultures were harvested and costained with CD11b-APC to label the DC. Mo-pDC had a 50% lower phagocytic capacity compared to mDC, when analyzing percentages in Q1, showing non-phagocytic DC compared to Q2, which defines DC that engulfed apoptotic Jurkat cells as shown by CD11b-CFSE double-staining (**Figure 14B**). The mo-pDC population expressed less CD11b compared to mDC, which corroborates literature data [99].

6.1.4 IFN- α production by mo-pDC

Since pDC were reported to be primary producers of IFN- α [6] and E2-2 deficient sources failed to produce type I interferons in response to the viral mimetic CpG [97], we checked the expression of IFN- α in TLR9-ligated mo-pDC or PBMC as controls. Therefore, we analyzed intracellular IFN- α [100] and surface expression of CD45RA by FACS. First, IFN- α production of human PBMC, containing primary blood pDC (**Figure 15A**), was compared with basal IFN- α of mo-pDC (**Figure 15B**). CD45RA⁺ cells of the TLR9-ligated PBMC fraction may comprise of monocytes, CD33⁺ myeloid cells, CD56⁺ NK cells, T cells, BDCA4⁺ DC and CD19⁺ B cells [101]. The occurrence of pDC in peripheral blood of human males is 0.11% \pm 0.06% and that of human females is 0.11% \pm 0.07% [17]. Thus, IFN- α producing cells in the CD45RA⁺ fraction of PBMC (~2%) were likely pDC. Whereas human pDC produced high IFN- α after TLR9 ligation [102], only few mo-pDC showed weak IFN- α intracellular expression. To be used in research and therapy as pDC equivalents, mo-pDC must produce high IFN- α . Since E2-2 is necessary for IFN- α production [25] and ID2 proteins are the major inhibitors E2-2 [26], we checked whether decreasing ID proteins would improve the IFN- α production

of mo-pDC. Interestingly, some vitamins were reported to have a profound impact on ID protein expression. 1α , 25-Dihydroxyvitamin D3 decreased both ID1 and ID2 expression [103].

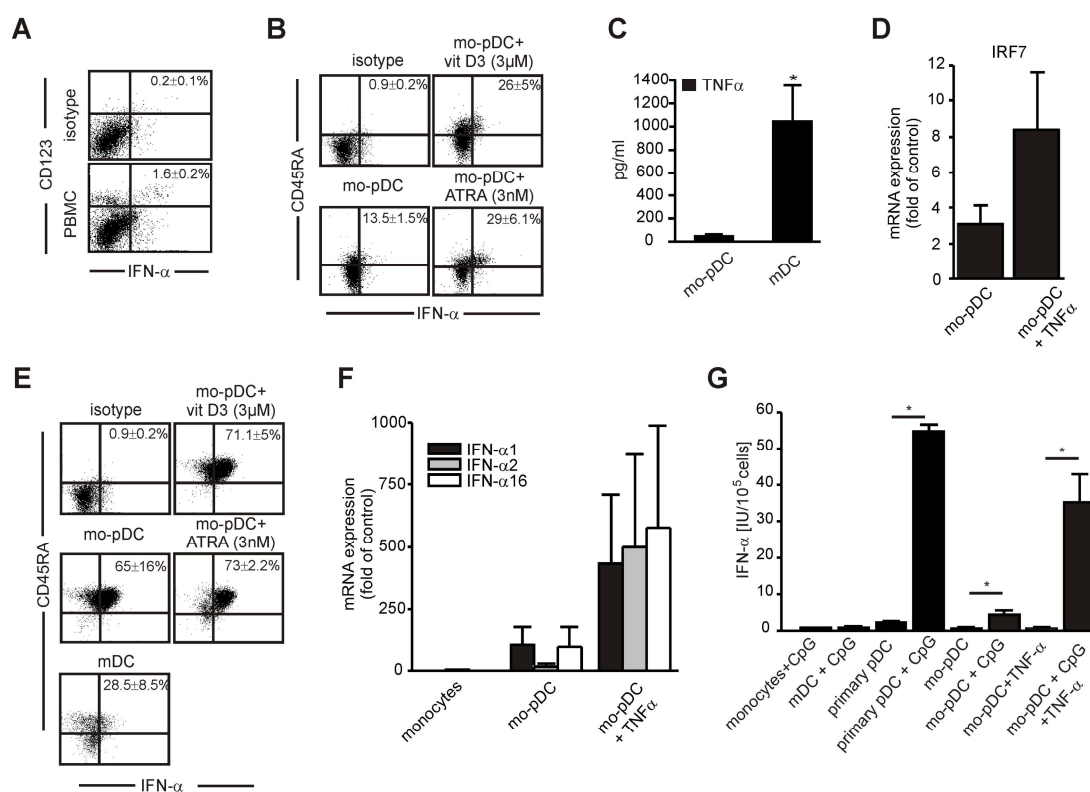


Figure 15. IFN- α production by mo-pDC. (A) PBMC were isolated from human peripheral blood. 5 μ g CpG ODN was added to PBMC for 2 h to induce IFN- α production followed by incubation with BFA for 2 h to stop anterograde protein transport. PBMC were then stained with anti-CD45RA antibody, fixed, permeabilized, co-stained with the anti-IFN- α antibody and analyzed by FACS. Representative FACS traces are shown. Experiments were repeated three times using different donors. Data are the mean \pm SEM. (B) Mo-pDC were generated from monocytes using Flt3-L alone or in combination with 3 μ M vitamin D3 or 3 nM ATRA for 5 days. Cells were incubated with 5 μ g CpG and intracellular IFN- α was analyzed as described for PBMC. Representative FACS traces are shown. Experiments were repeated three times using monocytes from different donors. Data are the mean \pm SEM. (C) TNF- α produced by immature mo-pDC and mDC was quantitated in supernatants using the CBA Human inflammation kit by FACS. Data are the mean \pm SEM of three experiments from different donors. Asterisk marks statistically significant differences ($p < 0.05$). (D) IRF-7 mRNA expression was quantitated by qPCR after TLR-9 agonism in mo-pDC without and with TNF- α pre-stimulation. qPCR data shown are normalized to 18s, with values for unstimulated mo-pDC set to 1. Data are mean \pm SEM of at least three experiments. (E) Immature mo-pDC

were pretreated overnight with 10 ng/ml TNF- α . TNF- α pretreated mo-pDC and immature mDC were incubated with CpG ODN and IFN- α intracellular staining was performed. Representative FACS traces are shown. Experiments were repeated three times using monocytes from different donors. Data are the mean \pm SEM. (F) IFN- α 1, 2 and 16 mRNA expression was quantitated by qPCR after TLR-9 agonism in mo-pDC without and with TNF- α pre-stimulation and in monocytes. (G) Bioactivity of IFN- α in the supernatants of CpG-treated monocytes, mDC, primary pDC and mo-pDC (without and with TNF- α pre-stimulation) was quantitated using bioassay. Experiments were repeated three times using monocytes from different donors. Data are the mean \pm SEM expressed in IU for 10^5 cells. Asterisks mark statistically significant differences ($p < 0.05$).

Also, all-trans retinoic acid (ATRA) decreased ID1 and ID2 expression [104]. Accordingly, we investigated the effects of vitamin D3 or ATRA on mo-pDC differentiation from monocytes, by adding them together with Flt3-L. IFN- α production increased during differentiation of mo-pDC with Flt3-L in combination with Vitamin D3 or ATRA (**Figure 15B**).

6.1.5 Augmenting IFN- α production by mo-pDC

Additionally, we asked whether triggering IFN- α upstream pathways enhances IFN- α production in mo-pDC. IRF7 is the critical transcriptional regulator of IFN- α [105] and TNF- α stimulates IRF7 expression through NF κ B [106]. Checking basal TNF- α produced we noticed that mo-pDC produced only insignificant amounts of TNF- α , especially when compared to mDC (**Figure 15C**). Therefore we checked the outcome of TNF- α pre-treatment on IRF-7 expression and further on CpG-elicited IFN- α expression. Indeed, IRF-7 mRNA expression in mo-pDC was increased after TNF- α prestimulation (**Figure 15D**).

In line, IFN- α production was strongly enhanced by TNF- α -priming and TNF- α -priming further increased CD45RA expression in mo-pDC (**Figure 15E**). During differentiation along with vitamin D3 or ATRA followed by priming with TNF- α , the number of cells producing high levels of IFN- α could be further enhanced. Here, IFN- α produced by TNF- α -pretreated mo-pDC was compared with TLR9 ligated mDC (**Figure 15E**). It was reported that pDC express CD45RA in comparison to mDC [94], which is also reflected by our

observations showing that mo-pDC are more CD45RA⁺ compared to mDC or with respect to their respective isotypes (**Figure 15E** and **Figure 15B**).

Primary human pDC are reported to show a certain IFN- α mRNA subtype profile compared to myeloid cells [107]. We checked the differential expression of representative IFN- α mRNA subtypes in mo-pDC after TLR9 agonism. TNF- α prestimulation increased the mRNA levels of all the three IFN- α subtypes that were tested (IFN- α 1, 2, 16) (**Figure 15F**). Interestingly, there was a nice correlation regarding the increase in IFN- α 2 expression between the intracellular staining that specifically detects IFN- α 2 and IFN- α 2 expression on mRNA levels with respect to TNF- α pre-stimulated and unprimed mo-pDC.

To finally confirm IFN- α production by mo-pDC, we first used a conventional ELISA to quantitatively validate the amount of IFN- α produced after TLR-9 agonism. However, the outcome was not satisfactory when compared to primary pDC (data not shown). Since there was no information available regarding the specific subtype of IFN- α detected in the ELISA, we next used a cell-based bioassay to detect biologically active IFN- α regardless of the subtype. IFN- α production was quantitated after TLR-9 agonism in monocytes, mDC, primary pDC, mo-pDC without and with TNF- α prestimulation (**Figure 15G**). As expected, primary pDC produced high amounts of biologically active IFN- α after CpG administration. Un-primed mo-pDC produced around 10% biologically IFN- α after TLR9 agonism compared to primary pDC, whereas secretion of bioactive IFN- α was strongly increased when mo-pDC were pre-stimulated with TNF- α (**Figure 15G**). Pre-stimulated mo-pDC produced more than 50% of bioactive IFN- α when compared with primary pDC. Thus, the data obtained by intracellular staining as well as by evaluating mRNA expression were reflected satisfactorily by the amount of secreted bioactive IFN- α .

6.1.6 Phenotypical differences between normoxia and hypoxia differentiated mo-pDC

Inflammation, infection [108] and cancer [109] share the occurrence of hypoxic episodes. Interestingly, pDC became non-functional when they infiltrated human head and neck carcinoma tissue [14].

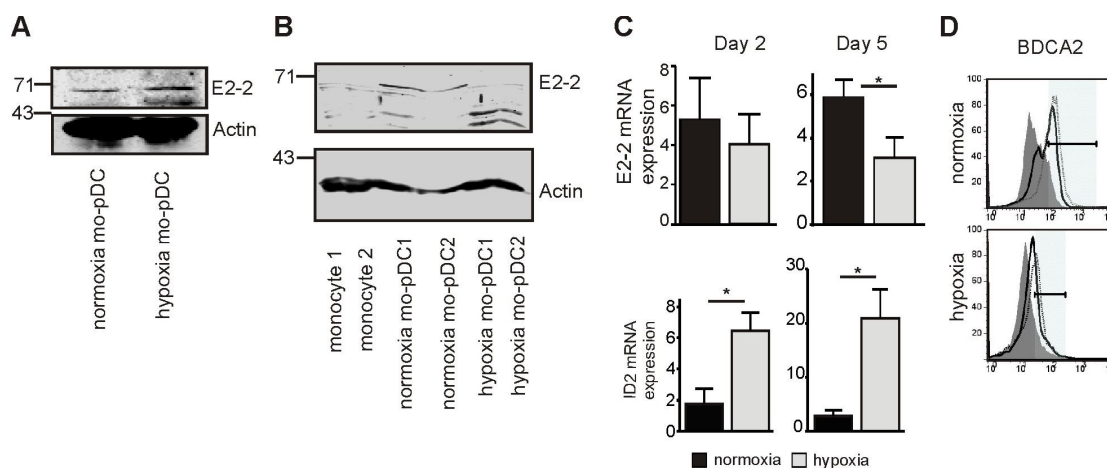


Figure 16. Expression of E2-2, ID2 and E2-2-controlled BDCA2 in normoxia and hypoxia differentiated mo-pDC. (A) Monocytes were differentiated with Flt3-L for 2 days under normoxia and hypoxia (1% O₂, 5% CO₂) and E2-2 expression was analyzed by Western blotting. Actin served as the loading control. A representative blot of three independent experiments using different donors is shown. (B) Immature mo-pDC from two donors were generated under normoxia and hypoxia for 5 days. E2-2 expression in these cells and monocytes from the same donors was analyzed by Western blotting. A representative blot of three independent experiments using different donors is shown. (C) E2-2 and ID2 mRNA expression of mo-pDC differentiated under normoxia or hypoxia for 2 or 5 days was quantitated by qPCR. Experiments were repeated three times using monocytes of different donors. Asterisk marks statistically significant differences ($p < 0.05$). (D) Surface expression of BDCA2 was measured by FACS after staining mo-pDC generated under normoxia or hypoxia for 2 or 5 days with an anti-BDCA2 antibody along with isotype controls. Representative FACS traces are shown. Isotype – shaded, day 2 - solid line, day 5 – dotted line. Experiments were repeated four times using monocytes of different donors. Data are the mean fluorescence intensity \pm SEM.

Besides, E2-2 is downregulated in human neuroblastoma cells exposed to hypoxia [110]. Therefore, we investigated the impact of hypoxia on E2-2 expression during differentiation of monocytes to mo-pDC. E2-2 expression was low in both normoxia and hypoxia differentiated mo-pDC, which were differentiated for two days with Flt3-L (**Figure 16A**).

However, at day 5, E2-2 protein was completely absent in hypoxia differentiated mo-pDC, compared to the expression of E2-2 in normoxia differentiated mo-pDC. E2-2 expression was absent in monocytes of the same donor (**Figure 16B**). Interestingly, we observed protein bands at a lower molecular weight in hypoxia treated mo-pDC, which were absent in monocytes or normoxic mo-pDC. We speculate that these might be E2-2 degradation products, although this phenomenon was not reported before. In order to substantiate the E2-2 Western data, we analyzed expression of E2-2 as well as its inhibitor ID2 on mRNA level. Concomitant with protein expression, E2-2 mRNA was similar 2 days after differentiation under hypoxia as compared to normoxia, but significantly decreased after 5 days. Strikingly, ID2 mRNA expression was increased under hypoxia already on day 2, but was substantially higher on day 5 (**Figure 16C**).

Table 2: Surface marker expression at normoxia versus hypoxia'

Surface markers	Mo-pDC			
	Normoxia day2	Hypoxia day2	Normoxia day 5	Hypoxia day5
BDCA2	48±4	21±5	51±3.5	22±2
CD86			56±3.4	44±5
MHCI			74±3	67±4.5

MFI ± S.D of surface marker expression displayed in **Figure 16D and 17C**

Since BDCA2 expression on pDC is under the control of the E2-2 transcription factor [97], we checked the expression of BDCA2 on mo-pDC generated under normoxia and hypoxia. The expression of BDCA2 was lower on hypoxia-differentiated mo-pDC compared to normoxia-differentiated counterparts, and the expression remained largely unchanged when differentiated until day 5 (**Figure 16D**). Quantification of the expression data is shown in **Table 2**.

Importantly, substantiating E2-2 expression data, hypoxia differentiated mo-pDC produced less IFN- α without (**Figure 17A**) as well as with TNF- α pretreatment as determined by intracellular staining (**Figure 17B**).

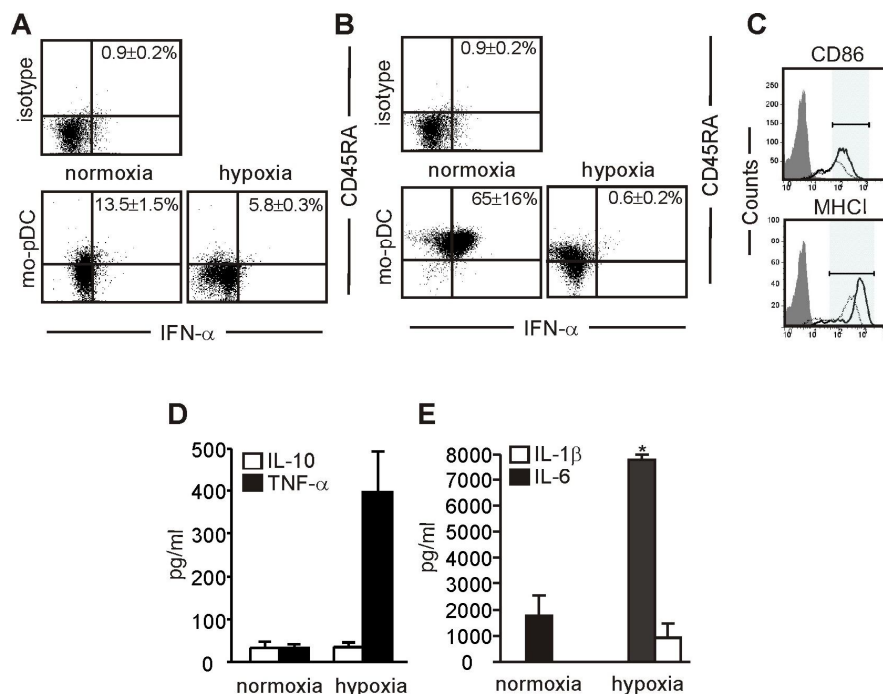


Figure 17. Mo-pDC generated under normoxia vs. hypoxia express different surface and functional markers. (A-E) Mo-pDC were matured with 5 μ g CpG ODN for 24 h under normoxia or hypoxia. The expression of IFN- α without (A) or with (B) 10 ng/ml TNF- α overnight pretreatment was quantitated by staining with respective antibodies and analysis in FACS. Representative FACS traces are shown. Experiments were repeated at least three times using monocytes of different donors. Data are the mean \pm SEM. (C) Surface expression of CD86 and MHCI was analyzed in FACS (shaded - isotype, solid - normoxia, dotted - hypoxia). (D, E) Supernatants from mo-pDC generated under normoxia or hypoxia were harvested and IL-10 and TNF- α (D) as well as IL-1 β and IL-6 (E) levels were quantitated with CBA using FACS. Data are the mean \pm SEM from three independent experiments using monocytes of different donors. Asterisks mark statistically significant differences ($p < 0.05$).

Hypoxia had a profound impact on the phenotype of human mDC [111] and down-regulated antigen uptake [112]. We thus compared the expression of CD86 and MHCI between mo-pDC differentiated under normoxia vs. hypoxia. Indeed mo-pDC differentiated under hypoxia showed decreased surface expression of CD86 and MHCI (**Figure 17C**). Quantification of the expression data is given in **Table 2**. DC do not only present antigens, but also produce a number of inflammatory cytokines in response to primary and secondary maturation signals. These cytokines participate in shaping T cell immunity.

Whereas mDC produce rather a Th1 cytokine response, pDC produce Th2 signatures and mediate Th2 differentiation [113]. Measuring inflammatory cytokine production using CBA, mo-pDC showed rather a Th2 profile as seen by low TNF- α but high IL-10 production. However, when mo-pDC were generated under hypoxia, they showed strong elevation of TNF- α production but similar IL-10 levels (**Figure 17D**). Remarkably, under hypoxia, mo-pDC produced higher IL-1 β and IL-6 levels (**Figure 17E**). Thus, hypoxia seemed to shift mo-pDC from producing primarily type I interferon and IL-10 to the production of high levels of Th1 cytokines

6.2 Study of mice pDC development under the influence of HIF-1 α and hypoxia

Based on the findings outlined above indicating defective development of human plasmacytoid dendritic cells (pDC) from monocytes under hypoxia *in vitro*, we wondered whether HIF-1 was involved in pDC differentiation using mouse bone marrow cultures.

6.2.1 Increased pDC frequency in HIF-1 $\alpha^{fl/fl}$ LysM-Cre mice

We noticed that pDC generation from human monocytes was attenuated under hypoxia (1% O₂). This is associated with up-regulation of the transcription factor ID2. ID2 opposes the function of the pDC lineage-determining transcription factor E2-2 [114] and is under the transcriptional control of HIF-1 α , at least in neuroblastoma cells [115]. Therefore, we questioned whether depletion of HIF-1 α in pDC progenitors would affect their development. To approach this question we used mice that lacked HIF-1 α in cells expressing lysozyme 2 (LysM), i.e. HIF-1 $\alpha^{fl/fl}$ LysM-Cre mice (**Figure 18**). The suitability of this system for studying HIF-1 α effects on pDC development might be surprising, since at least mature pDC do not express LysM as demonstrated in LysM-Cre reporter mice. However, MDP, which differentiate

into CDP and can further develop to pDC, express LysM although at a lower frequency compared to granulocytes or monocytes [116].

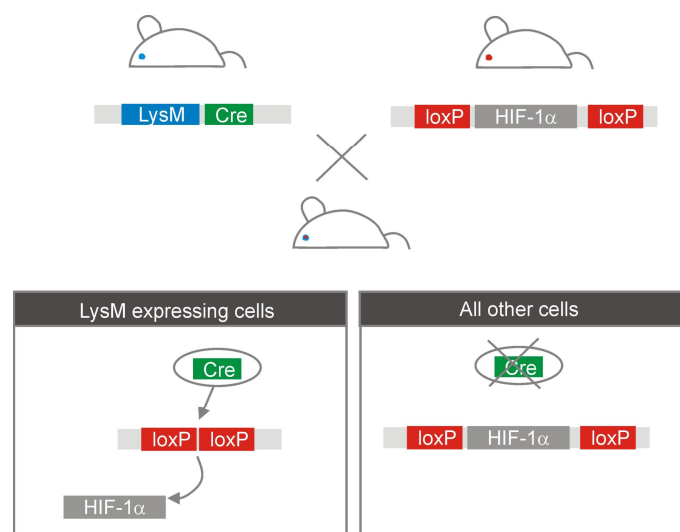


Figure 18: Generation of HIF-1 α ^{fl/fl} LysM-Cre mice. Mice expressing Cre recombinase downstream of the LysM promoter were crossed with mice genetically engineered to express HIF-1 α flanked by LoxP sites. In the resulting HIF-1 α ^{fl/fl} LysM-Cre mice, in LysM expressing cells, HIF-1 α will be deleted by Cre recombinase upon recognition of the LoxP sites. On the other hand, in cells that do not express LysM, HIF-1 α persists.

6.2.2 Hypoxia/HIF-1 represses pDC differentiation from whole bone marrow in vitro

We used the HIF-1 α ^{fl/fl} LysM-Cre system to investigate the function of hypoxia-induced HIF-1 in pDC development in detail. We started with differentiating whole bone marrow single cell suspensions derived from HIF-1 α ^{fl/fl} LysM-Cre or control mice to pDC using fms-related tyrosine kinase 3-ligand (Flt3-L) as described before [117] at high or low O₂ supply.

We used SiglecH as the determining marker for bone marrow-derived pDC [118, 119]. Most cells derived from the Flt3-L cultures were CD11b⁻ CD19⁻ CD11c⁺ SiglecH⁺ pDC that also expressed B220 (CD45RA) and CD317, also known as bone marrow stromal antigen-2 or tetherin (not shown). Whereas B220 and CD317 are highly but not exclusively expressed by pDC, SiglecH

appears to be pDC-restricted and is else only expressed by certain subsets of tissue-resident macrophages [120].

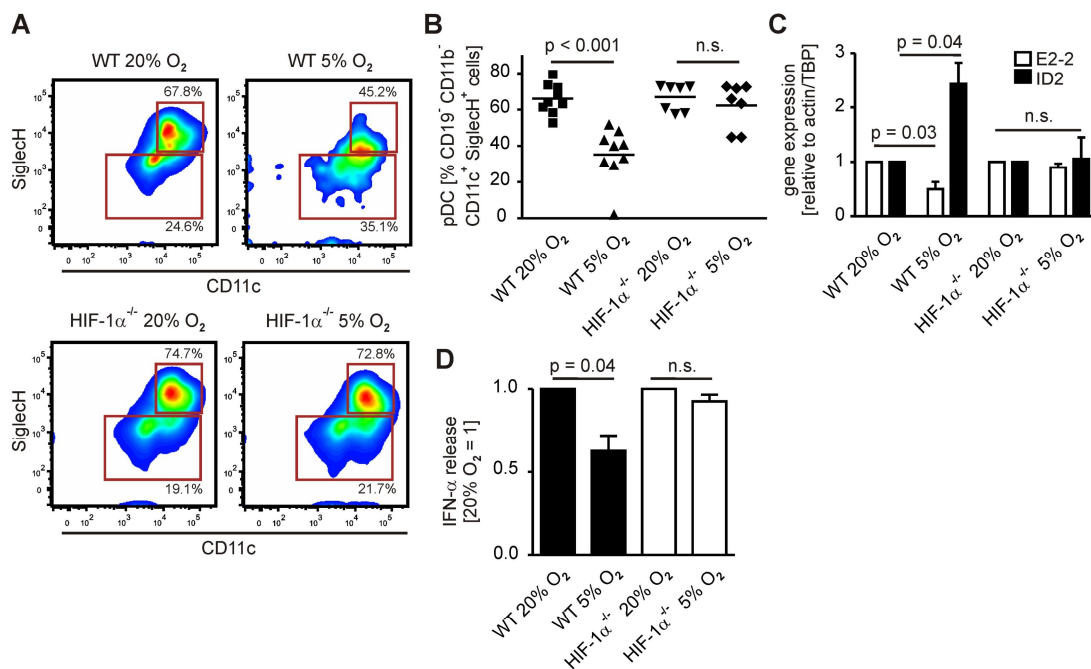


Figure 19. Hypoxia-induced HIF-1 suppresses pDC differentiation in vitro. Bone marrow single cell suspensions were harvested from C57BL/6 wildtype or HIF-1α^{fl/fl} LysM-Cre animals. 2×10^6 cells per ml were seeded in ultra-low attachment plates and incubated with 200 ng/ml murine recombinant Flt3-L at 20% or 5% O₂ for 9 d. (A) Representative FACS traces indicating relative amounts of CD11c⁺ SiglecH⁺ pDC in the CD11c⁺ CD19⁻ population of individual groups as indicated are shown. (B) Quantification of relative pDC amounts in bone marrow cultures. Individual data points and the mean value indicated by bars are shown, $n \geq 7$. (C) Relative mRNA expression of E2-2 and ID2 quantitated via qPCR is displayed. Data are means \pm SEM, $n = 4$. (D) Relative amount of IFN- α (normalized to the 20% O₂ group for each genotype) in 5 μ g/ml CpG-stimulated bone marrow cultures was determined by ELISA. Data are means \pm SEM, $n = 4$.

When we compared the generation of pDC within this population to cells differentiated under 20% O₂, we nevertheless noticed a strong reduction in SiglecH⁺ cells (**Figure 19A, B**). Thus, hypoxia, even at 5% O₂ interfered with bone marrow cell differentiation into pDC in vitro. This was clearly HIF-1 α -dependent as cells from HIF-1 α ^{fl/fl} LysM-Cre bone marrow effectively differentiated to pDC even at 5% O₂ (**Figure 19A, B**). This differentiation

pattern was reflected at the transcription factor level. Wildtype bone marrow cells differentiated for 9 days under 5% O₂ expressed significantly lower levels of E2-2 mRNA and higher levels of ID2 compared to cells differentiated at 20% O₂. In contrast, we observed neither a difference in E2-2 nor in ID2 mRNA levels of differentiated HIF-1 $\alpha^{fl/fl}$ LysM-Cre bone marrow-derived cells (**Figure 19C**). Importantly, activation of in vitro-generated pDC using 5 μ g/ml CpGA resulted in diminished production of IFN- α when pDC from wildtype bone marrow were cultured under 5% O₂ but not when pDC from HIF-1 $\alpha^{fl/fl}$ LysM-Cre bone marrow were generated under 5% O₂ (**Figure 19D**). Thus, limited pDC development due to HIF-1 was also demonstrated on a functional level. These data indicate that differentiation of pDC in vitro under low O₂ levels, which corresponds to in situ normoxia in the bone marrow [30], limits pDC generation in a HIF-1 α -dependent manner.

6.2.3 Altered immune cell populations in Flt3L-expanded bone marrow cultures dependent on O₂ supply

Next, we asked for the fate of cells that did not differentiate into pDC under 5% O₂ since we did not observe significant changes in overall cell numbers from 20% O₂ compared to 5% O₂ cultures (not shown). First, when analyzing the total single cell population, we observed a significant increase in the CD11b^{high} CD115⁻ cell population, which corresponds to cDC or their precursors [20] in 5% O₂ versus 20% O₂ cultures (**Figure 20A, B**). Furthermore, CD11b⁻ CD115⁺ cells, which likely are pDC precursors (not shown) were expanded under 5% O₂, whereas CD11b⁻ CD115⁻ pDC were significantly reduced (**Figure 20A, B**). These differences were strongly accentuated when analyzing only the specific Flt3-L expanded single cell population (**Figure 20A, C**). Our data imply that differentiation of bone marrow cells using Flt3-L in vitro gives rise to pDC under high levels of O₂, whereas their numbers are attenuated at low O₂ tension. In the latter case, the majority of pDC remain in a premature state, as reflected by reduced E2-2 expression (**Figure 19C**), but some cells seem to differentiate along an alternative route to cDC corresponding to increased expression of ID2 (**Figure 19C**).

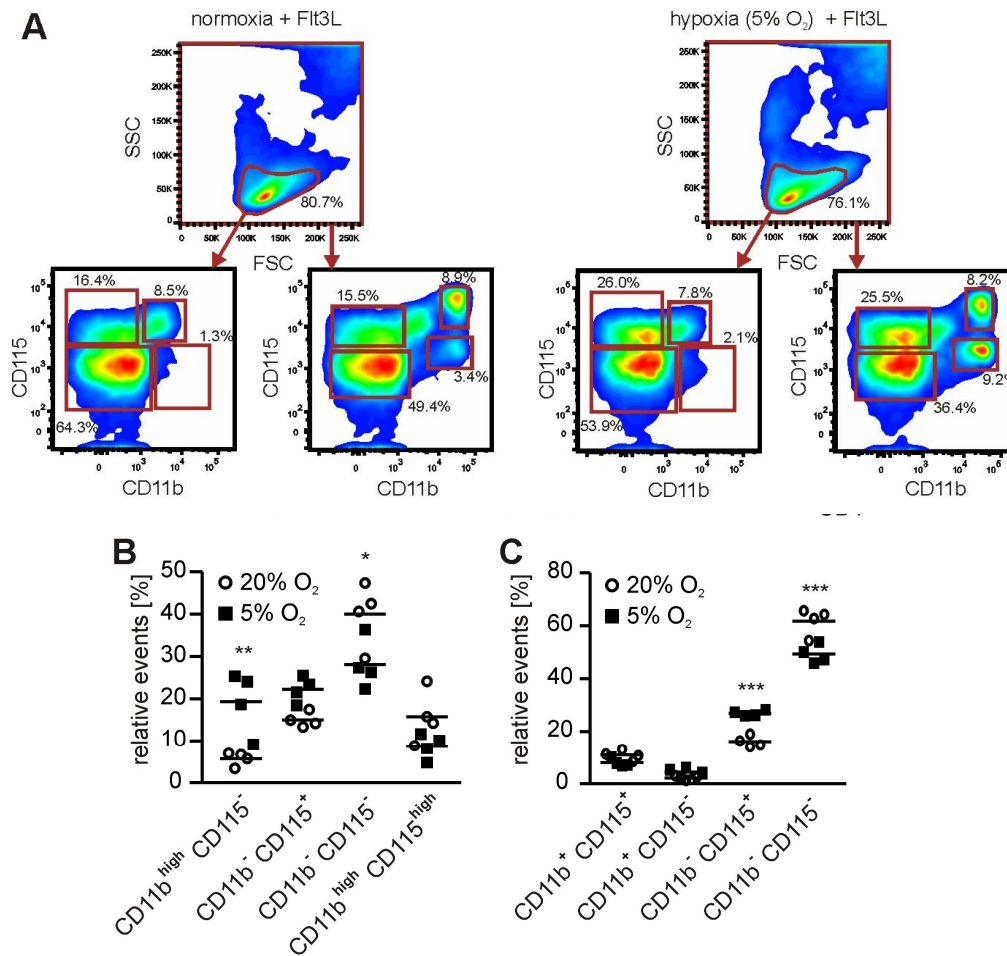


Figure 20. Differentiation of bone marrow under 5% O₂ blocks pDC differentiation and expands cDC. Bone marrow single cell suspensions were harvested from C57BL/6 wildtype. 2 x 10⁶ cells per ml were seeded in ultra-low attachment plates and incubated with 200 ng/ml murine recombinant Flt3-L at 20% or 5% O₂ for 9 d. (A) Representative FACS traces indicating expression of CD11b and CD115 in either total single cells (right density plots) or the specific Flt3-L-expanded population (left density plots) are shown. (B) Quantification of individual cell populations from total single cells based on CD11b and CD115 expression. (C) Quantification of individual cell populations from the Flt3-L-expanded single cell population based on CD11b and CD115 expression. Individual data points and the mean value indicated by bars are shown, n = 4. Asterisks indicate significant differences between groups, * = p < 0.05, ** = p < 0.01, *** = p < 0.01.

Taken together, our data indicate that HIF-1 α limits murine pDC differentiation from precursors *in vitro*. Low oxygen levels in the bone marrow might be an environmental explanation why pDC numbers in the body are low compared to other immune cell populations.

6.3 Generation of regulatory T cells by IL-27 secreting DC under the impact of apoptotic cell-derived factors

We aimed to investigate how priming of DC by factors/exosomes shed by dying versus living tumour cells affects their ability to initiate tumour cell-specific cytotoxic T cell responses. Conditioned media of apoptotic, necrotic, or viable MCF7 cells (ACM, NCM, VCM) were incubated with primary monocyte-derived human DC at a ratio of one tumour cell/DC. Higher ratios of tumour cells/DC induced cell death in DC, especially when using NCM (Figure 21A).

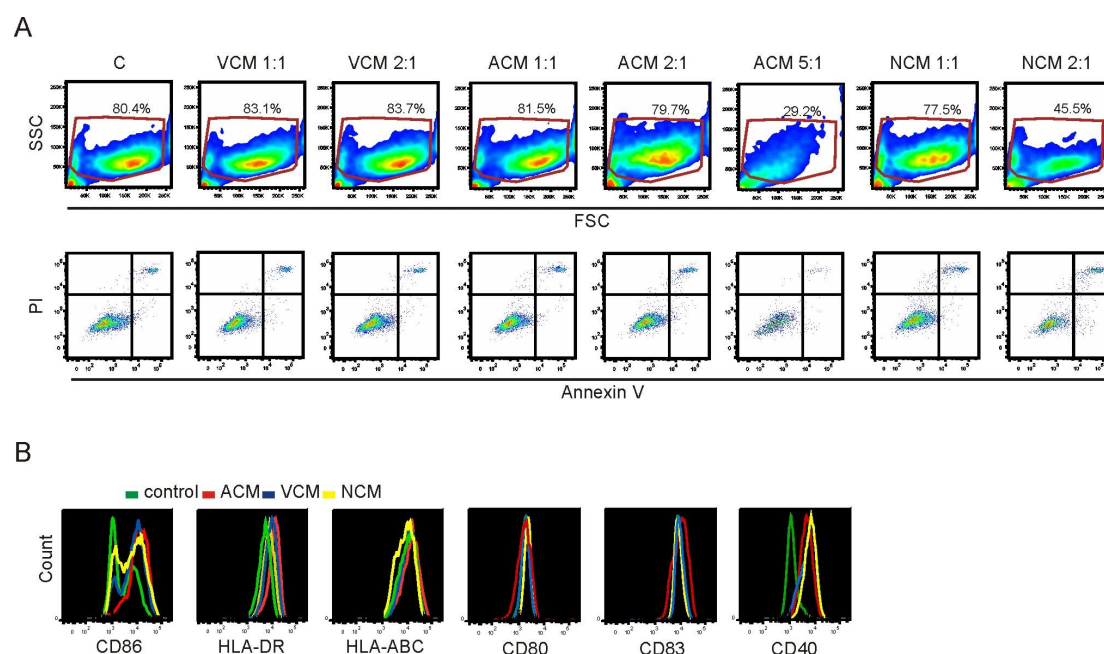


Figure 21. Basal DC phenotype upon activation with tumour cell supernatants. (A), Human monocyte-derived DC were incubated with supernatants of viable (VCM), apoptotic (ACM) or necrotic (NCM) MCF-7 cells at different ratios as indicated (1:1 = supernatant of 2×10^5 MCF-7 cells added to 2×10^5 DC) for 16 h, followed by staining with Annexin-V and propidium iodide (PI). Representative density plots of at least five independent experiments indicate size (FSC) and granularity (SSC) of the individual populations as well as the amount of dying cells (Annexin V versus PI). (B) Human monocyte-derived DC were controls or incubated with supernatants of viable (VCM), apoptotic (ACM) or necrotic (NCM) MCF-7 cells at a ratio of 1:1 for 16 h followed by FACS-analysis of CD86, HLA-DR, HLA-ABC, CD80, CD83 and CD40 surface expression. Representative histograms of at least four independent experiments are displayed.

This might be a mechanism of suppressing DC-dependent immunity by highly abundant dying tumour cells occurring e.g. after chemo/radiotherapy. Tumour cell supernatant-primed or unstimulated DC were co-cultured with IL-2-enriched autologous PBMC for 3 d (**Figure 22**).

6.3.1 Priming with apoptotic tumour cell supernatants suppresses DC-dependent tumour cell killing

IL-2 enriched PBMCs were mainly T cells, lacking significant amounts of mononuclear phagocytes, B cells or NK cells (< 1%) (not shown). Lymphocytes derived from these co-cultures were then added to living CellTracker Blue-stained MCF-7 cells for 4 h at different ratios and MCF-7/lymphocyte co-cultures were assessed for tumour cell death.

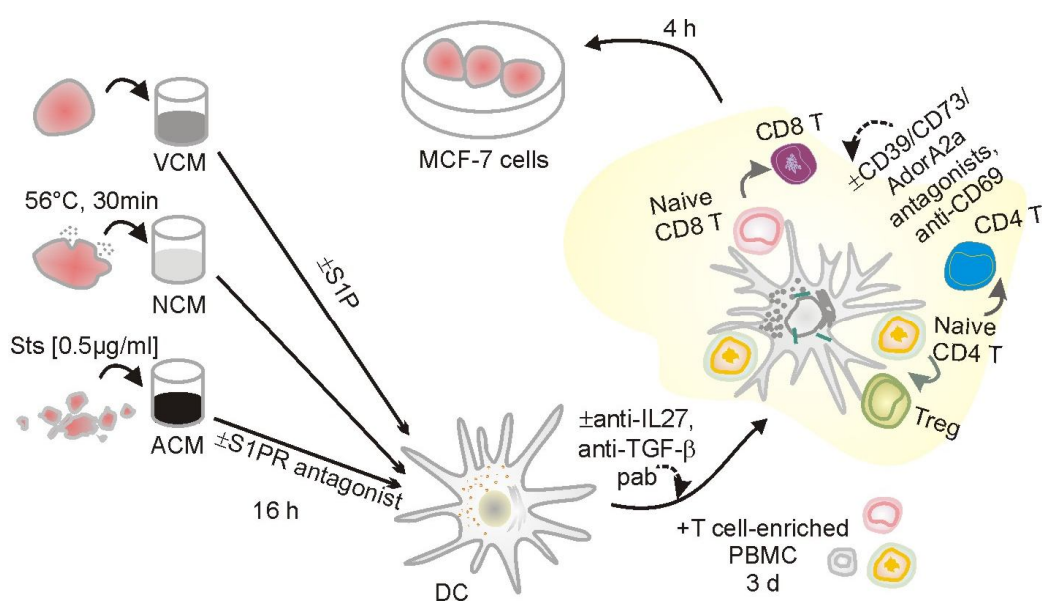


Figure 22. Experimental outline. Human monocyte-derived DC were controls or incubated with supernatants of viable (VCM), apoptotic (ACM) or necrotic (NCM) MCF-7 cells at a ratio of 1:1 (Supernatants of 2×10^5 MCF-7 added to 2×10^5 DC) for 16 h. Subsequently, supernatants were removed by washing and autologous T cell-enriched PBMC were added at a ratio of 10:1 (Tcells/DC) and cultured for another 3 d. The resulting polarized T cells were then co-cultured with living tumour cells for 4 h to determine cytotoxicity as described under Materials and Methods. Experimental interventions as outlined in the manuscript are indicated as dotted arrows.

Specific cytotoxicity was not observed in any experimental group up to a ratio of 1:2 (tumour cells to T cells) and reached a plateau at and above a ratio of 1:5 (**Figure 23A**).

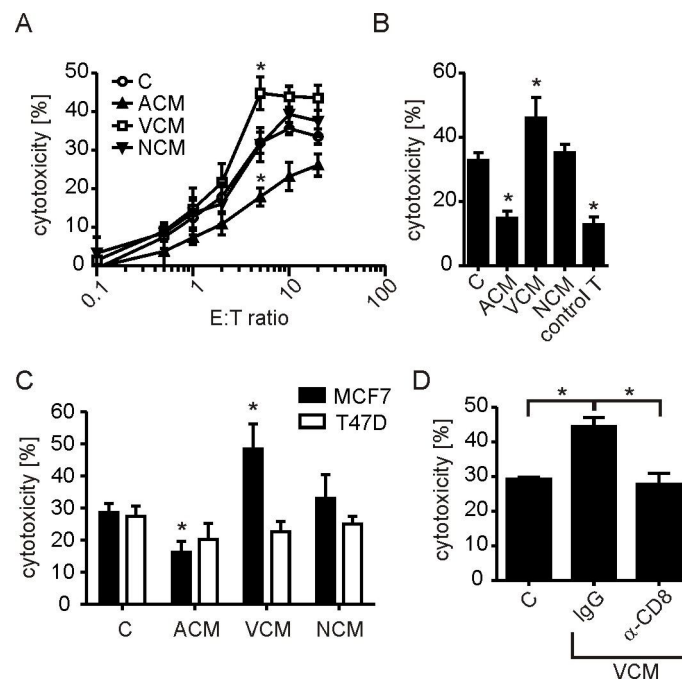


Figure 23. Viable cancer cell supernatants prime whereas supernatants of apoptotic cells suppress specific cytotoxicity. (A) CellTracker Blue-stained MCF-7 cells were incubated with T cells from individual co-cultures at effector to target (E:T) ratios of 0.1:1, 0.5:1, 1:1, 1:2, 1:5, 1:10, 1:20 for 4h. Cytotoxicity calculated for the ACM, VCM, NCM groups was compared to the control group. Data are means \pm SEM from five individual donors. (B) CellTracker Blue-stained MCF-7 cells were incubated with T cells from individual co-cultures as well as control T cells at ratios of 1:5 for 4 h. Cytotoxicity was calculated compared to non co-cultured MCF-7. Data are means \pm SEM from five individual donors. (C) CellTracker Blue-stained MCF7 (black bars) or T47D (white bars) breast carcinoma cells were incubated with T cells from individual co-cultures at 1:5 ratio for 4 h prior to cytotoxicity measurements. (D) T cells derived from VCM co-cultures were pre-incubated for 1h with anti-CD8 or the respective isotype control. These T cell were used to determine cytotoxicity against living MCF-7 cells compared to T cells from control co-cultures. Data are means \pm SEM from four individual donors. Asterisks indicate significant differences between groups, * = $p < 0.05$. p-values were calculated using ANOVA with Bonferroni's correction.

At a ratio of 1:5, the VCM group unexpectedly showed significantly higher cytotoxicity toward living MCF-7 cells compared to the control group, whereas T cells from the NCM group were not cytotoxic (**Figure 23A**). In contrast,

cytotoxicity towards living MCF-7 cells was reduced below controls when T cells from the ACM group were used. Cytotoxicity in this group was comparable to the basal cytotoxicity exhibited by IL-2 activated T cells without DC co-culture (**Figure 23B**). Importantly, VCM-induced cytotoxicity was cell-specific, since alterations in cytotoxicity were not observed when lymphocytes from MCF-7 supernatant-primed DC co-cultures were added to T47D cells (**Figure 23C**). In addition, CD8 depletion experiments suggested that CD8⁺ T cells were required for VCM-induced cytotoxicity in our system (**Figure 23D**).

6.3.2 Accumulation of CD39/CD69-expressing FoxP3⁺ Treg in ACM-primed co-cultures

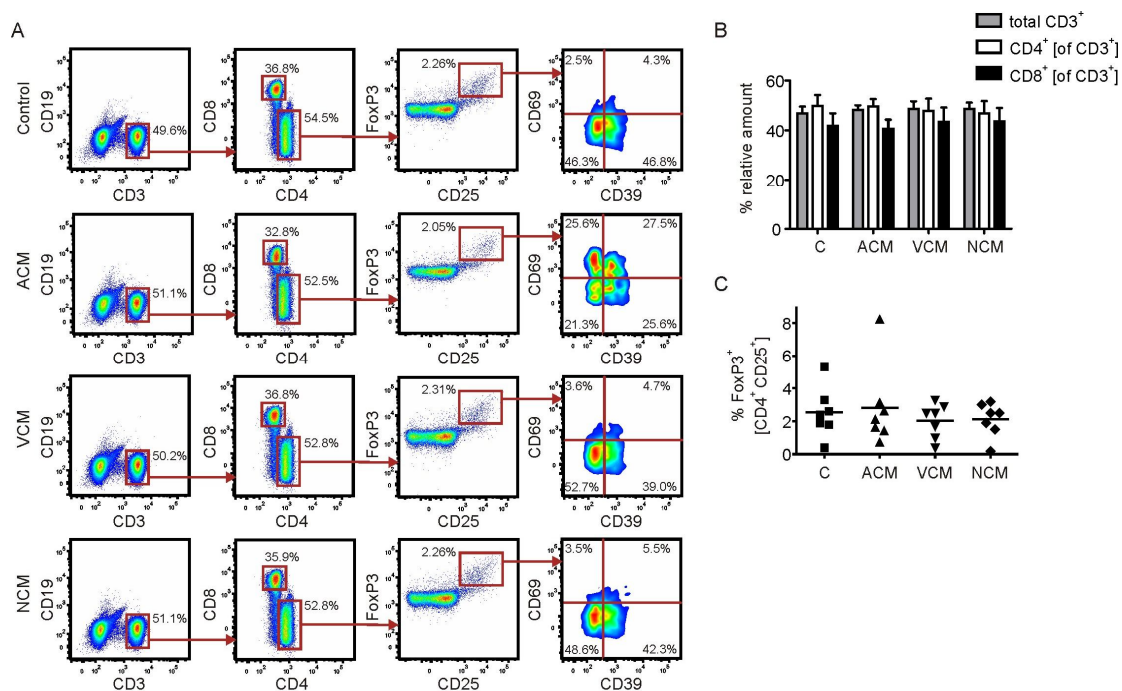


Figure 24. Relative amounts of T cell subsets and FoxP3-expressing Tregs. A-C, The profile of human T cell subpopulations from 3 d co-cultures with unprimed ACM-, VCM- or NCM-primed human monocyte-derived autologous DC were quantified using polychromatic flow cytometry. (A) Representative FACS traces for each co-culture setting are displayed. CD3⁺ T cells were sub-classed depending on expression of CD4 and CD8. CD4⁺ T cells were analyzed for expression CD25⁺ versus FoxP3⁺. CD4⁺CD25⁺FoxP3⁺ cells were further subdivided based on expression of CD39 and CD69. (B) Graphs display statistical quantitation of relative CD4 versus CD8 expression by CD3⁺ T cells. Data displayed as mean \pm SEM from

five individual donors. (C) Statistical quantification of FoxP3-expressing CD4⁺CD25⁺ T cells (Treg). Individual data points and the mean of seven individual donors are shown.

Since ACM-priming of DC suppressed cytotoxicity compared to the VCM- or NCM-primed groups, we determined whether alterations in the T cell populations occurred and if such alterations accounted for suppression of tumour cell killing. We analyzed the T cell profile in the co-cultures using polychromatic flow cytometry (**Figure 24A**). Regarding whole T cell numbers or basal T cell subsets, CD3⁺ T cell levels (not shown) and the ratio of CD4⁺ versus CD8⁺ T cells (**Figure 24B**) remained unchanged throughout the experimental groups. Next, we checked for a possible expansion of Treg, which were detected by intracellular staining of FoxP3 in CD4⁺CD25⁺ T cells (**Figure 24A**). The relative amount of FoxP3⁺ cells in the different experimental groups was unchanged (**Figure 24C**).

However, a different picture emerged when we investigated markers of Treg function. We stained Treg for expression of CD39 and CD69 (**Figure 24A**). The ectonucleotidase CD39 is expressed on naturally occurring FoxP3⁺ Treg [121], while the lymphocyte activation marker CD69 was shown to be expressed by Treg of cervical cancer patients [122].

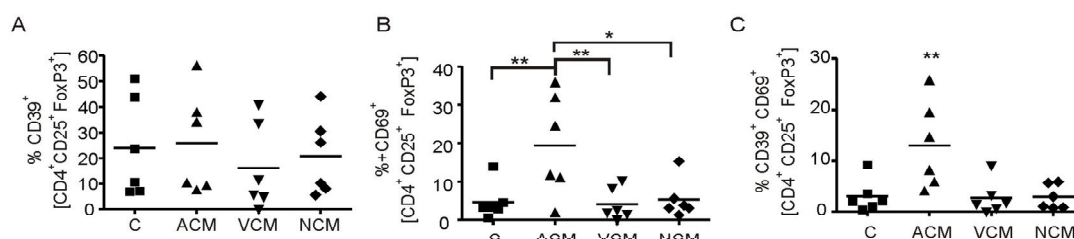


Figure 25. Apoptotic cell supernatants induce CD39 and CD69-expressing Treg. (A-C) Statistical quantification of CD39⁺ CD69⁻ Treg (A) CD39⁻ CD69⁺ Treg (B) CD39⁺ CD69⁺ Treg (C). Individual data points and the mean of six individual donors are shown. Asterisks indicate significant differences between groups, * = $p < 0.05$, ** = $p < 0.01$. p-values were calculated using ANOVA with Bonferroni's correction.

Whereas the expression of CD39 by Treg was not significantly different between the co-culture set-ups (**Figure 25A**), there were significant differences with regard to CD69 expression. CD69 was upregulated on Treg selectively in the ACM group (**Figure 25B**), which was most significant in the population co-expressing CD39 (**Figure 25C**).

This regulation pattern was Treg-specific, since neither CD39 nor CD69 were significantly upregulated in the total CD4⁺CD25⁺ population. CD39 was usually not expressed by CD8⁺ T cells. However, in approximately 20% of all donors, a small subpopulation of CD8⁺ T cells expressed CD39, which was selectively elevated in the ACM group, whereas CD69 expression was unaltered (not shown). Conclusively, ACM-primed, but not VCM or NCM-primed DC significantly induce surface CD69 expression in co-cultured CD39⁺ Treg.

Next, we asked if the accumulation of CD69-expressing Treg in the ACM group (**Figure 25B, 25C**) contributed to reduced MCF-7 cell killing (**Figure 23A**). In a first approach, we depleted Treg from unprimed, ACM-primed or VCM-primed co-cultures using commercial kits, before subjecting the remaining cells to the cytotoxicity assay.

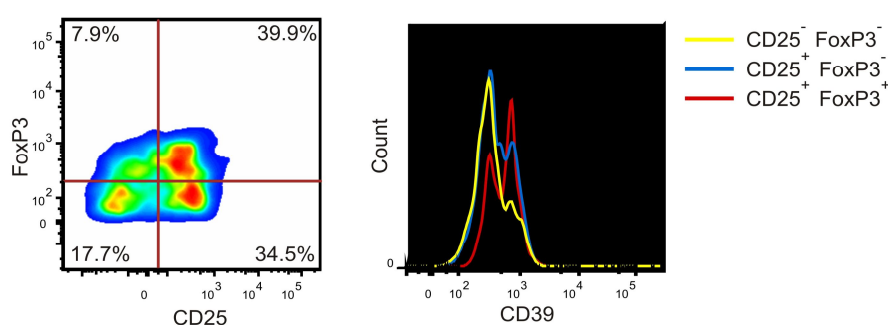


Figure 26. Purity of isolated CD4⁺CD25⁺ Treg. Left panel shows representative FACS trace indicating Foxp3 expression by CD4⁺CD25⁺ cells isolated from T cell co-cultures by magnetic bead sorting. Right panel displays co-expression of CD39 in subpopulations of isolated CD4⁺CD25⁺ T cells. T cell isolation was routinely controlled. Representative histograms of at least 6 independent experiments are displayed.

Of the isolated CD4⁺ CD25⁺ T cells, 40% expressed intracellular FoxP3, largely co-expressed CD39, and thus likely represent functional Treg (**Figure 26**).

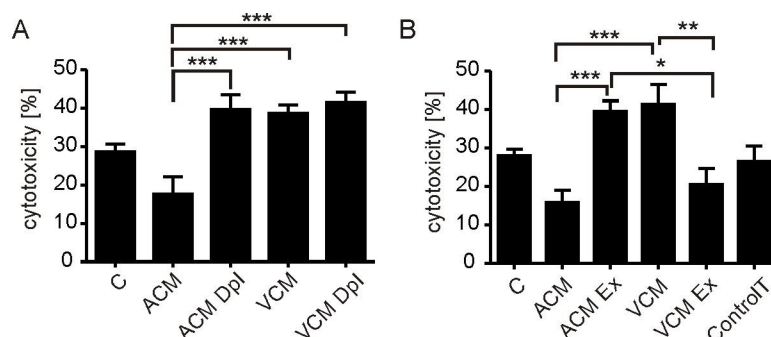


Figure 27. Treg confer ACM-induced suppression of cytotoxicity. (A) Treg were isolated from 2 d co-cultures of ACM- or VCM-primed human monocyte-derived autologous DC using automated magnetic bead-sorting. Residual T cells were added back to co-cultures for 24 h. MCF7 cells were then incubated with T cells from the ACM or VCM groups with or without (Dpl) Treg as well as controls and cytotoxicity was analyzed. Data are means \pm SEM from five individual donors. (B) Treg were isolated from 2 d co-cultures of ACM- or VCM-primed human monocyte-derived autologous DC using automated magnetic bead-sorting. Treg from ACM groups were then mixed with Treg-depleted T cells from VCM groups and vice versa and added back to the co-cultures for 24 h. MCF-7 cells were subsequently incubated with T cells from the Treg exchange groups (Ex) compared to non-exchanged groups and the control. T cells alone cultured without DC are indicated as control T. Data are means \pm SEM from six individual donors. Data are means \pm SEM from four individual donors. Asterisks indicate significant differences between groups, * = $p < 0.05$, ** = $p < 0.01$, *** = $p < 0.001$. p-values were calculated using ANOVA with Bonferroni's correction.

Interestingly, Treg-depleted lymphocytes from the ACM group were significantly more cytotoxic compared to the complete lymphocyte fraction, whereas Treg-depletion from the VCM-primed co-culture did not affect the enhanced cytotoxicity observed in the VCM group (**Figure 27A**).

Next, we asked whether the Treg-dependent suppression of cytotoxicity in the ACM group might be transferable. We isolated Treg from ACM-primed or VCM-primed co-cultures on day 2 and added the Treg from the ACM group to the Treg-depleted lymphocytes of the VCM group and vice versa. After another 24 h of co-incubation, these mixed lymphocyte populations were used

in the cytotoxicity assay. Indeed, Treg from the ACM group significantly suppressed cytotoxicity of Treg-depleted lymphocytes from the VCM group. On the other hand Treg from the VCM group were unable to suppress cytotoxicity in the ACM group (**Figure 27B**). Thus, ACM-priming provided FoxP3⁺ T cells with the ability to suppress cytotoxicity, which was correlated to expression of CD39 and CD69. Depletion of these cells restored cytotoxicity to a level comparable to the VCM-primed group.

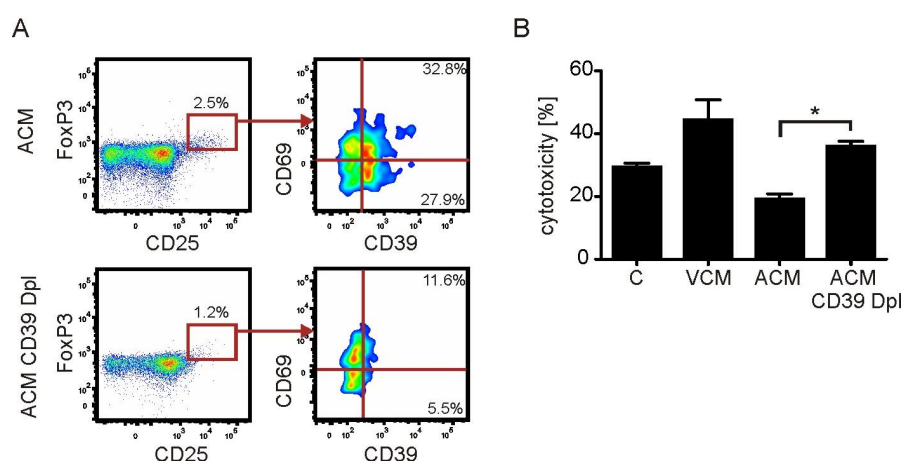


Figure 28. CD39 depletion restores ACM-induced suppression of cytotoxicity. (A, B) CD39⁺ cells were depleted from IL-2 enriched PBMC using anti-FITC microbeads after labeling with CD39-FITC antibody by automated magnetic bead-sorting. CD39-depleted (CD39 Dpl) T cells were added to co-cultures in the same ratio as unmodified T cells. (A) Representative FACS traces displaying the relative amount of CD39⁺CD69⁺ cells in CD4⁺CD25⁺FoxP3⁺ T cells in ACM co-cultures of CD39-depleted and unmodified T cells. (B) MCF7 cells were incubated with T cells from the VCM group, the ACM group with or without CD39⁺ T cell depletion (Dpl) as well as controls and cytotoxicity was analyzed. Data are means \pm SEM from four individual donors. Asterisks indicate significant differences between groups, * = $p < 0.05$, ** = $p < 0.01$, *** = $p < 0.001$. p-values were calculated using ANOVA with Bonferroni's correction.

We explored the relationship of CD39 and CD69-expressing Treg with suppression of cytotoxicity by further depleting CD39⁺ cells from IL-2-enriched lymphocytes before adding them to DC co-cultures. T cells from these co-cultures displayed lower levels of Treg and completely lacked the CD39⁺ subpopulation, indicating that CD39⁺ Treg upregulate CD69 expression in

ACM co-cultures, whereas upregulation of CD39 by CD69⁺ cells could be ruled out (**Figure 28A**). Importantly, depletion of CD39⁺ T cells restored cytotoxicity in the ACM group as observed when depleting total CD25⁺ cells (**Figure 28B**).

6.3.3 S1P in ACM confers suppression of cytotoxicity by activating S1PR4 on DC

Next, we performed experiments to interfere with the immunosuppressive properties of ACM in order to determine whether CD69 expression on FoxP3⁺ T cells accounted for reduced cytotoxicity.

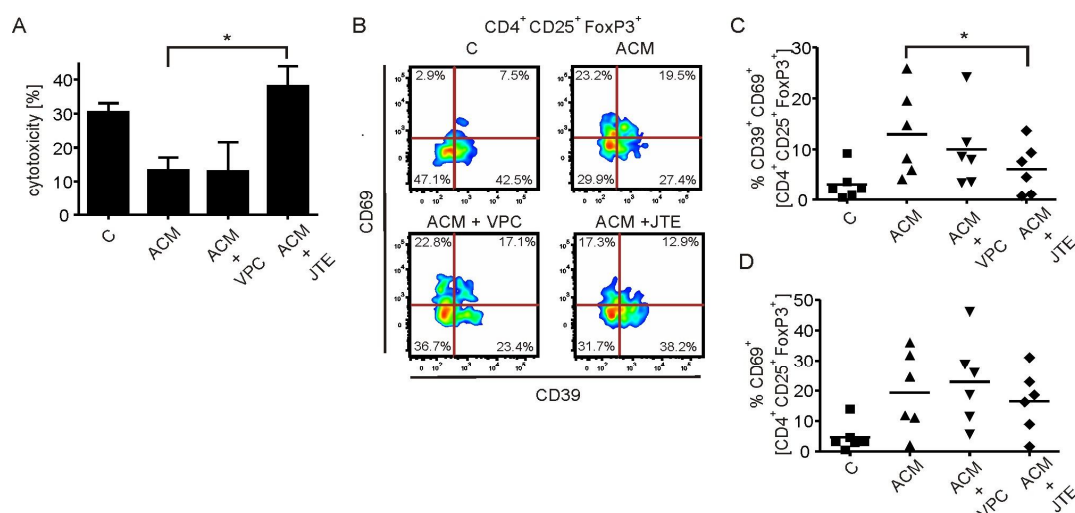


Figure 29. ACM-dependent suppression of cytotoxicity functions through S1P receptors. (A-D) T cells were co-cultured with control or ACM-primed autologous DC with or without the S1PR2/4 antagonist JTE-013 or the S1PR1/3 antagonist VPC23019. (A) Cytotoxicity induced by T cells from individual co-cultures towards living MCF-7 cells. Data are means \pm SEM from six individual donors. (B) Representative FACS traces of CD39 and CD69 expression by Treg from the individual co-cultures. C,D, Statistical evaluation of CD39⁺ CD69⁺ Treg (C) or CD39⁻ CD69⁺ Treg (D). Individual data points and the mean of six individual donors are shown. Asterisks indicate significant differences between groups, * = $p < 0.05$, ** = $p < 0.01$, *** = $p < 0.001$. p-values were calculated using ANOVA with Bonferroni's correction.

We asked for the factor(s) in ACM inducing DC-dependent suppression of cytotoxicity. Among the immunomodulatory factors secreted by AC is the lipid mediator S1P [67], which was present in ACM (~ 10 nM, determined routinely [123]). S1P couples to five specific receptors (S1PR), with human DC expressing S1PR1-4.

Pharmacological inhibition of S1PRs during ACM-priming of human DC was used to test an impact of AC-derived S1P on DC-dependent T cell activation. JTE-013, a partial inhibitor for S1PR2 (IC₅₀ 1.5 μ M) and a full inhibitor of S1PR4 (IC₅₀ 4.5 μ M) [124] significantly prevented ACM-induced suppression of cytotoxicity when used at high concentrations (15 μ M), whereas the S1PR1/3 inhibitor VPC23019 (1 μ M) did not (**Figure 29A**).

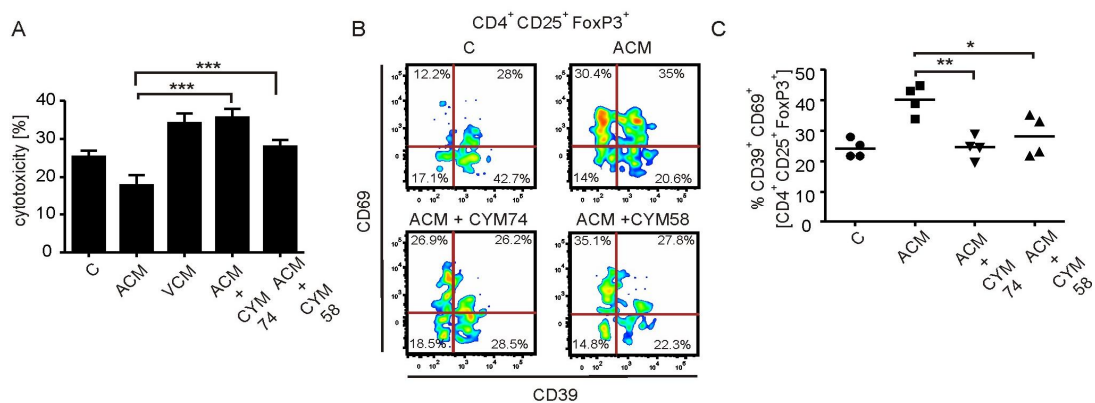


Figure 30. S1PR4 on DC conveys ACM-dependent suppression of cytotoxicity. (A-C) T cells were co-cultured with control or ACM-primed autologous DC with or without the S1PR4 antagonists CYM74 or CYM58 (A) Cytotoxicity induced by T cells from individual co-cultures towards living MCF-7 cells. Data are means \pm SEM from four individual donors. (B) Representative FACS traces of CD39 and CD69 expression by Treg from the individual co-cultures. (C) Statistical evaluation of CD39⁺ CD69⁺ Treg from individual co-cultures. Individual data points and the mean of four individual donors are shown. Asterisks indicate significant differences between groups, * = $p < 0.05$, ** = $p < 0.01$, *** = $p < 0.001$. p -values were calculated using ANOVA with Bonferroni's correction.

Diminishing cytotoxicity by the S1PR2/4 inhibitor JTE-013 correlated with a significant reduction of the CD39⁺CD69⁺ Treg population, whereas the relative proportion of CD69⁺CD39⁻ Treg population was unchanged (**Figure 29B-D**).

To substantiate these findings and to explicitly identify the S1PR subtype we used the recently described highly specific S1PR4 antagonists CYM50374 and CYM50358 (200 nM each) [84]. Both substances reversed suppression of cytotoxicity induced by ACM priming (**Figure 30A**) and decreased the expansion of CD39⁺CD69⁺ Treg (**Figure 30B, 30C**).

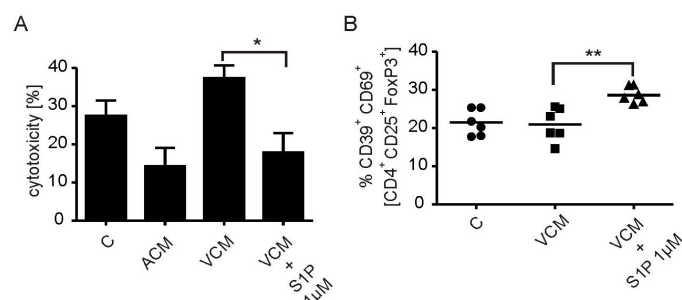


Figure 31. Addition of S1P to VCM mimics ACM (A,B) T cells were co-cultured with control, ACM- or NCM-primed autologous DC with or without adding 1 μ M S1P (A), Cytotoxicity induced by T cells from individual co-cultures towards living MCF-7 cells. Data are means \pm SEM from six individual donors. (B), Statistical evaluation of CD39⁺ CD69⁺ Treg from individual co-cultures. Individual data points and the mean of four individual donors are shown. Asterisks indicate significant differences between groups, * = $p < 0.05$, ** = $p < 0.01$, *** = $p < 0.001$. p-values were calculated using ANOVA with Bonferroni's correction.

Moreover, supplying S1P (1 μ M) during VCM-priming of DC suppressed the VCM-induced cytotoxicity (**Figure 31A**) and increased the amount of CD39⁺CD69⁺ Treg (**Figure 31B**). These findings indicate that S1PR4 activation by S1P in ACM enabled DC to induce CD69 expression on Treg, correlating to suppressed cytotoxicity.

6.3.4 ACM-primed DC secrete IL-27 to activate suppressive Treg

Apparently tumour-associated DC exist in different functional states depending on the microenvironment they are exposed to (i.e. tumour mass versus TDLN) [59]. We asked which parameters of DC functionality were altered by ACM. For maturation markers, each tumour supernatant slightly induced HLA-DR expression on DC as compared to the control group. CD80

expression remained unchanged. CD83 expression was induced slightly only in the ACM group. HLA-ABC expression remained largely unchanged, except for a reduction with NCM, whereas CD86 and CD40 expression were strongly induced with all conditioned media (**Figure 21B**). Conclusively, immunosuppression by ACM-priming was not dependent on altered maturation.

Apart from maturation, functional markers of tolerogenic DC include proteins such as IDO. IDO is an intracellular enzyme involved in tryptophan metabolism along the kynurenine pathway. IDO has been implicated in tolerance induction mediated through depleting tryptophan, which halts T cell proliferation and/or by accumulation of 3-hydroxykynurenine or 3-hydroxyanthranilic acid, which is toxic to lymphocytes [125]. IDO is expressed by DC interacting with AC [126]. We saw a marked upregulation of IDO protein expression in DC treated with ACM (**Figure 32A**).

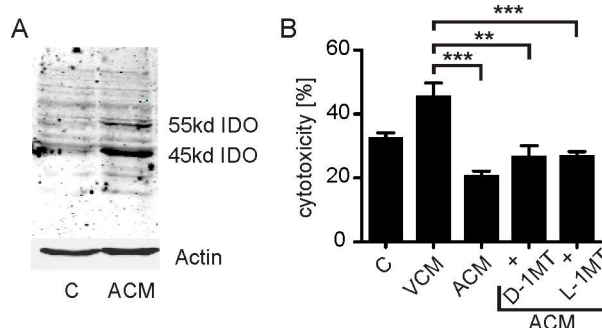


Figure 32. ACM-induced IDO expression and the effect of IDO inhibition on ACM-induced suppression of cytotoxicity. (A) IDO protein expression in untreated DC (C), or in ACM-stimulated DC (ACM) from the same donor was analyzed by Western blotting. Actin serves as a loading control. Representative blot of three independent experiments using different donors is shown. (B) DC were unprimed or treated with or treated with VCM, NCM or ACM with or without pre-incubation with 1mM of the IDO inhibitors D-1MT (dextro-1-methyl tryptophan) or L-1MT (levo-1-methyl tryptophan) for 2 h. These DC were co-cultured with autologous T cells for 3 d. Cytotoxicity of resulting T cells towards living MCF-7 cells is shown. Cytotoxicity was calculated compared to non co-cultured MCF-7. Data are means \pm SEM, n = 5. Individual data points and the mean of five individual donors are shown. Asterisks

indicate significant differences between groups, * = $p < 0.05$, ** = $p < 0.01$, *** = $p < 0.001$. p-values were calculated using ANOVA with Bonferroni's correction.

Thus, we asked whether this enzyme had any impact on the observed immunosuppression in the ACM co-cultures. We found that neither inhibition of IDO1 using D-1MT nor IDO2 with L-1MT was able to significantly restore cytotoxicity compared to the VCM group (**Figure 32B**). However, in some experiments L-1MT had minor efficiency in elevating cytotoxicity.

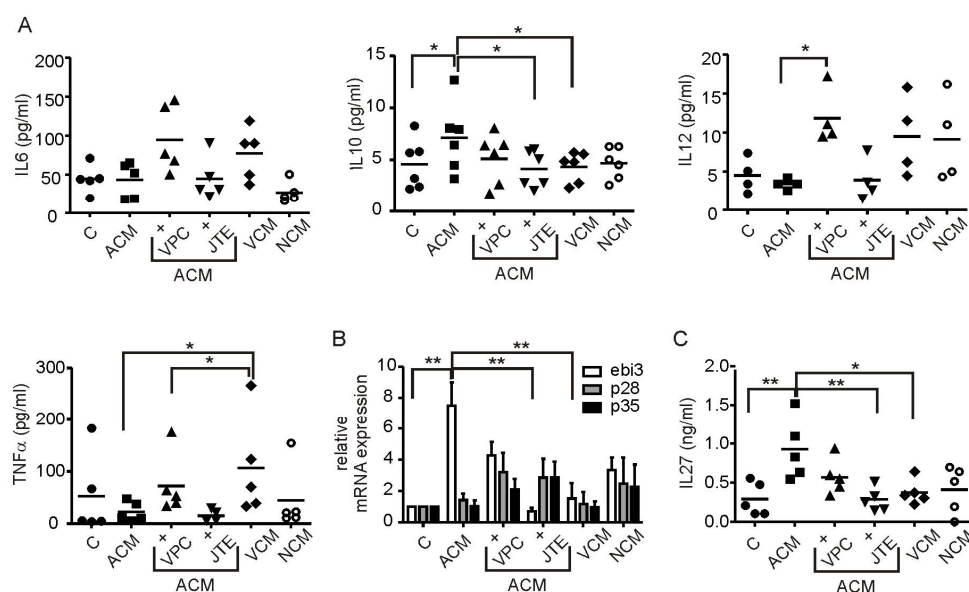


Figure 33. Influence of ACM on cytokine induction. (A-C) Human monocyte-derived DC were controls or incubated with VCM, NCM or ACM with or without the addition of JTE-013 (15 μ M) or VPC23019 (1 μ M) for 16 h. (A) Secreted cytokines were quantified using Human inflammatory cytokine Cytometric Bead Arrays. Quantification of IL-6, TNF- α , IL-12 and IL-10 in DC supernatants is shown. Individual data points and the mean of five individual donors are shown. (B) Relative mRNA expression of ebi3, p28 and p35 quantitated via qPCR is displayed. Data are means \pm SEM from four individual donors. (C) ELISA quantification of IL-27 protein secretion by DC from the individual groups is shown. Individual data points and the mean of five individual donors are shown. Asterisks indicate significant differences between groups, * = $p < 0.05$, ** = $p < 0.01$, *** = $p < 0.001$. p-values were calculated using ANOVA with Bonferroni's correction.

Next we measured the release of inflammatory cytokines by Cytometric Bead Arrays using flow cytometry 16 h after stimulation of DC with tumour cell

supernatants, including ACM stimulation in the presence of S1PR antagonists to detect meaningful regulation patterns. We did not observe release of significant amounts of IL-12, although there was a tendency towards enhanced IL-12 secretion by VCM-primed DC versus their ACM-primed counterparts (**Figure 33A**).

IL-6 showed a trend towards enhanced production in the VCM group, which was significant for TNF- α . However, compared to ACM, secretion of these cytokines was enhanced when using VPC23019, but not JTE-013, which did not correlate with changes in cytotoxicity. Release of the anti-inflammatory cytokine IL-10 followed a meaningful regulation pattern, since it was enhanced with ACM treatment as compared to all other treatments except for the ACM+VPC23019 group (**Figure 33A**). However, release of IL-10 was in the low pg/ml range, largely restricting its potential impact in the co-culture setting.

Searching for other candidates, we recognized that among cytokines that shape T cell-mediated immunity IL-12 family members play a central role. Despite having structurally similar subunits or even sharing identical subunits, these cytokines may enhance generation of Th1, Th17 or Treg [127].

For instance, the protein encoded by Epstein-Barr virus induced gene 3 (ebi3) is a common subunit of IL-35 and IL-27, both of which are recently emerging cytokines implicated in T cell biology. Analyzing mRNA expression in human DC in analogy to secreted cytokines as mentioned above, we noticed that ebi3 mRNA was upregulated upon incubation of DC with ACM after 16 h. This was S1PR2/4-dependent as determined by using JTE-013 or VPC23019 along with ACM (**Figure 33B**). Since expression of p28 and p35, the complementary subunits for IL-27 or IL-35 respectively, were unchanged with ACM treatment (**Figure 33B**); we quantified secretion of ebi3 subunit containing cytokines using commercial ELISA kits. While detecting IL-35 was unsuccessful, IL-27 was significantly upregulated in ACM-treated DC compared to controls or VCM-primed DC. This effect was completely abolished when inhibiting the S1PR2/4 (**Figure 33C**).

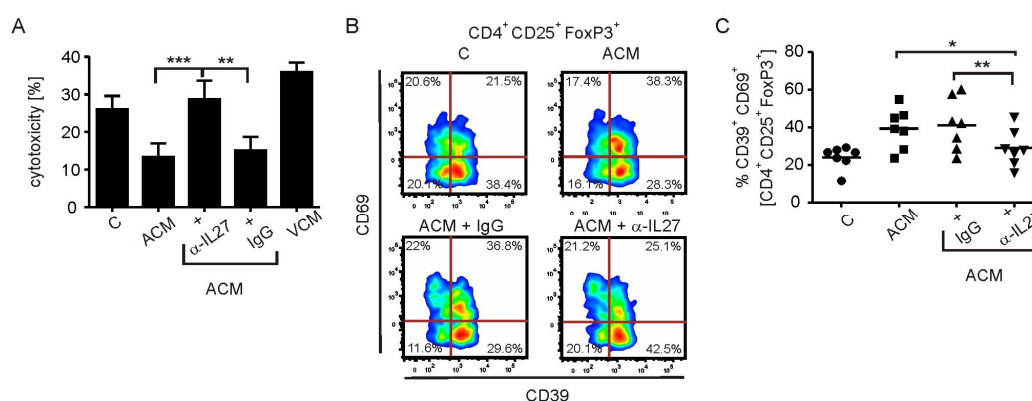


Figure 34. ACM induces IL-27 in DC in a S1PR4-dependent manner to generate Treg. (A-C) T cells were co-cultured with control, VCM- or ACM-primed autologous DC with or without the addition of an IL-27-neutralizing antibody (α -IL27) or the isotype control (IgG). (A) Cytotoxicity induced by T cells from individual co-cultures towards living MCF-7 cells. Data are means \pm SEM from seven individual donors. (B) Representative FACS traces of CD39 and CD69 expression by Treg from the individual co-cultures. (C) Statistical quantification of CD39⁺ CD69⁺ Treg. Individual data points and the mean of seven individual donors are shown, $n = 7$. Asterisks indicate significant differences between groups, * = $p < 0.05$, ** = $p < 0.01$, *** = $p < 0.001$. p -values were calculated using ANOVA with Bonferroni's correction.

To validate the role of IL-27 released by DC in generating suppressive Treg, we blocked its function by adding a specific IL-27-neutralizing antibody versus a non-specific isotype control (each 1 μ g/ml) to DC before adding autologous T cells. Blocking IL-27 potentially reduced ACM-induced suppression of cytotoxicity as compared to the isotype control (**Figure 34A**), which again correlated with attenuated ACM-induced CD69 expression in CD39⁺ Treg (**Figure 34B, 34C**).

We wondered whether induction of cell death using immunogenic drugs would deliver comparable results with regard to IL-27-dependent CD39⁺ CD69⁺ Treg expansion. When we compared effects of supernatants of oxaliplatin-treated MCF-7 cells (OXA-ACM) with staurosporine-treated cells (STS-ACM) on DC, we noticed significantly lower ebi-3 expression in OXA-ACM-treated DC (**Figure 35A**). Correlating to that, we observed reduced CD69⁺CD39⁺ Treg in OXA-ACM co-cultures compared to STS-ACM co-cultures (**Figure 35B**).

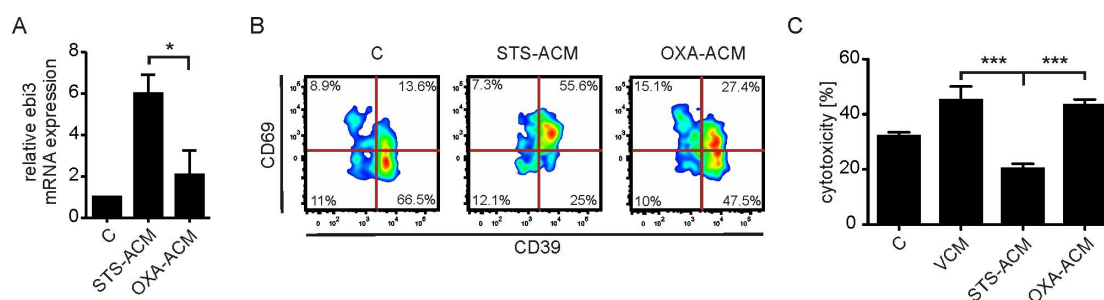


Figure 35. OXA-ACM exhibits higher cytotoxicity compared to STS-ACM. (A-C) MCF-7 cells were subjected to 0.5 $\mu\text{g/ml}$ staurosporine (STS) or 30 μM oxaliplatin (OXA) to induce cell death and supernatants were harvested. (A) Expression of *ebi3* mRNA in DC treated with STS-ACM or OXA-ACM compared to control DC is displayed. Data are means \pm SEM from four individual donors. (B) T cells were co-cultured with control, VCM-, or STS-ACM- or OXA-ACM-primed autologous DC. Representative FACS traces of CD39 and CD69 expression by Treg from the individual co-cultures are shown. (C) Cytotoxicity induced by T cells from individual co-cultures towards living MCF-7 cells. Data are means \pm SEM from five individual donors. Asterisks indicate significant differences between groups, * = $p < 0.05$, ** = $p < 0.01$, *** = $p < 0.001$. p-values were calculated using ANOVA with Bonferroni's correction.

This difference in the Treg population was again reflected by the cytotoxic potential of co-cultured T cells as T cells from the OXA-ACM group were significantly more cytotoxic compared to T cells from the STS-ACM group (**Figure 35C**). Hence, also in our hands oxaliplatin induced immunogenic cell death, which correlated with reduced *ebi-3* expression and thus, likely IL-27 production, as well as reduced CD69 expression on CD39⁺ Treg.

6.3.5 Suppression of cytotoxicity is reduced by interference with adenosine generation

We went on to identify a mechanism of how Treg suppressed cytotoxicity, which likely required functional CD8⁺ T cells. Analyzing the contents of the T cell-derived cytokines IFN- γ , IL-10, IL-4, IL-17, IL-2 from co-cultures after day 3, did not reveal any regulation patterns (not shown). Immunosuppression by Treg can be mediated by various mechanisms including production of effector cytokines such as TGF- β and IL-10 [128].

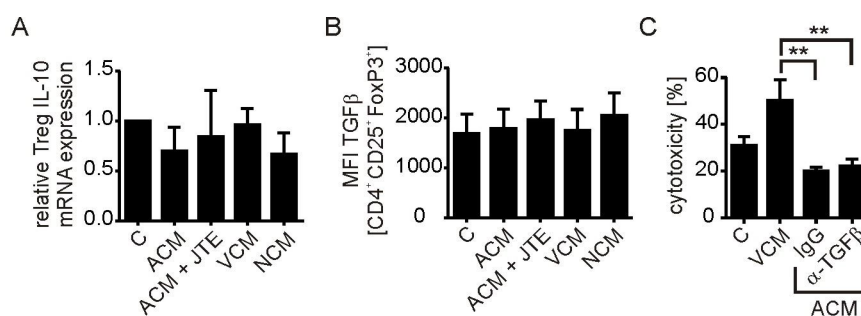


Figure 36. IL-10 and TGF- β are not involved in suppressing cytotoxicity. (A) Magnetic bead-isolated Treg from the individual co-cultures at day 3 were analyzed for relative IL-10 mRNA expression via qPCR. Data are means \pm SEM from five individual donors. (B) TGF- β expression in CD4⁺CD25⁺FoxP3⁺ Treg from whole individual co-cultures was determined via intracellular staining and polychromatic flow cytometry. Statistical evaluation TGF- β -dependent mean fluorescence intensity (MFI) is displayed. Data are means \pm SEM from four individual donors. (C) T cells were co-cultured with control, VCM- or ACM-primed autologous DC with or without the addition of a TGF- β -neutralizing antibody (α -TGF- β) or the isotype control (IgG). Cytotoxicity induced by T cells from individual co-cultures towards living MCF-7 cells was determined. Data are means \pm SEM from five individual donors. Asterisks indicate significant differences between groups, * = $p < 0.05$, ** = $p < 0.01$. p -values were calculated using ANOVA with Bonferroni's correction.

We checked the expression of these cytokines specifically in Treg using two different approaches. IL-10 expression was determined on mRNA level after isolation of Treg from the different treatment groups as mentioned above, whereas TGF- β was quantified by intracellular staining using flow cytometry. Unexpectedly, neither IL-10 (**Figure 36A**) nor TGF- β expression (**Figure 36B**) was significantly altered in Treg upon ACM-stimulation. In addition, neutralizing TGF- β in ACM co-cultures with a specific antibody did not restore cytotoxicity (**Figure 36C**), thus ruling out TGF- β as a candidate for immunosuppression in this set-up.

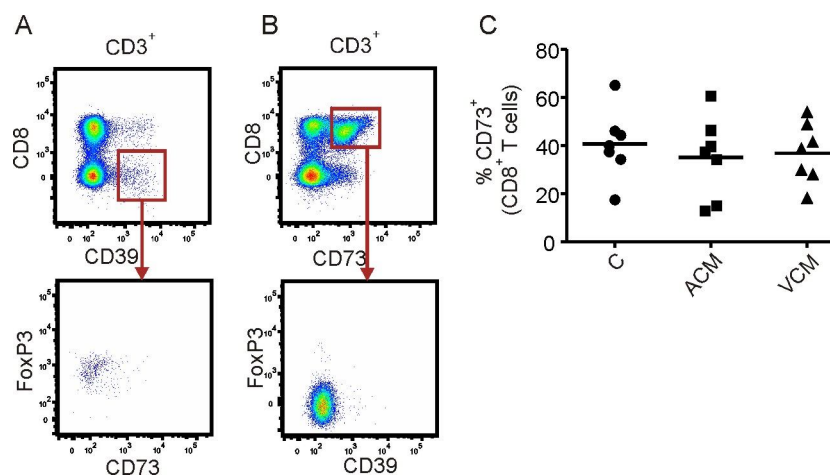


Figure 37. Relative expression of ectonucleotidases CD39 or CD73 by T cells. (A) Relative FACS traces indicating CD39⁺ expression by CD8⁺ T cells from control co-cultures. Gating on these cells and evaluation of FoxP3 versus CD73 expression reveals that CD39 is selectively expressed by CD4⁺ Treg. (B) Relative FACS traces indicating CD73⁺ expression by CD8⁺ T cells from control co-cultures. Gating on these cells and evaluation of FoxP3 versus CD39 expression reveals that CD73 is selectively expressed by CD8⁺ FoxP3⁻ T cells. (C) Quantification of CD73 expression by CD8⁺ T cells from individual co-cultures as indicated analyzed by flow cytometry is displayed. Individual data points and the mean of seven individual donors are shown. Asterisks indicate significant differences between groups, * = $p < 0.05$, ** = $p < 0.01$. p-values were calculated using ANOVA with Bonferroni's correction.

Another molecule known for its immunosuppressive function is the purine nucleotide adenosine. Extracellular adenosine inhibits various T cell functions among them proliferation and/or priming of CD8⁺ T cells [129]. We saw the involvement of CD8 T cells in VCM-induced cytotoxicity (**Figure 23D**). Adenosine is produced by the sequential breakdown of ATP by e.g. the ectonucleotidases CD39 and CD73.

Previous reports indicated that CD39 is expressed by human Treg, whereas CD73 might not be co-expressed by these cells [130], which we confirmed in our system. Whereas CD39 was mainly expressed by CD4⁺ Treg, which did not express CD73 (**Figure 37A**), CD73 was expressed by CD8⁺ cells (**Figure 37B**). We did not observe alterations in CD73 expression by CD8⁺ T cells upon priming with either ACM or VCM (**Figure 37C**).

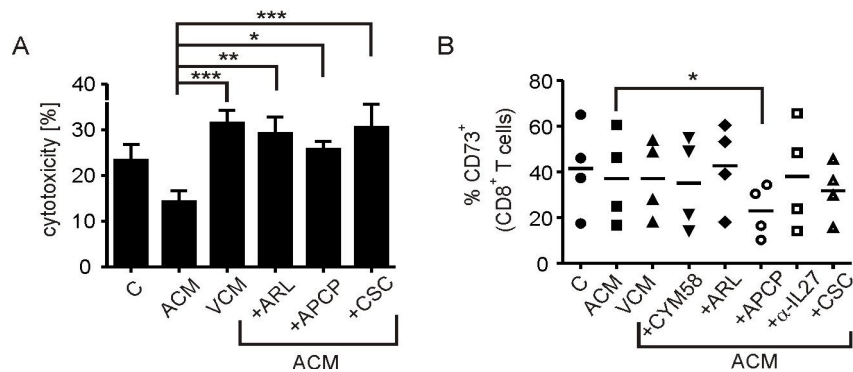


Figure 38. Inhibition of ectonucleotidases and adenosine receptor A2a restores cytotoxicity (A) T cells were co-cultured with control, VCM- or ACM-primed autologous DC with or without addition of the CD39 inhibitor (ARL) (250 μ M), the CD73 inhibitor (APCP) (100 μ M) or the adenosine receptor A2a (CSC) (10 mM). Cytotoxicity induced by T cells from individual co-cultures towards living MCF-7 cells is shown. Data are means \pm SEM from six individual donors. Asterisks indicate significant differences between groups, * = $p < 0.05$, ** = $p < 0.01$, *** = $p < 0.001$. p-values were calculated using ANOVA with Bonferroni's correction.

Adenosine seemed to be clearly involved in ACM- induced suppression of cytotoxicity in our system. Addition of the CD39 inhibitor ARL67156 as well as the CD73 inhibitor APCP [86] as well as the adenosine receptor A2a inhibitor CSC [87] to the co-cultures on day 2 restored cytotoxicity brought about by ACM-priming (**Figure 38A**). These suggested a role for adenosine generation and function in our system. None of the compounds altered expression of CD39 by Treg or of CD73 by CD8⁺ T cells except for the CD73 inhibitor APCP, which diminished surface expression of CD73 on CD8⁺ T cells, an unrecognized mechanism of its action (**Figure 38B**).

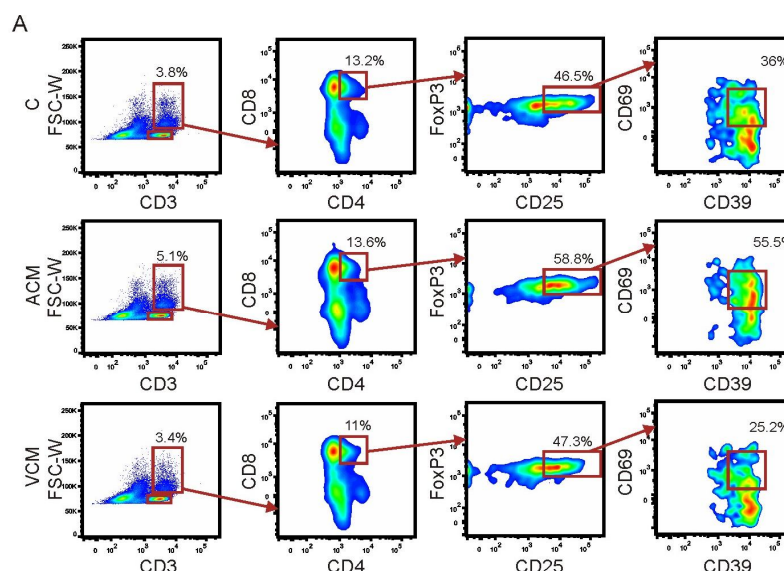


Figure 39. Surface profiling of doublet T cell populations. (A) Representative FACS traces show analysis of the FSC-W gated $CD3^+$ doublet population of cells from control, ACM- or VCM-primed co-cultures. $CD4^+CD8^+$ events in the doublets, most likely aggregates of $CD4^+$ and $CD8^+$ T cells were analyzed for expression of CD25, FoxP3, CD39 and CD69. Representative FACS traces are shown.

So far, we observed accumulation of CD69-expressing $CD39^+$ Treg in ACM-primed co-cultures, which directly correlated to suppression of cytotoxicity. We wondered whether CD69 expression on Treg might be directly involved in suppressing $CD8^+$ T cell function.

The concerted action of CD39 and CD73 seemed to be important for suppression of cytotoxicity induced by ACM-priming although these molecules were expressed by different cells. CD69 is a member of the c-type lectin family, proteins which regulate cell-cell contact. We hypothesize that CD69-bearing $CD39^+$ Treg might establish direct contact with CD73-expressing $CD8^+$ T cells to ensure efficient adenosine generation and subsequent immunosuppression.

To approach this question, we analyzed $CD4^+CD8^+$ events within $CD3^+$ doublets from control, ACM and VCM co-cultures using polychromatic flow cytometry. These $CD4^+CD8^+$ doublets were generally enriched in

CD25⁺FoxP3⁺ cells expressing CD69 (not shown). However this enrichment was strongly pronounced in the ACM group compared to the control or VCM groups (**Figure 39A, 40A**).

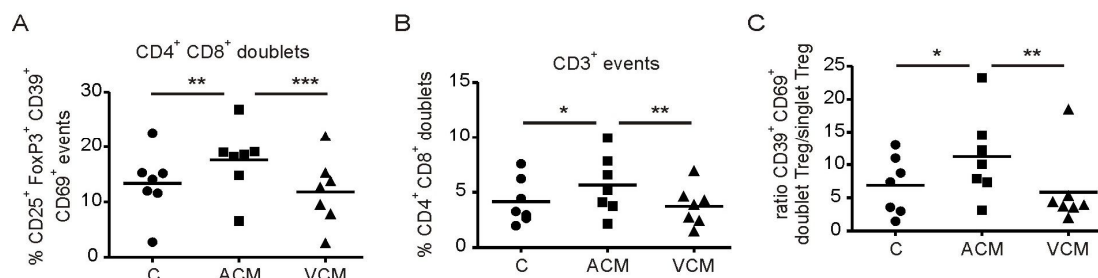


Figure 40. CD39/CD69-expressing Treg are enriched in CD4⁺CD8⁺ doublet events. (A) Quantification of CD25⁺FoxP3⁺CD39⁺CD69⁺ events in the doublet CD4⁺CD8⁺ population is shown. Individual data points and the mean of seven individual donors are shown. (B) The amount of CD4⁺ and CD8⁺ positive events in the CD3⁺ doublets was quantified. Individual data points and the mean of seven individual donors are shown. (C) The ratio of CD25⁺FoxP3⁺CD39⁺CD69⁺ events in doublets versus singlets in ACM-, VCM- or control co-cultures is shown. Individual data points and the mean of seven individual donors are shown. Asterisks indicate significant differences between groups, * = $p < 0.05$, ** = $p < 0.01$, *** = $p < 0.001$. p-values were calculated using ANOVA with Bonferroni's correction or paired Student's t-test.

Additionally, there was a significant reduction in enrichment of CD4⁺CD8⁺ events within whole CD3⁺ doublets in the ACM group as compared to the control or VCM co-cultures (**Figure 40B**). This pattern was also observed when analyzing whether CD25⁺CD39⁺CD69⁺ events were specifically enriched in doublets as compared to the singlet population (**Figure 40C**). Interestingly, though Treg numbers were generally lower in doublets compared to singlets, the percentages of CD25⁺CD39⁺CD69⁺ events was higher in doublets compared to singlets.

As a next step, we wondered whether antibody-mediated CD69 depletion would reduce CD4⁺CD8⁺ doublet formation as well as enrichment of CD25⁺CD39⁺CD69⁺ events in doublets of the ACM group.

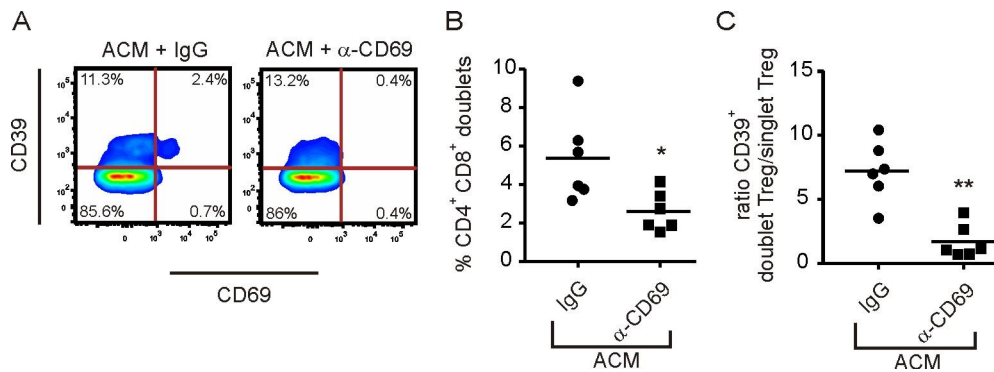


Figure 41. CD69 neutralization reduces the doublet T cell population (A) ACM co-cultures were treated with either anti-CD69 or the isotype control on day 2. Representative FACS traces show CD39 and CD69 expression in CD4⁺ T cells on day 3. (B) The amount of CD4⁺ and CD8⁺ positive events in CD3⁺ doublets in ACM-co-cultures with anti-CD69 (α -CD69) or the isotype control (IgG) on day 3 is displayed. Individual data points and the mean of six individual donors are shown, $n = 6$. (C) The ratio of CD25⁺FoxP3⁺CD39⁺ events in doublets versus singlets of ACM-co-cultures with anti-CD69 (α -CD69) or the isotype control (IgG) on day 3 is shown. Individual data points and the mean of six individual donors are shown. Asterisks indicate significant differences between groups, * = $p < 0.05$, ** = $p < 0.01$, *** = $p < 0.001$. p -values were calculated using ANOVA with Bonferroni's correction or paired Student's t -test.

CD69 depletion was efficiently induced in ACM co-cultures using CD69 antibody compared to the isotype, without altering the total amount of CD39⁺ cells (**Figure 41A**). Strikingly, CD4⁺CD8⁺ doublets (**Figure 41B**) as well as CD25⁺CD39⁺ events in the doublet population (**Figure 41C**) of the ACM group were decreased upon CD69 neutralization. These findings provide a first hint that CD69-expressing Treg may bind to an unidentified ligand on CD8⁺ T cells, which might aid efficient adenosine production and subsequent suppression of cytotoxicity.

7 Discussion

7.1 mo-pDC generation ex-vivo brought about by evoking pDC developmental genes

We successfully generated donor-specific plasmacytoid DC equivalents *ex vivo* from monocytes, which can be further manipulated by environmental stimuli such as hypoxia, vitamin D3 or ATRA. The availability of easy systems to generate mDC *ex vivo* made them attractive for cancer therapy with the advantage of manipulating DC during differentiation. Another subset of DC, the pDC are appreciated for their importance in therapy, to prevent allograft rejection, rheumatoid arthritis [15, 16] or cancer [12]. In mice, bone marrow cells have been used to generate pDC using Flt3-L [99], but in humans there is a need to generate pDC from easily available precursors instead of using cells from cumbersome sources such as bone marrow-derived cells. Peripheral blood monocytes constitute an available source of cells from human subjects to generate mo-pDC cells as demonstrated in this study. Since monocytes produce basal levels of GM-CSF [101], we asked whether differentiating them with Flt3-L could generate pDC equivalents. Our method offers the possibility to manipulate these cells during differentiation and to study the impact of various stimuli on their differentiation and maturation.

Flt3-L is a pDC-determining cytokine [22]. The expression of Flt3 on peripheral human monocytes made them responsive to Flt3-L. Mo-pDC obtained after differentiation of monocytes with Flt3-L exhibited surface marker profiles that characterize pDC such as high CD123 and BDCA4 but lower CD11c, CD86 and TLR4 expression. Whereas pDC do not express CD14 [131] the expression of CD14 seen in mo-pDC likely points to the partial retention of some monocyte phenotypical features, which was however lost upon long-term culture up to 10 days. Mo-pDC showed high TLR7 and TLR9 expression, making them likely candidates for being responsive to viruses and produce IFN- α . Though also mDC express high TLR9 levels, they express less IFN- α , as they are probably deficient in expression of proteins in the

upstream IFN- α pathway that are under transcriptional control of E2-2. Mo-pDC also expressed CXCR3 like their primary pDC counterpart, though in lower quantity. However, CXCR3 expression was higher compared to mDC. Thus, mo-pDC are likely to respond to CXCR3-dependent trafficking.

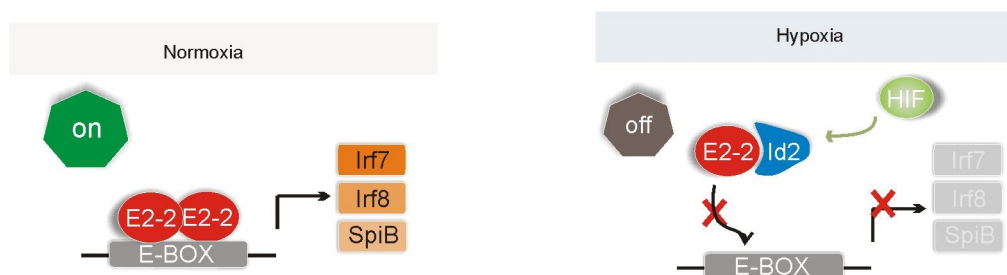


Figure 42: Transcription factors (TF) profile during pDC development under normoxia and hypoxia. (Left) In general, pDC express high levels of E2-2 but a low ID2. Under normoxia, the levels of these transcription factors are unaltered. In the absence of adequate levels of ID2, the E2-2 molecules are free to dimerize. The resulting, active E2-2 dimer binds to E-Box element in genes such as Irf-7/8, Spi-B and activates their transcription. (Right) However, under hypoxia, HIF induces ID2. In the presence of increased levels of E2-2 inhibiting TF ID2, E2-2 monomers are not able to dimerize. Since the E-Box is not occupied by the E2-2 dimer, the gene expression can not be initiated. Hence, the expression genes involved in pDC development and function are switched off under hypoxia.

E2-2 was identified as the critical pDC lineage determining marker, which is absent in conventional myeloid DC, monocytes and macrophages [25]. In humans it binds directly to the regulatory regions of multiple genes that are enriched in pDC such as ILT7, BDCA2, Spi-B, IRF7 and IRF8. A prominent E2-2 protein expression was observed in mo-pDC, whereas E2-2 expression was absent in monocytes of the same donor. Also, mo-pDC expressed significantly higher E2-2 and lower ID2 mRNA levels compared to mDC. Thus, mo-pDC might qualify as pDC equivalents, as they also differ in expression of pDC lineage markers compared to mDC generated from the same donor. Flt3-L most likely prompted E2-2 induction. Mo-pDC differentiated under hypoxia (1% O₂) for 2 days had similar levels of E2-2 like those differentiated under

normoxia, but with continuing differentiation under hypoxia, E2-2 expression was completely lost. It is interesting to note that E2a, another E protein like E2-2, was down-regulated after 1 to 3 days of exposure to hypoxia (1 % O₂) [132]. Likely, E2-2 as well as E2a was decreased under hypoxia by a yet unknown mechanism. ID proteins are the naturally occurring dominant negative inhibitors for E proteins. ID2 is a functional inhibitor of E2-2 (**Figure 42**) in human placenta [26]. On differentiation under hypoxia, we noticed that ID2 mRNA expression was progressively induced compared to normoxia. ID2 and ID3 inhibited development of pDC but not mDC [133]. 1 α , 25-Dihydroxyvitamin D3, an active form of vitamin D3 was reported to decrease both ID1 and ID2 expression [103]. Moreover, ATRA decreased ID1 and ID2 expression [104]. Consequently, we investigated the effect of vitamins on mo-pDC differentiation. As expected, mo-pDC differentiated with Flt3-L together with vitamin D3 or ATRA increased IFN- α production. Interestingly, vitamin D3 is reported to be beneficial for cancer treatment [134] and ATRA has been used along with GM-CSF and chemotherapy for treatment of acute myeloid leukaemia [135]. Besides, retinoic acid inhibited measles virus through type I interferon production [136]. Therefore, the anti-tumour and anti-virus effects of vitamins may hint towards increased production of type I interferons by pDC. In addition, ID2 is crucial for mDC development [27]. ID2 is expressed in human peripheral monocytes and its expression increases upon differentiation into terminal myeloid cells [137]. It is tempting to speculate that vitamins used in this study decreased ID proteins in monocytes. When ID levels are low, E2-2 may be free to form homodimers and activate downstream transcriptional pathways (**Figure 42**).

We checked the expression of markers in mo-pDC, which are reported to be under the control of E2-2. BDCA2 expression was higher in mo-pDC compared to mDC, which was likely due to a lack of E2-2 in the latter [25]. Furthermore, we determined the levels of IFN- α in E2-2 expressing mo-pDC. TLR9-ligated PBMC served as a positive control. IFN- α produced by mo-pDC was marginal compared to the high levels of IFN- α , which were produced by blood derived pDC [6]. Since mo-pDC expressed TLR7 and TLR9, we reasoned that the downstream IFN- α production machinery might be

incomplete. First we focussed on IRF-7, since the IRF-7 gene is transcriptionally activated by E2-2 [97] and it is critical to induce IFN- α production, which was impaired in pDC from E2-2 haplosufficient individuals [25]. IRF-7 gene expression could be stimulated by TNF- α through NF κ B [106]. Therefore, we checked the basal expression of TNF- α in mo-pDC and mDC. Mo-pDC produced significantly lower basal TNF- α amounts compared to mDC. Although IFN- α expression by mDC was low despite the high basal expression of TNF- α by these cells, priming of mo-pDC with TNF- α strongly increased their IFN- α expression on mRNA and protein level as well as secretion of bioactive IFN- α . Strikingly, TNF- α -treated mo-pDC expressed higher levels of IRF7 compared to control mo-pDC. However, basal TNF- α production from cells such as mDC alone was not sufficient to induce IFN- α . Rather, the cells had to be equipped with both the IFN- α -producing upstream machinery as well as IRF-7 expression, which is determined among others by E2-2 and was enhanced by TNF- α . The IRF7 gene promoter is reported to be located in a GC-rich area of the chromosome, which could be condensed and inaccessible. Thus, chromosome remodelling must take place in order to access the IRF7 promoter [106]. Whether E2-2 expression and TNF- α pre-stimulation improve IRF7 gene accessibility might be investigated further on.

Overall, mo-pDC generated by incubation of monocytes with Flt3-L were pDC-like cells, which still retained some characteristics of monocytes such as CD14 expression or a low basal ID2 expression. However, differentiation with vitamins or priming with TNF- α improved their function. Our method now provides an easily accessible system to study pDC differentiation and maturation using human cells.

7.2 Under hypoxia mo-pDC development is halted to produce non-functional cells

Hypoxia has a strong influence on the phenotype and functions of mDC. Immature DC undergo differentiation under hypoxia and further induce proliferation of T cells [111, 112]. In contrast, mo-pDC differentiated under

hypoxia became non-functional, based on decreased BDCA2 expression, attenuated IFN- α production, and a decreased CD86 as well as MHCII surface exposure. During differentiation under hypoxia, followed by maturation with CpG, mo-pDC also produced higher levels of TNF- α , IL-1 β and IL-6, but constant levels of IL-10 as compared to normoxia-differentiated mo-pDC. Induction of IL-6 by hypoxia is reported to result from activation of MAP kinase, HIF-1 and the NF- κ B pathway [138], which also might account for induction of TNF- α and IL-1 β . Overall, judging from cytokine data, hypoxia might strengthen NF- κ B-dependent transcription downstream of TLR9 ligation [139].

Decreased expression of BDCA2 and production of IFN- α might be a consequence of the lower E2-2 and higher ID2 levels at later stages of differentiation under hypoxia. Hypoxia might cause dedifferentiation of mo-pDC by decreasing E2-2 especially later during differentiation, since E2-2 expression was observed during early stages of differentiation under hypoxia as well as normoxia. The impact of hypoxia on E2-2 expression in later stages of mo-pDC development might have physiological implications e.g. in tumours, as it is reported that E2-2 predominantly regulates terminal development of pDC functions [97]. Therefore, properties of pDC under physiological hypoxia such as in tumours should be investigated. Interestingly, HIF-1 was described to induce ID2 in neuroblastoma cells during hypoxia [115]. Therefore, hypoxia and HIF-1-mediated ID2 induction may further contribute to the non-functionality or dedifferentiation of mo-pDC by inhibiting E2-2. To further evaluate this hypothesis, we went on to study the influence of hypoxia on pDC generation and function in the mouse system by using bone marrow progenitors that were deficient in expression of HIF-1 α .

7.3 Mouse pDC differentiation *in vitro* is inhibited by hypoxia-induced HIF-1

Indeed, on culturing mouse bone marrow cells with Flt3-L, a CD19⁻ CD11c⁺ Siglech⁺ pDC population was expanded that also expressed the mouse pDC

markers B220 (CD45R) and CD317 as described earlier [117]. But, when culturing these bone marrow cells under 5% O₂, differentiation to pDC was inhibited. This inhibition of differentiation was HIF-1 α -dependent as we observed an increase in pDC generation from progenitors lacking HIF-1 α in HIF-1 α ^{fl/fl} LysM-Cre mice under 5% O₂ compared to cells from wildtype mice. Besides, this absence differentiation was directly related to changes in the relative transcription factor levels and it was reflected on the diminished IFN- α production by these cells.

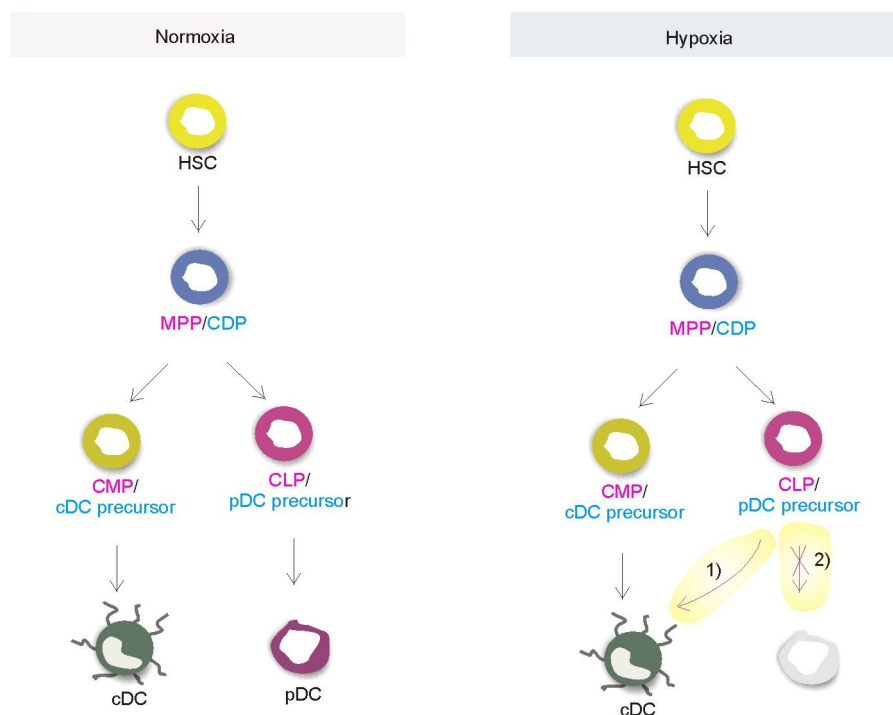


Figure 43: pDC development under normoxia and hypoxia: The differentiation of DC subsets may follow the hematopoietic stem cell (HSC)-multipotent progenitor (MPP)-common myeloid precursor (CMP)/common lymphoid precursor (CLP) path (HSC-MPP-CMP/CLP path) (depicted in pink) or the HSC-common DC progenitor (CDP)-cDC precursor/pDC precursor path (depicted in blue) (Left) (Left) Under normoxia, mDC develop from the CMP/cDC precursors and pDC develop from the CLP or pDC precursor. (Right) Under hypoxia mDC development is not affected, whereas pDC development is inhibited. Either the precursors are 1) developed into putative cDC or 2) arrested from differentiating to pDC.

It seems well-established that pDC in the bone marrow develop from common dendritic cell progenitors (CDP) that themselves arise from monocyte/DC progenitors (MDP) [20]. CDP in the bone marrow can give rise to either pDC

or progenitors of conventional DC (cDC) that leave the bone marrow to further differentiate along the DC lineage. Under hypoxia, pDC generation was inhibited whereas, the progenitors were retained as undifferentiated CD11b⁻ CD115⁺ cells [140] or the development was forked to generate a CD11b^{high} CD115⁻ cDC cell population. Thus, our data support the current view [21] that pDC mainly develop along a common pathway with cDC, which in the bone marrow might be the CDP (**Figure 43**).

Our data give first experimental evidence that one of the yet unidentified signals that encourage CDP differentiation to cDC might be the low oxygen level in the bone marrow, thereby limiting pDC generation [114, 140]. Indeed, the hypoxic milieu in the bone marrow might be a reason why pDCs constitute only a very small cell population in humans and mice. Since they are highly potent producers of type I interferons and are major drivers of autoimmune reactions [120], the identified mechanism might have evolved to limit their numbers and thus limit the magnitude of autoimmunity. To further elucidate the DC developmental program *in vitro* under the influence of hypoxia and HIF-1, detailed analysis for detecting progenitor populations could be performed

Recently, cancer immunotherapy using mDC along with pDC-activating CpG mimetic has proven successful against cancer [11, 12]. This is due to the capacity of pDC to produce type I interferon, which is crucial in preventing tumour growth by directly acting on tumour cells and on host hematopoietic cells [141]. We observed that there is a decrease in pDC differentiation under hypoxia. Furthermore, pDC function depends on continuous E2-2 expression [142], which might be decreased under hypoxia even in mature pDC, thereby limiting their functional properties. Thus tumour microenvironmental factors such as hypoxia may contribute to thwarting beneficial effects of such combinational immunotherapy which aims at pDC activation to check tumour growth.

7.4 Apoptotic cell priming in reducing cytotoxicity and inducing Tregs in DC dependent priming

A growing tumour or a tumour subjected to conventional therapy sheds tumour-derived factors/exosomes [143]. These factors released from dying tumour cells may be another crucial microenvironmental factor that may contribute to suppressing anti-tumour immunity. Over the last years it became apparent that the immune status of tumour-infiltrating lymphocytes is a crucial determinant for patient prognosis. In human colorectal cancer the presence of FoxP3⁺ Treg correlated positively with the presence of immunosuppressive DC and the absence of antigen-specific effector T cells [144]. In addition, accumulation of Treg can hinder beneficial effects of immunotherapy. Depletion of Treg using anti-CD25 or anti-CTLA4 along with T cell or DC immunotherapy was shown to successfully restore anti-tumour immunity [145]. Thus targeting Treg is a promising strategy to reduce tumour-driven immune suppression [146]. We analyzed the impact of factors released from dying tumour on the T cell-associated cytotoxicity mediated through DC. DC have been shown to internalize membrane material from living cells to mount CD8⁺ T cell immune responses [147]. Indeed we observed that factors shed from apoptotic tumour cells (ACM) reduced cytotoxicity; whereas priming with viable cell derived factors (VCM) increased cytotoxicity against living tumour cells. We propose that antigens contained in VCM exosomes might be responsible to induce cytotoxicity via CD8⁺ T cells, whereas Treg induced by immunosuppressive factors contained in ACM prevent cytotoxicity. Despite tumour cell-specific Tc might still be generated by ACM as indicated by the Treg depletion experiments, which restored cytotoxicity. Interestingly, the suppressive potential of ACM-induced Treg was transferable to VCM-primed lymphocytes. Hence apoptotic debris resulting from cytotoxic cancer therapy, which is known to induce immune paralysis [57], when shed, e.g., to the TDLN might culminate in generation of Treg that block potent endogenous tumour-killing CTL activity or CTL from an T cell adoptive-transfer immunotherapy.

Tumour-released factors modify functions of DC at the tumour site or in draining lymph nodes thereby, exploiting their tolerogenic function [148]. Generation of suppressive Treg required activation of S1PR4 on DC, likely due to S1P that is secreted by AC [149-151]. S1P is a potent lipid mediator that signals via specific G protein coupled receptors to control aspects of phagocyte biology [152]. We previously demonstrated that S1P is involved in activating macrophages to a potentially tumour-supportive phenotype [153, 154]. Furthermore, during LPS-induced maturation of DC, S1P inhibits Th1 responses by suppressing IL-12 release and instead promotes Th2 responses by increasing IL-4 and IL-10 production [152]. We observed that inhibition of S1PR1/3 upon treatment with ACM indeed marginally increased secretion of the pro-inflammatory cytokines IL-12, TNF- α and IL-6, while moderately increasing IL-10. This suggests that S1P acting on S1PR1/3 might be an intrinsic attenuating signal in AC-induced inflammation. However, for suppression of cytotoxicity these changes seemed irrelevant. Rather, S1P in ACM induced expression of ebi3 and the release of IL-27 through S1PR4. Whether IL-35, which was implicated in human Treg function [155], was upregulated by ACM could not be confirmed due to lack of a suitable IL-35 detection method. Although we cannot exclude a role for IL-35 in our system, IL-27 moderates suppressive Treg function, as demonstrated by antibody neutralization.

Generally, the function of IL-27 in T cell biology is ambiguous between pro-inflammatory (induction of Th1) and anti-inflammatory (immunosuppression) [156]. IL-27 induces expression of the Th1 transcription factor T-bet [157] and was recently shown to promote CD8⁺ T cell proliferation by activating STAT1 [158], which argues for IL-27 being pro-inflammatory. However, Treg also have been shown to express T-bet together with CXCR3. These specialized Treg migrate to areas of Th1 inflammation and contribute to immunosuppression [159], which might be a mechanism to dampen over-activation of immunity. This mechanism may be employed by ACM-primed DC expressing IL-27 to induce Treg that can in turn cause immunosuppression even in a milieu that is not strictly anti-inflammatory. Besides inducing T bet,

IL-27 potently reduces expression of the Th17 cell-determining transcription factor (TF) RORC as well as the Th2-determining TF GATA3, but not Foxp3 [160]. In our hands, interfering with IL-27 also had no effect on FoxP3 expression. Instead, IL-27 inhibition in the ACM group decreased the CD39⁺ CD69⁺ Treg population. This might be facilitated by a yet unknown mechanism similar to the one employed by IL-35, which shares the ebi3 subunit with IL-27, to induce CD39 expression on CD4⁺Foxp3⁺ Treg [161]. A mechanism how IL-27 upregulates CD69 remains to be discovered.

7.5 The Adenosine pathway is utilized by Treg to cause immunosuppression

The exact mechanism employed by Treg to suppress of anti-tumour responses in our system has yet to be defined. CD4⁺ Treg can be divided among others into CD4⁺ CD25⁺ Foxp3⁺ Treg and T regulatory type 1 (Tr1) FoxP3⁻ cells. IL-27 was shown to enhance the generation of IL-10 expressing Tr1 cells in mice [162] and to induce regulatory activity to NK cells which inturn, suppresses T cells [163]. In our system, using human cells, IL-27 did not upregulate IL-10 expression in the ACM group. The defining characteristic of the suppressive Treg subpopulation expanded by ACM-primed DC was expression of the ectonucleotidase CD39 and the activation marker CD69. It is reported that CD39 was nearly exclusively expressed by FoxP3⁺ cells [121]. CD39 metabolizes ATP and ADP to AMP, the former being produced by activated T cells that have undergone TCR engagement and calcium influx [164]. Since DC treated with ACM do not show deficiencies in maturation or activation, they might well engage the TCR of T effector cells to stimulate ATP release, which can be metabolized to AMP by CD39 present on the surface of Treg. Further on, AMP can be degraded to adenosine by CD73 present on CD8⁺ T cells in the co-culture. Extracellular adenosine was shown to inhibit many aspects of T cell functionality such as effector differentiation, activation (by increasing cAMP levels), cytokine production, metabolic activity and proliferation [129]. Interestingly ectonucleotidase expression and activity was increased in Treg of head and neck cancer patients, presumably contributing

to their immunosuppressive function [86]. A similar mechanism of immunosuppression is employed by ectonucleotidase-expressing ovarian carcinoma cells, which generate adenosine to inhibit $CD4^+$ T cell proliferation as well as NK cell cytotoxicity through activation of ADORA2A on these cells [165]. Hence adenosine generated through CD39 and CD73 expressed by Treg and $CD8^+$ T cells respectively might suppress the function of CTL in our system acting via ADORA2A, whose inhibition indeed restored cytotoxicity in the ACM group.

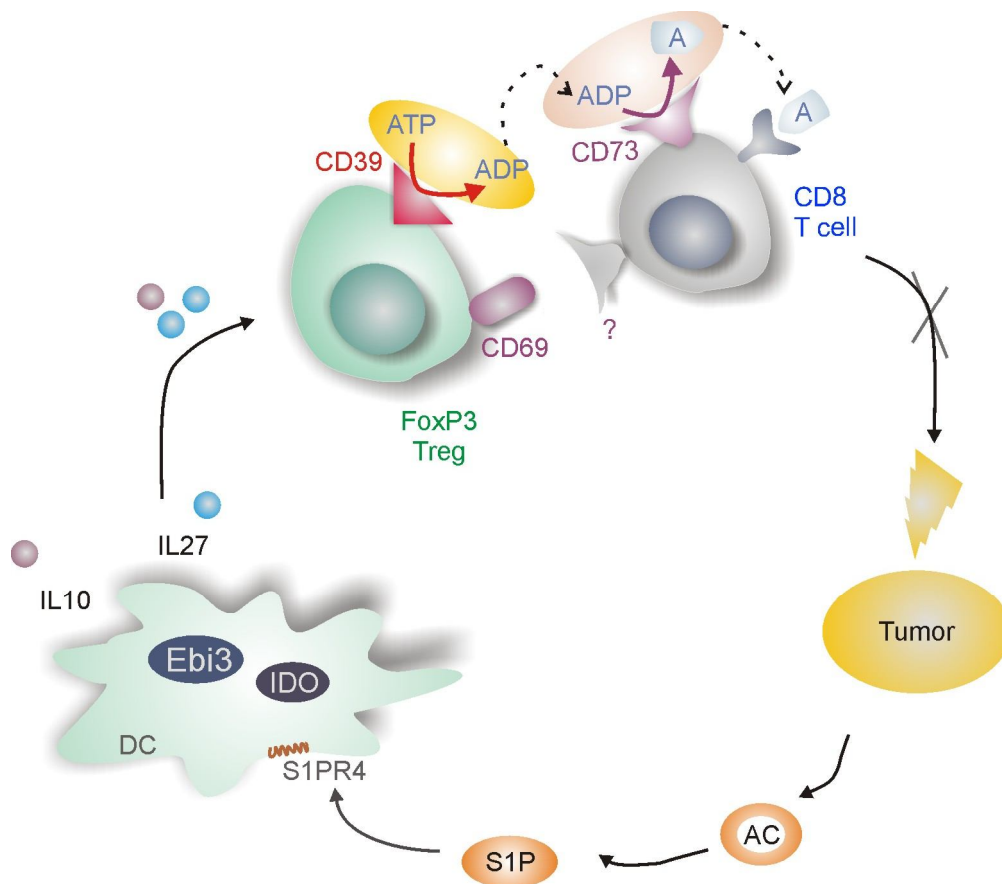


Figure 44: Pathway leading to suppression of anti-tumour immunity by apoptotic tumour cell priming of DC: Priming of DC with factors derived from apoptotic tumour cells (AC) induces expression of regulatory enzyme IDO and also expression of cytokine subunit ebi3. The ACM-polarized DC release cytokines such as IL-27 or IL-10, mediated through the S1PR4. IL-27 is responsible for up-regulation of CD69 on a Treg subpopulation that expresses FoxP3 and the ectonucleotidase CD39. The expression of CD39 on Treg along with an expression of ectonucleotidase CD73 on the surface $CD8^+$ T cells generates adenosine to mediate immunosuppression. This is likely transmitted through adenosine acting on adenosine receptors expressed on $CD8^+$ T cells. The CD69 molecule expressed by Treg might interact with a so far unidentified receptor on $CD8^+$ T cells forming a scaffold that supports adenosine generation to suppress the cytotoxic activity of $CD8^+$ T cells towards living tumour cells.

The most defining aspect of Treg from the ACM group was expression of CD69. CD69 expression on T cells inhibits S1P1 expression [166], which may act to maintain Treg in a suppressive state, since S1P has been shown to overcome FoxP3⁺ Treg-mediated suppression [167]. Besides, we hypothesize that CD69 on Treg might directly suppress the activity of effector T cells. CD69 is a C-type lectin, which can trigger e.g. TGF- β production [168]. Although TGF- β was connected with suppression of cytotoxic CD8⁺ T cells before [169], we did not observe significant up-regulation of TGF- β in Treg of the ACM group and TGF- β neutralizing did not restore cytotoxicity in our set-up. An alternative option might be binding of CD69 to a putative 'ligand/receptor' on the surface of CD8⁺ T cells, which is a common pattern for C-type lectins. This is true e.g. for interactions between cytotoxic lymphocytes and their targets [170]. However, a binding partner for CD69 is not known. If this putative molecule is expressed on CD8⁺ T cells, CD69-expressing Treg might bind to these cells to create a functional platform for adenosine production by bringing CD39 and CD73 in close proximity. Our analysis of CD4⁺CD8⁺ doublets is a first hint to support this hypothesis. Future experiments addressing the function and the putative ligand for CD69 are needed.

Ex-vivo priming of DC with tumour lysates and in vivo DC activation strategies have been employed in cancer immunotherapy [171]. Therefore, our data might add to the understanding how priming with viable or killed tumour cells might impact final anti-tumour activity and thus might aid in improving strategies for *ex vivo* DC activation. Conventional therapy will probably benefit from inhibition of intrinsic immunosuppressive pathways. Our results suggest that interfering with S1PR4 and/or IL-27 might prove beneficial. In the future, new findings regarding the putative CD69L could help to understand the significance of CD69 expression on Treg in modulating CTL responses.

8 Concluding remarks

Immune cells have evolved the capacity to act as a rheostat to control the amplitude of an immune response. DC are no exception to this rule and have a capacity to mount an inflammation or tolerance depending on the factors that they were primed with. Interestingly, pDC are immunoregulators that despite being present only in lesser numbers in the body participate in mounting an anti-viral immunity or induce tolerance. A protocol to easily differentiate pDC equivalents from human monocytes was attempted. The mo-pDC thus generated expressed some typical pDC surface markers. Besides, they also expressed pDC-determining transcription factor E2-2 whose expression was downregulated upon differentiation under hypoxia. pDC are principal IFN- α producers in the body. The capacity of mo-pDC to produce IFN- α was upregulated with TNF- α pretreatment. When differentiated under hypoxia, the IFN- α production by these mo-pDC was restricted, likely mediated through the increased ID2 production by the mo-pDC. ID2 inhibits E2-2 that controls the transcription of pDC differentiation genes. In addition, *in vitro* differentiation of bone marrow precursors from mice lacking HIF-1 α enhances pDC generation compared to culturing the precursors from wildtype mice under hypoxia, which limits pDC generation. The precursors are shunted to generate along the myeloid pathway to generate cDC or get arrested in an undifferentiated state. The lack of HIF-1 in progenitors of HIF-1 $\alpha^{fl/fl}$ LysM-Cre mice represses ID2 upregulation and encourages E2-2 function such as IFN- α production.

Hypoxia is one of the stress factors that encourages tumour growth. Another of such a stress factor is the presence of dying tumour cells, which maintains immune cells and tumour stromal cells in a state of alternative activation that ensures tumour cell survival. The influence of apoptotic or necrotic cell-derived factors on DC functions and phenotype could further help to understand their interactions with effector cells and tumour stroma in detail. Cancer immunosuppression brought about by apoptotic cells has lately become a topic of intense research [172]. Myeloid DC can be activated ex

vivo and used for tumour therapy. But the presence of tumour-derived factors has been known to offset benefits of tumour therapy. Chemotherapy and radiation therapy discharges large amounts of dying cell-released factors. However the exact mechanism of how the dying cell-discharged factors induce tolerance, in order to disrupt tumour cell killing, is not clear. We discovered that upon priming with the apoptotic cell-generated lipid S1P, DC undergo biochemical polarization via the S1P₄ receptor. The resulting release of the T cell-modulating cytokine IL-27 can direct a shift in T cell differentiation/activation and functions towards tolerance. In this study, the IL-27 released by DC upregulated a specific Treg subset. These CD39 and CD69 co-expressing FoxP3⁺ Treg suppressed the cytotoxic capability of CD8⁺ T cells through the adenosine pathway. This message as we speculate could be transmitted by the physical interaction of Treg with CD8⁺ T cells. Thus, the message of anti-tumour defence is relayed from 1) antigen presenting DC to 2) the T cells. Apoptotic cell-released factors; especially lipid messages can impact biochemical pathways at these two checkpoints. The role that IL-27, a newly discovered cytokine plays in Treg expansion under apoptotic cell priming is an interesting revelation. It will be of future interest to investigate the pathways activated downstream of IL-27R ligation in Treg and their contribution to Treg functions.

A fully functional immune system is essential for mounting an inflammatory response in the presence of a tumour. This is exemplified by the prevention of breast tumour destruction in individuals with a mutation in TLR4 [173]. Therefore, the efficacy of chemotherapeutics administered to cancer patients may also depend on their impact on the immune system. Chemotherapeutics may either kill tumour cells without immune involvement, which may or may not be immunogenic, may cause tumour cell death by activating immune cells or cause immunosuppression by also killing immune cells [174]. The immunological outcome depends on surface alterations of dying cells or, as seen in our system, on the apoptotic cell secretome, which depends on the cell death-inducing agent. In our studies, the immunogenic cell death inducer oxaliplatin did not induce immune suppression as opposed to staurosporine. One might speculate that this was due to the absence of S1P production by

oxaliplatin-treated MCF-7 cells. Finally, understanding how tumour microenvironmental factors cause altered phagocyte and effector function may greatly contribute to designing better immunotherapeutic approaches against tumours.

9 References

1. Schmid, M.C. and J.A. Varner, *Myeloid cells in the tumor microenvironment: modulation of tumor angiogenesis and tumor inflammation*. J Oncol, 2010. **2010**: p. 201026.
2. Curiel, T.J., et al., *Dendritic cell subsets differentially regulate angiogenesis in human ovarian cancer*. Cancer Res, 2004. **64**(16): p. 5535-8.
3. Yoong, K.F., et al., *Expression and function of CXC and CC chemokines in human malignant liver tumors: a role for human monokine induced by gamma-interferon in lymphocyte recruitment to hepatocellular carcinoma*. Hepatology, 1999. **30**(1): p. 100-11.
4. Palucka, K. and J. Banchereau, *Dendritic cells: a link between innate and adaptive immunity*. J Clin Immunol, 1999. **19**(1): p. 12-25.
5. Banchereau, J. and R.M. Steinman, *Dendritic cells and the control of immunity*. Nature, 1998. **392**(6673): p. 245-52.
6. Le Bon, A., et al., *Type I interferons potently enhance humoral immunity and can promote isotype switching by stimulating dendritic cells in vivo*. Immunity, 2001. **14**(4): p. 461-70.
7. Teleshova, N., J. Kenney, and M. Robbiani, *Dendritic cells and HIV infection: activating dendritic cells to boost immunity*. Adv Dent Res, 2006. **19**(1): p. 36-41.
8. Fonteneau, J.F., et al., *Human immunodeficiency virus type 1 activates plasmacytoid dendritic cells and concomitantly induces the bystander maturation of myeloid dendritic cells*. J Virol, 2004. **78**(10): p. 5223-32.
9. Chen, W., et al., *The indoleamine 2,3-dioxygenase pathway is essential for human plasmacytoid dendritic cell-induced adaptive T regulatory cell generation*. J Immunol, 2008. **181**(8): p. 5396-404.
10. Palucka, K., et al., *Dendritic cells and immunity against cancer*. J Intern Med, 2011. **269**(1): p. 64-73.
11. Lonsdorf, A.S., et al., *Intratumor CpG-oligodeoxynucleotide injection induces protective antitumor T cell immunity*. J Immunol, 2003. **171**(8): p. 3941-6.
12. Lou, Y., et al., *Plasmacytoid dendritic cells synergize with myeloid dendritic cells in the induction of antigen-specific antitumor immune responses*. J Immunol, 2007. **178**(3): p. 1534-41.
13. Diamond, M.S., et al., *Type I interferon is selectively required by dendritic cells for immune rejection of tumors*. J Exp Med, 2011. **208**(10): p. 1989-2003.
14. Hartmann, E., et al., *Identification and functional analysis of tumor-infiltrating plasmacytoid dendritic cells in head and neck cancer*. Cancer Res, 2003. **63**(19): p. 6478-87.
15. Colvin, B.L., et al., *Allostimulatory activity of bone marrow-derived plasmacytoid dendritic cells is independent of indoleamine dioxygenase but regulated by inducible costimulator ligand expression*. Hum Immunol, 2009.
16. Lebre, M.C. and P.P. Tak, *Dendritic cells in rheumatoid arthritis: Which subset should be used as a tool to induce tolerance?* Hum Immunol, 2009.
17. Ueda, Y., et al., *Frequencies of dendritic cells (myeloid DC and plasmacytoid DC) and their ratio reduced in pregnant women: comparison with umbilical cord blood and normal healthy adults*. Hum Immunol, 2003. **64**(12): p. 1144-51.
18. Colonna, M., G. Trinchieri, and Y.J. Liu, *Plasmacytoid dendritic cells in immunity*. Nat Immunol, 2004. **5**(12): p. 1219-26.
19. Yang, G.X., et al., *Plasmacytoid dendritic cells of different origins have distinct characteristics and function: studies of lymphoid progenitors versus myeloid progenitors*. J Immunol, 2005. **175**(11): p. 7281-7.
20. Geissmann, F., et al., *Development of monocytes, macrophages, and dendritic cells*. Science, 2010. **327**(5966): p. 656-61.
21. Ishikawa, F., et al., *The developmental program of human dendritic cells is operated independently of conventional myeloid and lymphoid pathways*. Blood, 2007. **110**(10): p. 3591-660.
22. Pulendran, B., et al., *Flt3-ligand and granulocyte colony-stimulating factor mobilize distinct human dendritic cell subsets in vivo*. J Immunol, 2000. **165**(1): p. 566-72.

23. Gotze, K.S., et al., *Flt3high and Flt3low CD34⁺ progenitor cells isolated from human bone marrow are functionally distinct*. Blood, 1998. **91**(6): p. 1947-58.
24. Kingston, D., et al., *The concerted action of GM-CSF and Flt3-ligand on in vivo dendritic cell homeostasis*. Blood, 2009.
25. Cisse, B., et al., *Transcription factor E2-2 is an essential and specific regulator of plasmacytoid dendritic cell development*. Cell, 2008. **135**(1): p. 37-48.
26. Liu, Y.P., et al., *Id2 is a primary partner for the E2-2 basic helix-loop-helix transcription factor in the human placenta*. Mol Cell Endocrinol, 2004. **222**(1-2): p. 83-91.
27. Hacker, C., et al., *Transcriptional profiling identifies Id2 function in dendritic cell development*. Nat Immunol, 2003. **4**(4): p. 380-6.
28. Nagasawa, M., et al., *Development of human plasmacytoid dendritic cells depends on the combined action of the basic helix-loop-helix factor E2-2 and the Ets factor Spi-B*. Eur J Immunol, 2008. **38**(9): p. 2389-400.
29. Ghosh, H.S., et al., *Continuous expression of the transcription factor e2-2 maintains the cell fate of mature plasmacytoid dendritic cells*. Immunity, 2010. **33**(6): p. 905-16.
30. Ivanovic, Z., *Hypoxia or in situ normoxia: The stem cell paradigm*. J Cell Physiol, 2009. **219**(2): p. 271-5.
31. Eliasson, P. and J.I. Jonsson, *The hematopoietic stem cell niche: low in oxygen but a nice place to be*. J Cell Physiol, 2010. **222**(1): p. 17-22.
32. Winkler, I.G., et al., *Positioning of bone marrow hematopoietic and stromal cells relative to blood flow in vivo: serially reconstituting hematopoietic stem cells reside in distinct nonperfused niches*. Blood, 2010. **116**(3): p. 375-85.
33. Parmar, K., et al., *Distribution of hematopoietic stem cells in the bone marrow according to regional hypoxia*. Proc Natl Acad Sci U S A, 2007. **104**(13): p. 5431-6.
34. Majmundar, A.J., W.J. Wong, and M.C. Simon, *Hypoxia-inducible factors and the response to hypoxic stress*. Mol Cell, 2010. **40**(2): p. 294-309.
35. Takubo, K., et al., *Regulation of the HIF-1alpha level is essential for hematopoietic stem cells*. Cell Stem Cell, 2010. **7**(3): p. 391-402.
36. Fatrai, S., et al., *Identification of HIF2alpha as an important STAT5 target gene in human hematopoietic stem cells*. Blood, 2011. **117**(12): p. 3320-30.
37. Yoon, D., P. Ponka, and J.T. Prchal, *Hypoxia. 5. Hypoxia and hematopoiesis*. Am J Physiol Cell Physiol, 2011. **300**(6): p. C1215-22.
38. Kojima, H., et al., *Abnormal B lymphocyte development and autoimmunity in hypoxia-inducible factor 1alpha -deficient chimeric mice*. Proc Natl Acad Sci U S A, 2002. **99**(4): p. 2170-4.
39. Biswas, S.K. and A. Mantovani, *Macrophage plasticity and interaction with lymphocyte subsets: cancer as a paradigm*. Nat Immunol, 2010. **11**(10): p. 889-96.
40. Dhodapkar, M.V., K.M. Dhodapkar, and A.K. Palucka, *Interactions of tumor cells with dendritic cells: balancing immunity and tolerance*. Cell Death Differ, 2008. **15**(1): p. 39-50.
41. Berzofsky, J.A. and M. Terabe, *NKT cells in tumor immunity: opposing subsets define a new immunoregulatory axis*. J Immunol, 2008. **180**(6): p. 3627-35.
42. Olex, A.L., et al., *Dynamics of dendritic cell maturation are identified through a novel filtering strategy applied to biological time-course microarray replicates*. BMC Immunol, 2010. **11**: p. 41.
43. Gelin, C., et al., *Regulation of MHC II and CD1 antigen presentation: from ubiquity to security*. J Leukoc Biol, 2009. **85**(2): p. 215-24.
44. Raghavan, M., et al., *MHC class I assembly: out and about*. Trends Immunol, 2008. **29**(9): p. 436-43.
45. Zhu, J. and W.E. Paul, *Heterogeneity and plasticity of T helper cells*. Cell Res, 2010. **20**(1): p. 4-12.
46. Schroder, K., et al., *Interferon-gamma: an overview of signals, mechanisms and functions*. J Leukoc Biol, 2004. **75**(2): p. 163-89.
47. Gutcher, I. and B. Becher, *APC-derived cytokines and T cell polarization in autoimmune inflammation*. J Clin Invest, 2007. **117**(5): p. 1119-27.
48. Nakamura, T., et al., *Roles of IL-4 and IFN-gamma in stabilizing the T helper cell type 1 and 2 phenotype*. J Immunol, 1997. **158**(6): p. 2648-53.
49. Dong, C., *TH17 cells in development: an updated view of their molecular identity and genetic programming*. Nat Rev Immunol, 2008. **8**(5): p. 337-48.

50. Chatila, T.A., *Regulatory T cells: key players in tolerance and autoimmunity*. *Endocrinol Metab Clin North Am*, 2009. **38**(2): p. 265-72, vii.
51. Jiang, H. and L. Chess, *An integrated view of suppressor T cell subsets in immunoregulation*. *J Clin Invest*, 2004. **114**(9): p. 1198-208.
52. Piersma, S.J., M.J. Welters, and S.H. van der Burg, *Tumor-specific regulatory T cells in cancer patients*. *Hum Immunol*, 2008. **69**(4-5): p. 241-9.
53. Munn, D.H. and A.L. Mellor, *The tumor-draining lymph node as an immune-privileged site*. *Immunol Rev*, 2006. **213**: p. 146-58.
54. Thompson, E.D., et al., *Tumor masses support naive T cell infiltration, activation, and differentiation into effectors*. *J Exp Med*, 2010. **207**(8): p. 1791-804.
55. Wang, H.Y., et al., *Tumor-specific human CD4⁺ regulatory T cells and their ligands: implications for immunotherapy*. *Immunity*, 2004. **20**(1): p. 107-18.
56. Tan, W., et al., *Tumour-infiltrating regulatory T cells stimulate mammary cancer metastasis through RANKL-RANK signalling*. *Nature*, 2011. **470**(7335): p. 548-53.
57. Zitvogel, L., et al., *Immunological aspects of cancer chemotherapy*. *Nat Rev Immunol*, 2008. **8**(1): p. 59-73.
58. Zou, W., *Immunosuppressive networks in the tumour environment and their therapeutic relevance*. *Nat Rev Cancer*, 2005. **5**(4): p. 263-74.
59. Lin, A., et al., *Dendritic cells integrate signals from the tumor microenvironment to modulate immunity and tumor growth*. *Immunol Lett*, 2010. **127**(2): p. 77-84.
60. McDonnell, A.M., B.W. Robinson, and A.J. Currie, *Tumor antigen cross-presentation and the dendritic cell: where it all begins?* *Clin Dev Immunol*. **2010**: p. 539519.
61. Bell, D., et al., *In breast carcinoma tissue, immature dendritic cells reside within the tumor, whereas mature dendritic cells are located in peritumoral areas*. *J Exp Med*, 1999. **190**(10): p. 1417-26.
62. Iero, M., et al., *Tumour-released exosomes and their implications in cancer immunity*. *Cell Death Differ*, 2008. **15**(1): p. 80-8.
63. Thery, C., M. Ostrowski, and E. Segura, *Membrane vesicles as conveyors of immune responses*. *Nat Rev Immunol*, 2009. **9**(8): p. 581-93.
64. Gregory, C.D. and J.D. Pound, *Cell death in the neighbourhood: direct microenvironmental effects of apoptosis in normal and neoplastic tissues*. *J Pathol*, 2010. **223**(2): p. 177-94.
65. Albert, M.L., *Death-defying immunity: do apoptotic cells influence antigen processing and presentation?* *Nat Rev Immunol*, 2004. **4**(3): p. 223-31.
66. Burgdorf, S., et al., *Spatial and mechanistic separation of cross-presentation and endogenous antigen presentation*. *Nat Immunol*, 2008. **9**(5): p. 558-66.
67. Zitvogel, L., O. Kepp, and G. Kroemer, *Decoding cell death signals in inflammation and immunity*. *Cell*, 2010. **140**(6): p. 798-804.
68. Sims, G.P., et al., *HMGB1 and RAGE in inflammation and cancer*. *Annu Rev Immunol*, 2010. **28**: p. 367-88.
69. Tesniere, A., et al., *Immunogenic cancer cell death: a key-lock paradigm*. *Curr Opin Immunol*, 2008. **20**(5): p. 504-11.
70. Nowak, A.K., et al., *Induction of tumor cell apoptosis in vivo increases tumor antigen cross-presentation, cross-priming rather than cross-tolerizing host tumor-specific CD8 T cells*. *J Immunol*, 2003. **170**(10): p. 4905-13.
71. Morelli, A.E. and A.W. Thomson, *Tolerogenic dendritic cells and the quest for transplant tolerance*. *Nat Rev Immunol*, 2007. **7**(8): p. 610-21.
72. Panaretakis, T., et al., *Mechanisms of pre-apoptotic calreticulin exposure in immunogenic cell death*. *Embo J*, 2009. **28**(5): p. 578-90.
73. van der Most, R.G., et al., *Decoding dangerous death: how cytotoxic chemotherapy invokes inflammation, immunity or nothing at all*. *Cell Death Differ*, 2008. **15**(1): p. 13-20.
74. Feng, H., et al., *Stressed apoptotic tumor cells stimulate dendritic cells and induce specific cytotoxic T cells*. *Blood*, 2002. **100**(12): p. 4108-15.
75. Soule, H.D., et al., *A human cell line from a pleural effusion derived from a breast carcinoma*. *J Natl Cancer Inst*, 1973. **51**(5): p. 1409-16.
76. Exley, M.A., B. Wilson, and S.P. Balk, *Isolation and functional use of human NKT cells*. *Curr Protoc Immunol*, 2010. **Chapter 14**: p. Unit 14 11.

77. Deenick, E.K., A.V. Gett, and P.D. Hodgkin, *Stochastic model of T cell proliferation: a calculus revealing IL-2 regulation of precursor frequencies, cell cycle time, and survival*. J Immunol, 2003. **170**(10): p. 4963-72.
78. Ryan, H.E., J. Lo, and R.S. Johnson, *HIF-1 alpha is required for solid tumor formation and embryonic vascularization*. EMBO J, 1998. **17**(11): p. 3005-15.
79. Clausen, B.E., et al., *Conditional gene targeting in macrophages and granulocytes using LysMcre mice*. Transgenic Res, 1999. **8**(4): p. 265-77.
80. Brawand, P., et al., *Murine plasmacytoid pre-dendritic cells generated from Flt3 ligand-supplemented bone marrow cultures are immature APCs*. J Immunol, 2002. **169**(12): p. 6711-9.
81. Weigert, A., et al., *Apoptotic cells promote macrophage survival by releasing the antiapoptotic mediator sphingosine-1-phosphate*. Blood, 2006. **108**(5): p. 1635-42.
82. Lauber, K., et al., *Apoptotic cells induce migration of phagocytes via caspase-3-mediated release of a lipid attraction signal*. Cell, 2003. **113**(6): p. 717-30.
83. Segundo, C., et al., *Surface molecule loss and bleb formation by human germinal center B cells undergoing apoptosis: role of apoptotic blebs in monocyte chemotaxis*. Blood, 1999. **94**(3): p. 1012-20.
84. Guerrero, M., et al., *Discovery, design and synthesis of the first reported potent and selective sphingosine-1-phosphate 4 (S1P(4)) receptor antagonists*. Bioorg Med Chem Lett, 2011. **21**(12): p. 3632-6.
85. Qian, F., et al., *Efficacy of levo-1-methyl tryptophan and dextro-1-methyl tryptophan in reversing indoleamine-2,3-dioxygenase-mediated arrest of T-cell proliferation in human epithelial ovarian cancer*. Cancer Res, 2009. **69**(13): p. 5498-504.
86. Mandapathil, M., et al., *Increased ectonucleotidase expression and activity in regulatory T cells of patients with head and neck cancer*. Clin Cancer Res, 2009. **15**(20): p. 6348-57.
87. Eltzschig, H.K., et al., *Endogenous adenosine produced during hypoxia attenuates neutrophil accumulation: coordination by extracellular nucleotide metabolism*. Blood, 2004. **104**(13): p. 3986-92.
88. Herr, B., et al., *The supernatant of apoptotic cells causes transcriptional activation of hypoxia-inducible factor-1alpha in macrophages via sphingosine-1-phosphate and transforming growth factor-beta*. Blood, 2009. **114**(10): p. 2140-8.
89. Zimmermann, S.Y., et al., *A novel four-colour flow cytometric assay to determine natural killer cell or T-cell-mediated cellular cytotoxicity against leukaemic cells in peripheral or bone marrow specimens containing greater than 20% of normal cells*. J Immunol Methods, 2005. **296**(1-2): p. 63-76.
90. Campanelli, R., et al., *Human CD8 co-receptor is strictly involved in MHC-peptide tetramer-TCR binding and T cell activation*. Int Immunol, 2002. **14**(1): p. 39-44.
91. Albee, L., B. Shi, and H. Perlman, *Aspartic protease and caspase 3/7 activation are central for macrophage apoptosis following infection with Escherichia coli*. J Leukoc Biol, 2007. **81**(1): p. 229-37.
92. Weis, N., et al., *Heme oxygenase-1 contributes to an alternative macrophage activation profile induced by apoptotic cell supernatants*. Mol Biol Cell, 2009. **20**(5): p. 1280-8.
93. Hiasa, M., et al., *GM-CSF and IL-4 induce dendritic cell differentiation and disrupt osteoclastogenesis through M-CSF receptor shedding by up-regulation of TNF-alpha converting enzyme (TACE)*. Blood, 2009. **114**(20): p. 4517-26.
94. Briere, F., et al., *Origin and filiation of human plasmacytoid dendritic cells*. Hum Immunol, 2002. **63**(12): p. 1081-93.
95. Dzionek, A., et al., *Plasmacytoid dendritic cells: from specific surface markers to specific cellular functions*. Hum Immunol, 2002. **63**(12): p. 1133-48.
96. Jarrossay, D., et al., *Specialization and complementarity in microbial molecule recognition by human myeloid and plasmacytoid dendritic cells*. Eur J Immunol, 2001. **31**(11): p. 3388-93.
97. Esashi, E. and S.S. Watowich, *Dendritic cells: transcriptional control of plasmacytoid dendritic cell development by E2-2*. Immunol Cell Biol, 2009. **87**(1): p. 1-2.
98. Grouard, G., et al., *The enigmatic plasmacytoid T cells develop into dendritic cells with interleukin (IL)-3 and CD40-ligand*. J Exp Med, 1997. **185**(6): p. 1101-11.
99. Smit, J.J., et al., *The balance between plasmacytoid DC versus conventional DC determines pulmonary immunity to virus infections*. PLoS One, 2008. **3**(3): p. e1720.

100. Meier, A., et al., *Sex differences in the Toll-like receptor-mediated response of plasmacytoid dendritic cells to HIV-1*. *Nat Med*, 2009. **15**(8): p. 955-9.
101. Su, A.I., et al., *A gene atlas of the mouse and human protein-encoding transcriptomes*. *Proc Natl Acad Sci U S A*, 2004. **101**(16): p. 6062-7.
102. Takauji, R., et al., *CpG-DNA-induced IFN-alpha production involves p38 MAPK-dependent STAT1 phosphorylation in human plasmacytoid dendritic cell precursors*. *J Leukoc Biol*, 2002. **72**(5): p. 1011-9.
103. Fernandez-Garcia, N.I., et al., *1alpha,25-Dihydroxyvitamin D3 regulates the expression of Id1 and Id2 genes and the angiogenic phenotype of human colon carcinoma cells*. *Oncogene*, 2005. **24**(43): p. 6533-44.
104. Nigten, J., et al., *ID1 and ID2 are retinoic acid responsive genes and induce a G0/G1 accumulation in acute promyelocytic leukemia cells*. *Leukemia*, 2005. **19**(5): p. 799-805.
105. Barchet, W., et al., *Virus-induced interferon alpha production by a dendritic cell subset in the absence of feedback signaling in vivo*. *J Exp Med*, 2002. **195**(4): p. 507-16.
106. Lu, R., P.A. Moore, and P.M. Pitha, *Stimulation of IRF-7 gene expression by tumor necrosis factor alpha: requirement for NFkappa B transcription factor and gene accessibility*. *J Biol Chem*, 2002. **277**(19): p. 16592-8.
107. Greenway, A.L., et al., *Selective production of interferon-alpha subtypes by cultured peripheral blood mononuclear cells and lymphoblastoid cell lines*. *Immunology*, 1992. **75**(1): p. 182-8.
108. Murdoch, C., M. Muthana, and C.E. Lewis, *Hypoxia regulates macrophage functions in inflammation*. *J Immunol*, 2005. **175**(10): p. 6257-63.
109. Kunz, M. and S.M. Ibrahim, *Molecular responses to hypoxia in tumor cells*. *Mol Cancer*, 2003. **2**: p. 23.
110. Jogi, A., et al., *Human neuroblastoma cells exposed to hypoxia: induction of genes associated with growth, survival, and aggressive behavior*. *Exp Cell Res*, 2004. **295**(2): p. 469-87.
111. Rama, I., et al., *Hypoxia stimulus: An adaptive immune response during dendritic cell maturation*. *Kidney Int*, 2008. **73**(7): p. 816-25.
112. Jantsch, J., et al., *Hypoxia and hypoxia-inducible factor-1 alpha modulate lipopolysaccharide-induced dendritic cell activation and function*. *J Immunol*, 2008. **180**(7): p. 4697-705.
113. Rissoan, M.C., et al., *Reciprocal control of T helper cell and dendritic cell differentiation*. *Science*, 1999. **283**(5405): p. 1183-6.
114. Reizis, B., *Regulation of plasmacytoid dendritic cell development*. *Curr Opin Immunol*, 2010. **22**(2): p. 206-11.
115. Lofstedt, T., et al., *Induction of ID2 expression by hypoxia-inducible factor-1: a role in dedifferentiation of hypoxic neuroblastoma cells*. *J Biol Chem*, 2004. **279**(38): p. 39223-31.
116. Jakubzick, C., et al., *Lymph-migrating, tissue-derived dendritic cells are minor constituents within steady-state lymph nodes*. *J Exp Med*, 2008. **205**(12): p. 2839-50.
117. Lau-Kilby, A.W., et al., *Interleukin-2 inhibits FMS-like tyrosine kinase 3 receptor ligand (flt3L)-dependent development and function of conventional and plasmacytoid dendritic cells*. *Proc Natl Acad Sci U S A*, 2011. **108**(6): p. 2408-13.
118. Zhang, J., et al., *Characterization of Siglec-H as a novel endocytic receptor expressed on murine plasmacytoid dendritic cell precursors*. *Blood*, 2006. **107**(9): p. 3600-8.
119. Blasius, A.L., et al., *Siglec-H is an IPC-specific receptor that modulates type I IFN secretion through DAP12*. *Blood*, 2006. **107**(6): p. 2474-6.
120. Swiecki, M. and M. Colonna, *Unraveling the functions of plasmacytoid dendritic cells during viral infections, autoimmunity, and tolerance*. *Immunol Rev*, 2010. **234**(1): p. 142-62.
121. Borsellino, G., et al., *Expression of ectonucleotidase CD39 by Foxp3⁺ Treg cells: hydrolysis of extracellular ATP and immune suppression*. *Blood*, 2007. **110**(4): p. 1225-32.
122. Battaglia, A., et al., *Metastatic tumour cells favour the generation of a tolerogenic milieu in tumour draining lymph node in patients with early cervical cancer*. *Cancer Immunol Immunother*, 2009. **58**(9): p. 1363-73.

123. Weigert, A., et al., *Cleavage of sphingosine kinase 2 by caspase-1 provokes its release from apoptotic cells*. *Blood*, 2010. **115**(17): p. 3531-40.
124. Wetter, J.A., C. Revankar, and B.J. Hanson, *Utilization of the Tango beta-arrestin recruitment technology for cell-based EDG receptor assay development and interrogation*. *J Biomol Screen*, 2009. **14**(9): p. 1134-41.
125. Lob, S., et al., *Inhibitors of indoleamine-2,3-dioxygenase for cancer therapy: can we see the wood for the trees?* *Nat Rev Cancer*, 2009. **9**(6): p. 445-52.
126. Williams, C.A., R.A. Harry, and J.D. McLeod, *Apoptotic cells induce dendritic cell-mediated suppression via interferon-gamma-induced IDO*. *Immunology*, 2008. **124**(1): p. 89-101.
127. Gee, K., et al., *The IL-12 family of cytokines in infection, inflammation and autoimmune disorders*. *Inflamm Allergy Drug Targets*, 2009. **8**(1): p. 40-52.
128. Shevach, E.M., *Mechanisms of foxp3⁺ T regulatory cell-mediated suppression*. *Immunity*, 2009. **30**(5): p. 636-45.
129. Linnemann, C., et al., *Adenosine regulates CD8 T-cell priming by inhibition of membrane-proximal T-cell receptor signalling*. *Immunology*, 2009. **128**(1 Suppl): p. e728-37.
130. Kisley, L.R., et al., *Genetic ablation of inducible nitric oxide synthase decreases mouse lung tumorigenesis*. *Cancer Res*, 2002. **62**(23): p. 6850-6.
131. Marmey, B., et al., *CD14 and CD169 expression in human lymph nodes and spleen: specific expansion of CD14⁺CD169- monocyte-derived cells in diffuse large B-cell lymphomas*. *Hum Pathol*, 2006. **37**(1): p. 68-77.
132. Yun, Z., Q. Lin, and A.J. Giaccia, *Adaptive myogenesis under hypoxia*. *Mol Cell Biol*, 2005. **25**(8): p. 3040-55.
133. Spits, H., et al., *Id2 and Id3 inhibit development of CD34⁺ stem cells into predendritic cell (pre-DC)2 but not into pre-DC1. Evidence for a lymphoid origin of pre-DC2*. *J Exp Med*, 2000. **192**(12): p. 1775-84.
134. Leibowitz, S.B. and P.W. Kantoff, *Differentiating agents and the treatment of prostate cancer: Vitamin D3 and peroxisome proliferator-activated receptor gamma ligands*. *Semin Oncol*, 2003. **30**(5): p. 698-708.
135. Shin, H.J., et al., *A Pilot Study of Priming With Granulocyte Macrophage Colony-Stimulating Factor Plus All-trans Retinoic Acid Combined With Remission Induction Chemotherapy in Patients With Acute Myeloid Leukemia*. *Am J Clin Oncol*, 2009.
136. Trottier, C., et al., *Retinoids inhibit measles virus through a type I IFN-dependent bystander effect*. *Faseb J*, 2009.
137. Ishiguro, A., et al., *Id2 expression increases with differentiation of human myeloid cells*. *Blood*, 1996. **87**(12): p. 5225-31.
138. Jeong, H.J., et al., *Hypoxia-induced IL-6 production is associated with activation of MAP kinase, HIF-1, and NF-kappaB on HEI-OC1 cells*. *Hear Res*, 2005. **207**(1-2): p. 59-67.
139. Baccala, R., et al., *TLR-dependent and TLR-independent pathways of type I interferon induction in systemic autoimmunity*. *Nat Med*, 2007. **13**(5): p. 543-51.
140. Liu, K., et al., *In vivo analysis of dendritic cell development and homeostasis*. *Science*, 2009. **324**(5925): p. 392-7.
141. Smyth, M.J., *Type I interferon and cancer immunoediting*. *Nat Immunol*, 2005. **6**(7): p. 646-8.
142. Reizis, B., et al., *Plasmacytoid dendritic cells: recent progress and open questions*. *Annu Rev Immunol*, 2011. **29**: p. 163-83.
143. Zeelenberg, I.S., et al., *Antigen localization controls T cell-mediated tumor immunity*. *J Immunol*, 2011. **187**(3): p. 1281-8.
144. Nagorsen, D., et al., *Tumor-infiltrating macrophages and dendritic cells in human colorectal cancer: relation to local regulatory T cells, systemic T-cell response against tumor-associated antigens and survival*. *J Transl Med*, 2007. **5**: p. 62.
145. von Bergwelt-Baildon, M.S., et al., *CD25 and indoleamine 2,3-dioxygenase are up-regulated by prostaglandin E2 and expressed by tumor-associated dendritic cells in vivo: additional mechanisms of T-cell inhibition*. *Blood*, 2006. **108**(1): p. 228-37.
146. Curiel, T.J., *Tregs and rethinking cancer immunotherapy*. *J Clin Invest*, 2007. **117**(5): p. 1167-74.
147. Matheoud, D., et al., *Cross-presentation by dendritic cells from live cells induces protective immune responses in vivo*. *Blood*, 2010. **115**(22): p. 4412-20.

148. Schuler, G., *Dendritic cells in cancer immunotherapy*. Eur J Immunol, 2010. **40**(8): p. 2123-30.
149. Weigert, A., et al., *Cleavage of sphingosine kinase 2 by caspase-1 provokes its release from apoptotic cells*. Blood, 2010. **115**(17): p. 3531-40.
150. Gude, D.R., et al., *Apoptosis induces expression of sphingosine kinase 1 to release sphingosine-1-phosphate as a "come-and-get-me" signal*. Faseb J, 2008. **22**(8): p. 2629-38.
151. Gu, Y., et al., *Epithelial cell extrusion requires the sphingosine-1-phosphate receptor 2 pathway*. J Cell Biol, 2011. **193**(4): p. 667-76.
152. Rivera, J., R.L. Proia, and A. Olivera, *The alliance of sphingosine-1-phosphate and its receptors in immunity*. Nat Rev Immunol, 2008. **8**(10): p. 753-63.
153. Weigert, A., et al., *Sphingosine kinase 2 deficient tumor xenografts show impaired growth and fail to polarize macrophages towards an anti-inflammatory phenotype*. Int J Cancer, 2009. **125**(9): p. 2114-21.
154. Brecht, K., et al., *Macrophages programmed by apoptotic cells promote angiogenesis via prostaglandin E2*. Faseb J, 2011.
155. Collison, L.W., et al., *IL-35-mediated induction of a potent regulatory T cell population*. Nat Immunol, 2010. **11**(12): p. 1093-101.
156. Yoshida, H., M. Nakaya, and Y. Miyazaki, *Interleukin 27: a double-edged sword for offense and defense*. J Leukoc Biol, 2009. **86**(6): p. 1295-303.
157. Kamiya, S., et al., *An indispensable role for STAT1 in IL-27-induced T-bet expression but not proliferation of naive CD4⁺ T cells*. J Immunol, 2004. **173**(6): p. 3871-7.
158. Schneider, R., et al., *IL-27 increases the proliferation and effector functions of human naive CD8⁺ T lymphocytes and promotes their development into Tc1 cells*. Eur J Immunol, 2011. **41**(1): p. 47-59.
159. Sindrilaru, A., et al., *Wound healing defect of Vav3^{-/-} mice due to impaired {beta}2-integrin-dependent macrophage phagocytosis of apoptotic neutrophils*. Blood, 2009. **113**(21): p. 5266-76.
160. Murugaiyan, G., et al., *IL-27 is a key regulator of IL-10 and IL-17 production by human CD4⁺ T cells*. J Immunol, 2009. **183**(4): p. 2435-43.
161. Kochetkova, I., et al., *IL-35 stimulation of CD39⁺ regulatory T cells confers protection against collagen II-induced arthritis via the production of IL-10*. J Immunol, 2010. **184**(12): p. 7144-53.
162. Batten, M., et al., *Cutting edge: IL-27 is a potent inducer of IL-10 but not FoxP3 in murine T cells*. J Immunol, 2008. **180**(5): p. 2752-6.
163. Laroni, A., et al., *IL-27 imparts immunoregulatory function to human NK cell subsets*. PLoS One, 2011. **6**(10): p. e26173.
164. Schenk, U., et al., *Purinergic control of T cell activation by ATP released through pannexin-1 hemichannels*. Sci Signal, 2008. **1**(39): p. ra6.
165. Hausler, S.F., et al., *Ectonucleotidases CD39 and CD73 on OvCA cells are potent adenosine-generating enzymes responsible for adenosine receptor 2A-dependent suppression of T cell function and NK cell cytotoxicity*. Cancer Immunol Immunother, 2011.
166. Shioh, L.R., et al., *CD69 acts downstream of interferon-alpha/beta to inhibit S1P1 and lymphocyte egress from lymphoid organs*. Nature, 2006. **440**(7083): p. 540-4.
167. Liu, G., et al., *The receptor S1P1 overrides regulatory T cell-mediated immune suppression through Akt-mTOR*. Nat Immunol, 2009. **10**(7): p. 769-77.
168. Sancho, D., M. Gomez, and F. Sanchez-Madrid, *CD69 is an immunoregulatory molecule induced following activation*. Trends Immunol, 2005. **26**(3): p. 136-40.
169. Chen, M.L., et al., *Regulatory T cells suppress tumor-specific CD8 T cell cytotoxicity through TGF-beta signals in vivo*. Proc Natl Acad Sci U S A, 2005. **102**(2): p. 419-24.
170. Vogler, I. and A. Steinle, *Vis-a-vis in the NKC: genetically linked natural killer cell receptor/ligand pairs in the natural killer gene complex (NKC)*. J Innate Immun, 2011. **3**(3): p. 227-35.
171. Le, D.T., D.M. Pardoll, and E.M. Jaffee, *Cellular vaccine approaches*. Cancer J, 2010. **16**(4): p. 304-10.
172. Gregory, C.D. and J.D. Pound, *Cell death in the neighbourhood: direct microenvironmental effects of apoptosis in normal and neoplastic tissues*. J Pathol, 2011. **223**(2): p. 177-94.

173. Apetoh, L., et al., *Toll-like receptor 4-dependent contribution of the immune system to anticancer chemotherapy and radiotherapy*. *Nat Med*, 2007. **13**(9): p. 1050-9.
174. Zitvogel, L., O. Kepp, and G. Kroemer, *Immune parameters affecting the efficacy of chemotherapeutic regimens*. *Nat Rev Clin Oncol*, 2011. **8**(3): p. 151-60.

10 Publications

Weigert A, **Sekar D**, Brüne B., Tumour-associated macrophages as targets for tumour immunotherapy, *Immunotherapy*. 2009. Jan;1(1):83-95.

Weigert A, Schiffmann S, **Sekar D**, Ley S, Menrad H, Werno C, Grosch S, Geisslinger G, Brüne B., Sphingosine kinase 2 deficient tumour xenografts show impaired growth and fail to polarize macrophages towards an anti-inflammatory phenotype. *Int J Cancer* 2009. Nov 1;125(9):2114-21.

Sekar D, Brüne B, Weigert A., Technical advance: Generation of human pDC equivalents from primary monocytes using Flt3-L and their functional validation under hypoxia. *J Leukoc Biol*. 2010 Aug;88(2):413-24.

Sekar D, Hahn C, Brüne B, Roberts E, Weigert A., Apoptotic tumour cells induce IL-27 release from human DC to activate regulatory T cells that express CD69 and attenuate cytotoxicity. *Eur J Immunol*. accepted, ahead of print: DOI: 10.1002/eji.201142093.

Weigert A, Weichand B, **Sekar D**, Essler S, Dehne N, Brüne B, HIF-1 α is a negative regulator of plasmacytoid DC development *in vitro* and *in vivo*, submitted.

Meeting abstract (selected for oral presentation)

Sekar D, Brüne B, Weigert A., Dendritic cell and subsequent effector T cell polarization by dying tumour cells. 1st International Conference of Immunotherapy, Institut Curie, Paris, France. 17-18 Oct 2008

11 Acknowledgements

I am greatly indebted to my PhD supervisor Prof. Brüne, for supporting me in these 4 years of research study by providing the top notch lab equipments, reagents, scientific advice and constructive criticism. Transparent modes of working and professionalism under Prof. Brüne made it easier to devote all the energy on the projects itself.

I am thankful to have worked under the guidance of Dr. Andreas Weigert who is encouraging, creative and critical. His constantly driven scientific-radar and the thirst to get the projects to completion helped immensely.

Getting an education in a foreign country is a challenging enterprise. I am deeply thankful to my colleagues in *Biochemie Eins* for the support and patience during the countless times I stuttered with understanding Deutsch or the etiquettes. Not to forget the *Kuchen/Torte* that many colleagues brought to the lab. Each *Schicht*, was a sugar-pump for moving the PhD days forward.

To my best friends.

To my family.

To my sister: For that thing which is my life's constant.

To my love.

To sea shells.

12 Curriculum Vitae

Name: Divya Sekar
Date of birth: 19.01.1985
Place of birth: Shimoga, India
Nationality: Indian
Marital status: Married
Address: Cranachstrasse 15
60596 Frankfurt/Main
Tel: 069-47890830
Mail: div.sek@gmail.com

Academic profile:

1999 - 00 X, Senior secondary school, India
2001 - 02 XII, Higher secondary school, India
2002 – 05 BSc Biochemistry, University of Madras, 6th rank
2005 – 06 Project Saraswathi All India Scholarship
to Support Post Graduate studies
2005 – 07 MSc Microbial gene technology,
Madurai Kamaraj University, India
Oct 2007 – Sep 2009 Frankfurt International Research school
for translational medicine,
stipend for PhD studies
Oct 2007 – Sep 2011 PhD Research student, Institut für Biochemie I
(Prof. Bernhard Brüne), Klinikum der Johann
Wolfgang Goethe-Universität, Frankfurt am Main

13 Ehrenwörtliche Erklärung

Ich erkläre ehrenwörtlich, dass ich die dem Fachbereich Medizin der Johann Wolfgang Goethe-Universität Frankfurt am Main zur Promotionsprüfung eingereichte Arbeit mit dem Titel

“Impact of tumour microenvironmental factors on dendritic cell differentiation and function”

Im Institut für Biochemie I – Pathobiochemie unter Betreuung und Anleitung von Prof. Dr. Bernhard Brüne ohne sonstige Hilfe selbst durchgeführt und bei der Abfassung der Arbeit keine anderen als die in der Dissertation angeführten Hilfsmittel benutzt habe.

Ich habe bisher an keiner in- oder ausländischen Universität ein Gesuch um Zulassung zur Promotion eingereicht. Die vorliegende Arbeit wurde bisher nicht als Dissertation eingereicht.

Teile der vorliegenden Arbeit wurden in den folgenden Publikationsorganen veröffentlicht:

J Leukoc Biol. 2010 Aug;88(2):413-24.

Eur J Immunol. ahead of print, DOI: 10.1002/eji.201142093.

Frankfurt am Main, den